

Search for triboson $W^\pm W^\pm W^\mp$ production in pp collisions at $\sqrt{s} = 8$ TeV with the ATLAS detector

ATLAS Collaboration*

CERN, 1211 Geneva 23, Switzerland

Received: 18 October 2016 / Accepted: 10 February 2017 / Published online: 2 March 2017

© CERN for the benefit of the ATLAS collaboration 2017. This article is published with open access at Springerlink.com

Abstract This paper reports a search for triboson $W^\pm W^\pm W^\mp$ production in two decay channels ($W^\pm W^\pm W^\mp \rightarrow \ell^\pm \nu \ell^\pm \nu \ell^\mp \nu$ and $W^\pm W^\pm W^\mp \rightarrow \ell^\pm \nu \ell^\pm \nu jj$ with $\ell = e, \mu$) in proton-proton collision data corresponding to an integrated luminosity of 20.3 fb^{-1} at a centre-of-mass energy of 8 TeV with the ATLAS detector at the Large Hadron Collider. Events with exactly three charged leptons, or two leptons with the same electric charge in association with two jets, are selected. The total number of events observed in data is consistent with the Standard Model (SM) predictions. The observed 95% confidence level upper limit on the SM $W^\pm W^\pm W^\mp$ production cross section is found to be 730 fb with an expected limit of 560 fb in the absence of SM $W^\pm W^\pm W^\mp$ production. Limits are also set on $WWWW$ anomalous quartic gauge couplings.

1 Introduction

The triple gauge couplings (TGCs) and quartic gauge couplings (QGCs) that describe the strengths of the triple and quartic gauge boson self-interactions are completely determined by the non-Abelian nature of the electroweak $SU(2)_L \times U(1)_Y$ gauge structure in the Standard Model (SM). These interactions contribute directly to diboson and triboson production at colliders. Studies of triboson production can test these interactions and any possible observed deviation from the theoretical prediction would provide hints of new physics at a higher energy scale. Compared with TGCs, QGCs are usually harder to study due to the, in general, smaller production cross sections of the relevant processes.

In the SM, charged QGC interactions ($WWWW$, $WWZZ$, $WWZ\gamma$ and $WW\gamma\gamma$) are allowed whereas neutral QGC interactions ($ZZZZ$, $ZZZ\gamma$, $ZZ\gamma\gamma$, $Z\gamma\gamma\gamma$ and $\gamma\gamma\gamma\gamma$) are forbidden. Searches have been performed by the LEP experiments for $WW\gamma\gamma$, $WWZ\gamma$, and $ZZ\gamma\gamma$ QGCs [1–6], by the Tevatron experiments for $WW\gamma\gamma$ [7],

and by the LHC experiments for $WW\gamma\gamma$, $WWZ\gamma$, $WWZZ$, $ZZ\gamma\gamma$, $Z\gamma\gamma\gamma$, and $WWWW$ QGCs [8–17].

Previous studies of $WWWW$ QGC interactions [8, 16] used $W^\pm W^\pm$ vector-boson scattering events, whereas this paper presents the first search for $WWWW$ QGC interactions via triboson $W^\pm W^\pm W^\mp$ production and sets the first limit on the total SM $W^\pm W^\pm W^\mp$ production cross-section using proton-proton (pp) collision data collected with the ATLAS detector and corresponding to an integrated luminosity of 20.3 fb^{-1} [18] at a centre-of-mass energy of 8 TeV. Two decay channels, $W^\pm W^\pm W^\mp \rightarrow \ell^\pm \nu \ell^\pm \nu \ell^\mp \nu$ and $W^\pm W^\pm W^\mp \rightarrow \ell^\pm \nu \ell^\pm \nu jj$, with $\ell = e$ or μ , are considered and are hereafter referred to simply as $\ell\nu\ell\nu\ell\nu$ and $\ell\nu\ell\nu jj$ channels, respectively.

2 The ATLAS detector

The ATLAS detector [19] is composed of an inner tracking detector (ID) surrounded by a thin superconducting solenoid providing a 2 T axial magnetic field, electromagnetic and hadronic calorimeters, and a muon spectrometer (MS). The ID consists of three subsystems: the pixel and silicon microstrip detectors that cover $|\eta| < 2.5$ in pseudorapidity,¹ and the outer transition radiation tracker that has an acceptance range of $|\eta| < 2.0$. The finely-segmented electromagnetic calorimeter is composed of lead absorbers with liquid argon (LAr) as the active material, spanning $|\eta| < 3.2$. In the region $|\eta| < 1.8$, a pre-sampler detector using a thin layer of LAr is used to correct for the energy loss by electrons and photons upstream of the calorimeter. The hadronic

¹ The ATLAS experiment uses a right-handed coordinate system with its origin at the nominal interaction point (IP) in the centre of the detector. The x -axis points from the IP to the centre of the LHC ring, the y -axis points upward, and the z -axis is along one of the proton beam directions. Cylindrical coordinates (r, ϕ) are used in the transverse plane, ϕ being the azimuthal angle around the beam pipe. The pseudorapidity is defined in terms of the polar angle θ as $\eta = -\ln \tan(\theta/2)$. Transverse momentum (p_T) is defined relative to the beam axis and is calculated as $p_T = p \sin \theta$ where p is the momentum.

* e-mail: atlas.publications@cern.ch

tile calorimeter ($|\eta| < 1.7$) consists of steel absorbers and scintillating tiles and is located directly outside the envelope of the barrel electromagnetic calorimeter. The endcap hadronic calorimeters use LAr as active material, with copper as absorber material, while the forward calorimeters use LAr as active material, with copper absorber for the first layer, dedicated to electromagnetic measurements, and tungsten for other layers, dedicated to hadronic measurements. The MS is composed of three large superconducting air-core toroidal magnets, a system of three stations of tracking chambers in the range $|\eta| < 2.7$, and a muon trigger system in the range $|\eta| < 2.4$. The precision muon momentum measurement is performed by monitored drift tubes everywhere except in the innermost layer for the range $|\eta| > 2.0$ where cathode strip chambers are used instead. The muon trigger system is composed of resistive plate chambers in the barrel region ($|\eta| < 1.05$) and thin gap chambers in the endcap region ($1.05 < |\eta| < 2.4$).

The ATLAS trigger system has three distinct levels referred to as L1, L2, and the event filter. Each trigger level refines the decisions made at the previous level. The L1 trigger is implemented in hardware and uses a subset of detector information to reduce the event rate to a design value of at most 75 kHz. The L2 and event filter are software-based trigger levels and together reduce the event rate to about 400 Hz.

Events used were selected by single-lepton triggers with a transverse momentum, p_T , threshold of 24 GeV for both muons and electrons, along with an isolation requirement. The single-lepton triggers are complemented with triggers having a higher p_T threshold (60 GeV for electrons and 36 GeV for muons) and no isolation requirement in order to increase the acceptance at high p_T .

3 Object reconstruction and event selection

Each event is required to have at least one primary vertex reconstructed from at least three tracks with $p_T > 400$ MeV. If there are multiple primary vertices reconstructed in the event due to additional pp interactions (pile-up) in the same or a neighbouring bunch crossing, the vertex with the highest $\sum p_T^2$, calculated using all associated tracks, is taken as the primary collision vertex. The mean number of interactions per bunch crossing in this data set is 20.7.

Electron candidates [20] are required to have $p_T > 20$ GeV and $|\eta| < 2.47$. Candidates within the transition region between the barrel and endcap calorimeters ($1.37 < |\eta| < 1.52$) are rejected. In addition, they must satisfy the *tight* quality definition described in Ref. [21]. Muon candidates are reconstructed by combining tracks in the ID with tracks in the MS and have $p_T > 20$ GeV and $|\eta| < 2.5$. The ID tracks associated with these muons must pass a number of quality requirements [22].

To ensure that lepton candidates originate from the primary vertex, a requirement is placed on the longitudinal impact parameter, z_0 , multiplied by the sine of the track polar angle, θ , such that the absolute value is smaller than 0.5 mm ($|z_0 \times \sin \theta| < 0.5$ mm). A requirement is also placed on the transverse impact parameter, d_0 , divided by its resolution (σ_{d_0}), such that $|d_0/\sigma_{d_0}| < 3$. To suppress the contribution from hadronic jets which are misidentified as leptons, signal leptons are required to be isolated in both the ID and the calorimeter. The calorimeter isolation is defined as $E_T^{\text{Cone}X}/E_T$ whereas the ID isolation is defined as $p_T^{\text{Cone}X}/p_T$, where $E_T^{\text{Cone}X}$ ($p_T^{\text{Cone}X}$) is the transverse energy (momentum) deposited in the calorimeter (the scalar sum of the p_T of tracks with $p_T > 1$ GeV) within a cone of size $\Delta R = \sqrt{(\Delta\eta)^2 + (\Delta\phi)^2} = X$ around the lepton. The transverse momentum from the lepton itself is excluded in the calculations of $E_T^{\text{Cone}X}$ and $p_T^{\text{Cone}X}$. Different lepton isolation criteria are applied in the two channels to maximize the signal efficiency while suppressing the backgrounds. In the $\ell\nu\ell\nu\ell\nu$ channel, $E_T^{\text{Cone}0.2}/E_T < 0.1$ and $p_T^{\text{Cone}0.2}/p_T < 0.04$ are required for both the electrons and muons; in the $\ell\nu\ell\nu jj$ channel, $E_T^{\text{Cone}0.3}/E_T < 0.14$ and $p_T^{\text{Cone}0.3}/p_T < 0.06$ are required for electrons whereas $E_T^{\text{Cone}0.3}/E_T < 0.07$ and $p_T^{\text{Cone}0.3}/p_T < 0.07$ are required for muons.

Jets are reconstructed from clusters of energy in the calorimeter using the anti- k_t algorithm [23] with radius parameter $R = 0.4$. Jet energies are calibrated using energy- and η -dependent correction factors derived using Monte Carlo (MC) simulation and validated by studies of collision data [24]. For jets with $p_T < 50$ GeV and $|\eta| < 2.4$, at least 50% of the summed scalar p_T of the tracks within a cone of size $\Delta R = 0.4$ around the jet axis must originate from the primary vertex. This requirement reduces the number of jet candidates originating from pile-up vertices. Jets containing b -hadrons (“ b -jets”) with $|\eta| < 2.5$ and $p_T > 25$ GeV are identified using the impact parameter significance of tracks in the jet and secondary vertices reconstructed from these tracks [25, 26]. In the $\ell\nu\ell\nu\ell\nu$ and $\ell\nu\ell\nu jj$ channels, the efficiency of the b -tagging algorithm used is 85 and 70%, respectively.

The measurement of the two-dimensional missing transverse momentum vector, \vec{p}_T^{miss} , is based on the measurement of all topological clusters in the calorimeter and muon tracks reconstructed in the ID and MS [27]. Calorimeter cells associated with reconstructed objects, such as electrons, photons, hadronically decaying τ leptons, and jets, are calibrated at their own energy scale, whereas calorimeter cells not associated with any object are calibrated at the electromagnetic energy scale and taken into account as a so-called “soft term” in the calculation of \vec{p}_T^{miss} . The magnitude of the missing transverse momentum vector is referred to as the missing transverse energy, $E_T^{\text{miss}} = |\vec{p}_T^{\text{miss}}|$.

Table 1 Selection criteria for the $l\nu l\nu l\nu$ channel, split based on the number of SFOS lepton pairs: 0 SFOS, 1 SFOS, and 2 SFOS

$l\nu l\nu l\nu$	0 SFOS	1 SFOS	2 SFOS
Preselection	Exactly three charged leptons with $p_T > 20$ GeV		
E_T^{miss}	–	$E_T^{\text{miss}} > 45$ GeV	$E_T^{\text{miss}} > 55$ GeV
Same-flavour dilepton mass	$m_{\ell\ell} > 20$ GeV	–	–
Angle between tripleton and \vec{p}_T^{miss}	–	$ \phi^{3\ell} - \phi^{\vec{p}_T^{\text{miss}}} > 2.5$	–
Z boson veto	$ m_{ee} - m_Z > 15$ GeV	$m_Z - m_{\text{SFOS}} > 35$ GeV or $m_{\text{SFOS}} - m_Z > 20$ GeV	$ m_{\text{SFOS}} - m_Z > 20$ GeV
Jet veto	At most one jet with $p_T > 25$ GeV and $ \eta < 4.5$		
b -jet veto	No identified b -jets with $p_T > 25$ GeV and $ \eta < 2.5$		

The experimental signature of the $l\nu l\nu l\nu$ channel is the presence of three charged leptons and E_T^{miss} . The signature of the $l\nu l\nu jj$ channel is the presence of two same-charge leptons, E_T^{miss} , and two jets with an invariant mass close to 80 GeV. The selection requirements used to define the signal regions described in the following are obtained from a multi-dimensional optimization to maximize the sensitivity to the $W^\pm W^\pm W^\mp$ process and to reduce the contributions from SM background processes.

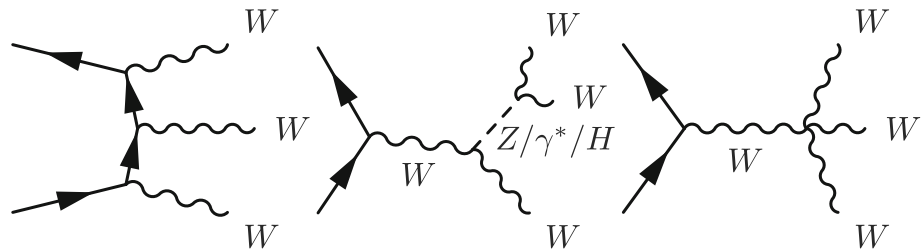
To select $l\nu l\nu l\nu$ candidates, events are required to have exactly three charged leptons with $p_T > 20$ GeV, at most one jet with $p_T > 25$ GeV and $|\eta| < 4.5$, and no identified b -jets. In addition, the absolute value of the azimuthal angle between the tripleton system and the \vec{p}_T^{miss} , $|\phi^{3\ell} - \phi^{\vec{p}_T^{\text{miss}}}|$, is required to be above 2.5. Eight different final states with equal production probability are considered based on the flavour and the charge of the leptons, namely $e^\pm e^\pm e^\mp$, $e^\pm e^\mp \mu^\pm$, $e^\pm e^\mp \mu^\mp$, $e^\pm e^\pm \mu^\mp$, $\mu^\pm \mu^\mp e^\pm$, $\mu^\pm \mu^\mp e^\mp$, $\mu^\pm \mu^\pm e^\mp$, and $\mu^\pm \mu^\pm \mu^\mp$. Three separate signal regions are defined based on the number of same-flavour opposite-sign (SFOS) lepton pairs in the event: 0 SFOS ($e^\pm e^\pm \mu^\mp$ and $\mu^\pm \mu^\pm e^\mp$), 1 SFOS ($e^\pm e^\mp \mu^\pm$, $e^\pm e^\mp \mu^\mp$, $\mu^\pm \mu^\mp e^\pm$, and $\mu^\pm \mu^\mp e^\mp$), and 2 SFOS ($e^\pm e^\pm e^\mp$ and $\mu^\pm \mu^\pm \mu^\mp$). In the 0-SFOS case, the invariant mass of the same-flavour lepton pair, $m_{\ell\ell}$, is required to be greater than 20 GeV. If there are at least two electrons in the event, the di-electron invariant mass, m_{ee} , is required to have $|m_{ee} - m_Z| > 15$ GeV, where m_Z is the pole mass of the Z boson [28]. No requirement is applied on the E_T^{miss} variable, as it was found to not discriminate between signal and backgrounds. In the 1-SFOS case, the SFOS dilepton invariant mass, m_{SFOS} , is required to be outside of the region $m_Z - 35$ GeV $< m_{\text{SFOS}} < m_Z + 20$ GeV. In addition, events are required to satisfy $E_T^{\text{miss}} > 45$ GeV. Finally,

in the 2-SFOS case, the SFOS dilepton invariant masses are required to have $|m_{\text{SFOS}} - m_Z| > 20$ GeV while the E_T^{miss} must be greater than 55 GeV. The selection criteria for m_{SFOS} and E_T^{miss} are mainly used to reduce the contributions from the Z+jets and WZ+jets processes. Table 1 shows the kinematic selection criteria used for the $l\nu l\nu l\nu$ channel.

To select $l\nu l\nu jj$ candidates, events are required to have exactly two leptons with the same electric charge, at least two jets, and no identified b -jets. Three different final states are considered based on the lepton flavour, namely $e^\pm e^\pm$, $e^\pm \mu^\pm$, and $\mu^\pm \mu^\pm$. The lepton p_T (E_T^{miss}) threshold is set to 30 (55) GeV to reduce the SM background contributions, though the E_T^{miss} criterion is not applied for the $\mu^\pm \mu^\pm$ final state due to the smaller Z+jets background expected in this channel. The leading (sub-leading) p_T jet must have $p_T > 30$ (20) GeV and $|\eta| < 2.5$. The two jets are required to have 65 GeV $< m_{jj} < 105$ GeV and $|\Delta\eta_{jj}| < 1.5$ in order to distinguish the signal from the $W^\pm W^\pm$ backgrounds, where m_{jj} is the dijet invariant mass and $\Delta\eta_{jj}$ is the pseudorapidity separation between the two jets. The dilepton system is required to have $m_{\ell\ell} > 40$ GeV and in the case of the $e^\pm e^\pm$ final state, m_{ee} must have $m_{ee} < 80$ GeV or $m_{ee} > 100$ GeV in order to suppress events with two opposite-sign prompt leptons where the charge of one of the electrons is misidentified. To reduce the contributions from WZ+jets and ZZ+jets production, events are removed if they contain additional leptons reconstructed with $p_T > 6$ GeV passing looser identification quality requirements, with a *medium* identification requirement for electrons as defined in Ref. [21] and the minimum identification required for muon reconstruction. Table 2 shows the kinematic selection criteria used for the $l\nu l\nu jj$ channel.

Table 2 Selection criteria for the $\ell\nu\ell\nu jj$ channel, split based on the lepton flavour: $e^\pm e^\pm$, $e^\pm \mu^\pm$, and $\mu^\pm \mu^\pm$

$\ell\nu\ell\nu jj$	$e^\pm e^\pm$	$e^\pm \mu^\pm$	$\mu^\pm \mu^\pm$
Lepton	Exactly two same-charge leptons with $p_T > 30$ GeV		
Jets	At least two jets with $p_T(1) > 30$ GeV, $p_T(2) > 20$ GeV and $ \eta < 2.5$		
$m_{\ell\ell}$	$m_{\ell\ell} > 40$ GeV		
E_T^{miss}	$E_T^{\text{miss}} > 55$ GeV		
m_{jj}	$65 \text{ GeV} < m_{jj} < 105 \text{ GeV}$		
$\Delta\eta_{jj}$	$ \Delta\eta_{jj} < 1.5$		
Z boson veto	$m_{ee} < 80 \text{ GeV}$ or $m_{ee} > 100 \text{ GeV}$		
Third-lepton veto	No third lepton with $p_T > 6$ GeV and $ \eta < 2.5$ passing looser identification requirements		
b -jet veto	No identified b -jets with $p_T > 25$ GeV and $ \eta < 2.5$		

Fig. 1 Feynman graphs contributing at LO to $W^\pm W^\pm W^\mp$ production

4 Signal fiducial cross sections

At leading order (LO), the production of three W bosons can take place through radiation from a fermion, from an associated W and $Z/\gamma^*/H$ production with the intermediate $Z/\gamma^*/H$ boson decaying to two opposite-sign W bosons, or from a $WWWW$ QGC vertex. Representative Feynman graphs for each of these production processes are shown in Fig. 1. Calculations are available including corrections at next-to-leading order (NLO) in QCD with all spin correlations involved in the vector-boson decays, the effects due to intermediate Higgs boson exchange, and off-shell contributions correctly taken into account [29]. Electroweak NLO corrections have been calculated recently [30]. However, they are not considered in this analysis.

In order to determine $W^\pm W^\pm W^\mp$ production cross sections, events are generated at NLO in QCD using MADGRAPH5_aMC@NLO [31] including on-shell diagrams as well as Higgs associated diagrams. The CT10 NLO parton distribution function (PDF) [32] is used. Subsequent decays of unstable particles and parton showers are handled by PYTHIA8 [33]. Fiducial cross sections are calculated using the generator-level lepton, jet, and E_T^{miss} definitions as described in Ref. [34]. Generator-level prompt leptons (those not originating from hadron and τ lepton decays) are dressed with prompt photons within a cone of size $\Delta R = 0.1$. Generator-level jets are reconstructed by applying the anti- k_t algorithm with radius parameter $R = 0.4$ on all final-state particles after parton showering and hadronisation. The E_T^{miss} variable is calculated using all generator-level neutrinos. The

same kinematic selection criteria as listed in Tables 1 and 2 are applied on these objects, with the exception of the b -jet veto requirements in the $\ell\nu\ell\nu\ell\nu$ channel and the lepton quality requirements. To take into account the effect of the lepton isolation in the fiducial region, any lepton pairs must satisfy $\Delta R(\ell, \ell) > 0.1$, and in the $\ell\nu\ell\nu jj$ channel any lepton-jet pairs must satisfy $\Delta R(j, \ell) > 0.3$. Electrons or muons from τ decays are not included.

The fiducial cross section is predicted to be 309 ± 7 (stat.) ± 15 (PDF) ± 8 (scale) ab in the $\ell\nu\ell\nu\ell\nu$ channel and 286 ± 6 (stat.) ± 15 (PDF) ± 10 (scale) ab in the $\ell\nu\ell\nu jj$ channel. Uncertainties due to the PDFs are computed using an envelope of the CT10, NNPDF3.0 [35], and MSTW2008 [36] NLO PDF 68 or 90% (for CT10) confidence level (CL) uncertainties, following the recommendation of Ref. [37]. The renormalization and factorization scales are set to the invariant mass of the WWW system. Scale uncertainties are estimated by varying the two scales independently up and down by a factor of two and taking the largest variation from the nominal cross-section values.

In order to combine the measurements from the two decay channels, a common phase space is defined where each W boson can decay either leptonically (including τ leptons) or hadronically, $pp \rightarrow W^\pm W^\pm W^\mp + X$, with no kinematic requirements placed on the final-state leptons but with jets restricted to have $p_T > 10$ GeV. The extrapolation factor from the fiducial phase space to the total phase space is large, but it is mainly due to the well-known W boson decay branching ratios. The total cross section in this common phase space is 241.5 ± 0.1 (stat.) ± 10.3 (PDF) ± 6.3 (scale) fb.

In order to determine the detector reconstruction effects on the signal selection, $W^\pm W^\pm W^\mp$ signal samples are generated with VBFNLO [29,38–40] at LO. The parton shower and hadronisation are performed by PYTHIA8. The fiducial cross sections are seen to be consistent between VBFNLO and MADGRAPH5_aMC@NLO when computed at the same order. The VBFNLO LO fiducial cross sections are normalized to the NLO fiducial cross section predicted by MADGRAPH5_aMC@NLO for the signal yield calculations. These events are processed through the full ATLAS detector simulation [41] based on GEANT 4 [42]. To simulate the effect of multiple pp interactions occurring during the same or a neighbouring bunch crossing, minimum-bias interactions are generated and overlaid on the hard-scattering process. These events are then processed through the same object reconstruction and identification algorithms as used on data. MC events are reweighted so that the pile-up conditions in the simulation match the data. Additional corrections are made to the simulated samples to account for small differences between the simulation and the data for the object identification and reconstruction efficiencies, the trigger efficiencies, and the energy and momentum scales and resolutions. While excluded in the fiducial cross-section definition, the contribution from events with $W \rightarrow \tau\nu \rightarrow \ell\nu\nu\nu$ decays are counted as signal in the VBFNLO signal sample used in the final event selection. These events contribute up to 20% of the predicted signal yield. This approach is used to ease comparisons of the obtained cross-section limits with alternative cross-section predictions that may not simulate tau decays.

5 Backgrounds

5.1 Background estimation

The SM processes that mimic the $W^\pm W^\pm W^\mp$ signal signature can be grouped into five categories:

- The WZ/γ^*+jets process that produces three prompt leptons or two prompt leptons with the same electric charge (referred to as “ WZ background”);
- The $W\gamma+jets$ or $Z\gamma+jets$ processes where the photon is misreconstructed as a lepton (referred to as “ $V\gamma$ background”, where $V = W, Z$);
- Processes other than WZ/γ^*+jets that produce three prompt leptons or two prompt leptons with the same electric charge (referred to as “other prompt background”);
- Processes that produce two or three prompt charged leptons, but the charge of one lepton is misidentified (referred to as “charge-flip background”);
- Processes that have one or two non-prompt leptons originating either from misidentified jets or from hadronic decays (referred to as “fake-lepton background”).

The dominant irreducible background originates from the $WZ(\rightarrow \ell^\pm\nu\ell^\pm\ell^\mp)+jets$ process and is estimated using simulated events. In the $\ell\nu\ell\nu\ell\nu$ channel these events are generated with POWHEG-BOX [43–46] and hadronised with PYTHIA8 and in the $\ell\nu\ell\nu jj$ channel they are generated with SHERPA [47]. In the $\ell\nu\ell\nu\ell\nu$ channel, the inclusive $WZ+jets$ cross section is normalized using a scale factor (1.08 ± 0.10) derived from a WZ -enriched region in data. This region is obtained by requiring exactly one SFOS lepton pair with $|m_{SFOS} - m_Z| < 15$ GeV. In the $\ell\nu\ell\nu jj$ channel, the cross section is normalized to the NLO calculation in QCD from VBFNLO [48] in the specified fiducial phase space with a normalization factor of 1.04 ± 0.09 .

The $V\gamma$ background contributes when the photon is misidentified as an electron. In the $\ell\nu\ell\nu\ell\nu$ channel, this originates primarily from the $Z\gamma$ process and its contribution is estimated using events generated with SHERPA. In the $\ell\nu\ell\nu jj$ channel, this comes primarily from electroweak and strong production of $W\gamma jj$ events. Strong production of $W\gamma jj$ [49] is estimated using ALPGEN [50] interfaced to HERWIG [51] and JIMMY [52] for simulation of the parton shower, fragmentation, hadronisation and the underlying event. The electroweak production of $W\gamma jj$ [53] is modelled using SHERPA.

Other SM processes that produce multiple prompt leptons include $ZZ, t\bar{t}V, ZWW, ZZZ, W^\pm W^\pm jj$ production, and double parton scattering processes. The production of ZZ is modelled with POWHEG-BOX [46] and hadronised with PYTHIA8 in the $\ell\nu\ell\nu\ell\nu$ channel and is modelled with SHERPA in the $\ell\nu\ell\nu jj$ channel. The $t\bar{t}V$ [54], ZWW [55], and ZZZ [55] processes are modelled using MADGRAPH5_aMC@NLO together with PYTHIA8 for both channels. The non-resonant $W^\pm W^\pm jj$ background [56] is only important for the $\ell\nu\ell\nu jj$ channel and its contribution is estimated using SHERPA. Contributions from double parton scattering processes are found to be negligible in both channels.

The charge-flip background originates from processes where the charge of at least one prompt lepton is misidentified. This occurs primarily when a lepton from a hard bremsstrahlung photon conversion is recorded instead of the signal lepton. It mainly contributes to the 0-SFOS signal region in the $\ell\nu\ell\nu\ell\nu$ channel and the $e^\pm e^\pm / e^\pm \mu^\pm$ signal regions in the $\ell\nu\ell\nu jj$ channel. The electron charge misidentification rate is measured using $Z \rightarrow e^+e^-$ events. In the $\ell\nu\ell\nu\ell\nu$ channel, the charge-flip background is estimated by using these rates to re-weight the MC estimate of WZ and ZZ events based on the probability for opposite-sign events of this kind to migrate into the 0-SFOS category. In the $\ell\nu\ell\nu jj$ channel, the background is estimated by applying these rates on data events satisfying all signal selection criteria except the two leptons are required to have opposite-sign.

Contributions from fake-lepton backgrounds are estimated in data, using different approaches in the two chan-

Table 3 Expected numbers of signal and background events in the VRs compared to the numbers of events observed in data. The first uncertainty is statistical and the second is systematic

Validation region	Signal	Background	Observed
<i>ℓνℓνℓν</i>			
Preselection	$9.78 \pm 0.04 \pm 0.45$	$2392 \pm 7 \pm 298$	2472
Fake-lepton	$0.15 \pm 0.01 \pm 0.02$	$15 \pm 1 \pm 10$	18
$Z\gamma$	$0.32 \pm 0.01 \pm 0.02$	$119 \pm 3 \pm 20$	119
<i>ℓνℓνjj</i>			
Charge-flip	$0.98 \pm 0.04 \pm 0.06$	$21 \pm 1 \pm 2$	22
$WZ + 2$ -jets	$0.55 \pm 0.03 \pm 0.04$	$52 \pm 1 \pm 10$	56
b -tagged	$1.00 \pm 0.05 \pm 0.07$	$69 \pm 1 \pm 23$	78
W mass sideband	$3.35 \pm 0.08 \pm 0.43$	$48 \pm 2 \pm 6$	53
≤ 1 jet	$1.62 \pm 0.06 \pm 0.40$	$139 \pm 3 \pm 18$	145

nels. In the $\ell\nu\ell\nu\ell\nu$ channel, the probabilities of prompt leptons or non-prompt leptons to satisfy the signal lepton criteria are computed using a tag-and-probe method whereby a well-reconstructed “tag” lepton is used to identify the event and a second “probe” lepton is used to study the probabilities without bias. A tag lepton must satisfy the signal lepton requirements while a looser lepton selection criterion is defined for probe leptons with the lepton isolation requirements removed and the electron quality requirement loosened to *medium* as defined in Ref. [21]. The probability for a prompt lepton to satisfy the signal lepton criteria is estimated using $Z \rightarrow \ell^+\ell^-$ events with the tag-and-probe lepton pair required to have the same-flavour, opposite-sign and an invariant mass within 10 GeV of the pole mass of the Z boson. The probability for a non-prompt lepton from hadronic activity to satisfy the signal lepton requirement is estimated using the tag-and-probe method in a W +jets-enriched region with $E_T^{\text{miss}} > 10$ GeV, the tag lepton is a muon with $p_T > 40$ GeV, and the tag and probe leptons have the same electric charge. The probabilities are calculated separately for electrons and muons. A loosely identified set of data is also selected by requiring at least three loose leptons as defined above. This set of data, along with these probabilities are then used to estimate the background in the signal region with the matrix method [57].

In the $\ell\nu\ell\nu jj$ channel, events that contain one signal lepton and one “lepton-like” jet are selected. A “lepton-like” jet satisfies all signal lepton selection criteria except that the isolation requirements are $0.14 < E_T^{\text{Cone}0.3}/p_T < 2$ and $0.06 < p_T^{\text{Cone}0.3}/p_T < 2$ for electrons, and $0.07 < E_T^{\text{Cone}0.3}/p_T < 2$ and $0.07 < p_T^{\text{Cone}0.3}/p_T < 2$ for muons. In addition, the $|d_0/\sigma_{d_0}|$ and $|z_0 \times \sin\theta|$ selection criteria are loosened to 10 mm and 5 mm, respectively. These events are dominated by non-prompt leptons and are scaled by a fake factor to estimate the non-prompt background. The fake factor is the ratio of the number of jets satisfying the signal lepton identification criteria to the number of jets satisfying the “lepton-like” jet criteria. It is measured as a function of the jet p_T and η from a dijet-enriched sample selected by

requiring a lepton back-to-back with a jet ($\Delta\phi_{j\ell} > 2.8$) and $E_T^{\text{miss}} < 40$ GeV.

5.2 Validation of background estimates

The background predictions are tested in several validation regions (VRs). These VRs are defined to be close to the signal region with a few selection criteria removed or inverted. They generally have dominant contributions from one or two background sources and a negligible contribution from the signal process. The signal and background predictions are compared to data for each VR in Table 3.

In the $\ell\nu\ell\nu\ell\nu$ channel, three VRs are considered. The first VR, called the pre-selection region, tests the modelling of the WZ +jets background by requiring exactly three signal leptons. The distribution of the trilepton transverse mass, $m_T^{3\ell} = \sqrt{2p_T^{3\ell} E_T^{\text{miss}} (1 - \cos(\phi^{3\ell} - \phi^{\vec{p}_T^{\text{miss}}}))}$ where $p_T^{3\ell}$ is the p_T of the trilepton system, is shown at the top left of Fig. 2. This VR includes the three signal regions (0, 1, and 2 SFOS), but the effect of the signal is considered negligible at this stage of the selection, as shown in Table 3. The WZ +jets purity is estimated to be around 70% in this region. The second region, called the fake-lepton region, tests the modelling of the fake-lepton background by requiring exactly three signal leptons with no SFOS lepton pairs and at least one b -jet. The distribution of the jet multiplicity, N_{jet} , is shown at the top right of Fig. 2. The purity of the fake-lepton background is estimated to be around 80% in this region. The third region, called $Z\gamma$ region, tests the modelling of the $Z\gamma$ background by requiring the presence of only $\mu^+\mu^-e^\pm$ events where the trilepton invariant mass is close to the Z resonance peak. This restricts the main contributions to originate from the $Z\gamma \rightarrow \mu^+\mu^-\gamma$ and $Z \rightarrow \mu^+\mu^- \rightarrow \mu^+\mu^-\gamma$ processes. The $Z\gamma$ purity is estimated to be around 70% in this region. The data are seen to be well described by the background in all three VRs.

In the $\ell\nu\ell\nu jj$ channel, five VRs are considered. The modelling of the charge-flip background is tested using $e^\pm e^\pm$ events with $80 \text{ GeV} < m_{\ell\ell} < 100 \text{ GeV}$. The purity of the

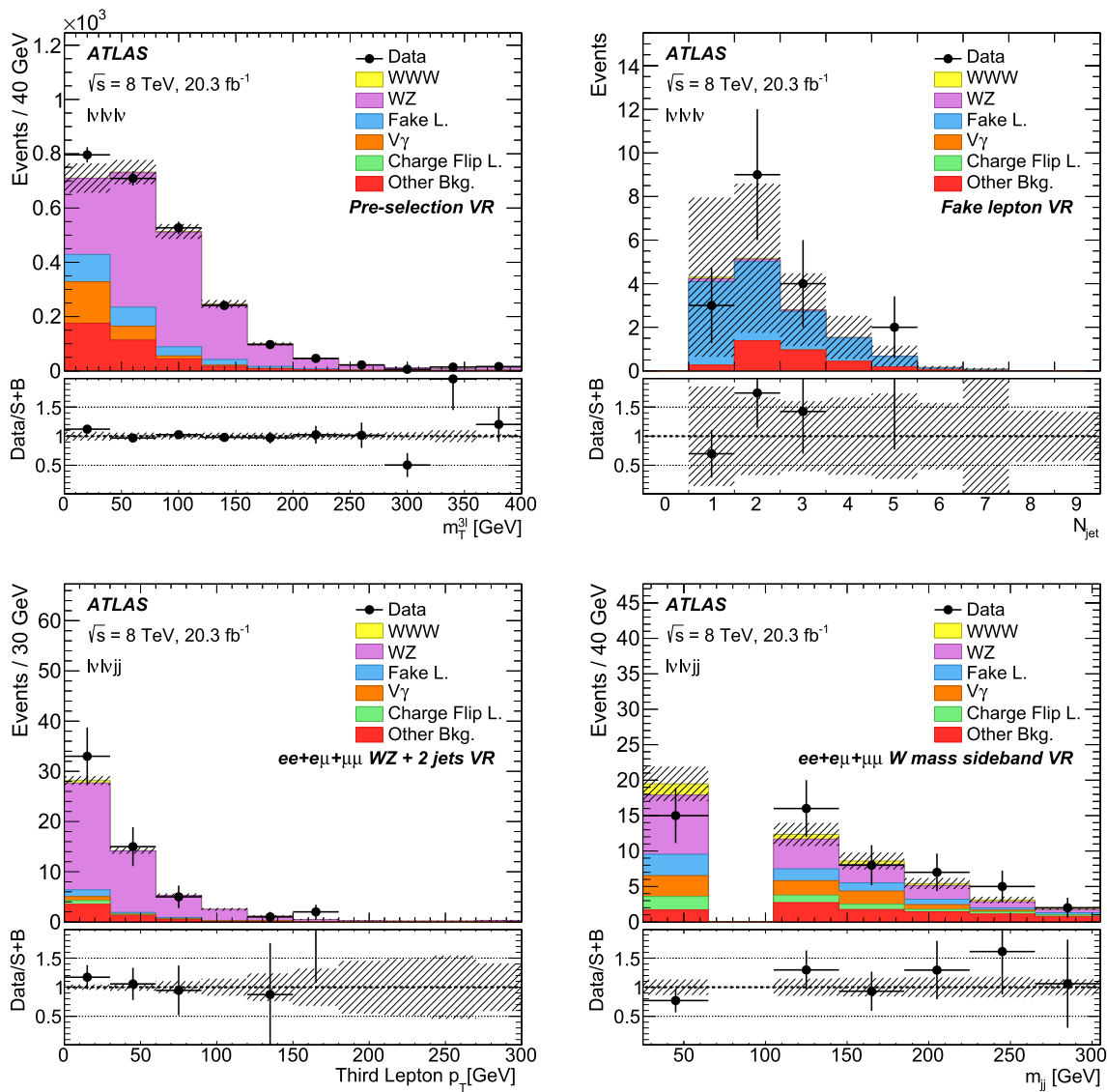


Fig. 2 Distributions in four different VRs, two corresponding to the $l\nu l\nu l\nu$ channel (top) and two to the $l\nu l\nu jj$ channel (bottom). For the $l\nu l\nu l\nu$ channel the m_T^{3l} distribution in the preselection region (top left) and the jet multiplicity distribution in the fake-lepton region (top right) are shown. For the $l\nu l\nu jj$ channel the third-lepton p_T in the $WZ + 2$ -

jets region (bottom left) and the m_{jj} distribution in the W mass sideband region (bottom right) are shown. The “other backgrounds” contain prompt leptons and are estimated from MC. The hashed band represents total uncertainties on the signal-plus-background prediction. The highest bin also includes events falling out of the range shown

charge-flip background is estimated to be around 80% in this region. The modelling of the $WZ + 2$ -jets background is checked in a $WZ + 2$ -jets region requiring the presence of an additional lepton. The p_T of this third lepton is shown at the bottom left of Fig. 2. The purity of the $WZ + 2$ -jets is estimated to be around 60% in this region. The modelling of backgrounds from non-prompt leptons is tested in a b -tagged region that requires at least one b -jet. The purity of the non-prompt lepton background is estimated to be around 80% in this region. The m_{jj} modelling is checked by examining events with masses m_{jj} in the regions $m_{jj} < 65$ GeV or $m_{jj} > 105$ GeV. The distribution of m_{jj} in this region is

shown at the bottom right of Fig. 2. Finally, conversion and prompt backgrounds are tested in a region with at most one jet, called the ≤ 1 jet region. The purity of the conversion and prompt backgrounds is estimated to be around 70% in this region. As for the $l\nu l\nu l\nu$ channel, good agreement is observed between the data and the prediction in all five VRs.

6 Systematic uncertainties

Systematic uncertainties in the signal and background predictions arise from the measurement of the integrated lumi-

Table 4 The effect of the various systematic uncertainties on the total signal and background yields (in percent) for both channels

Source of uncertainty	$l\nu l\nu l\nu$		$l\nu l\nu jj$	
	Signal (%)	Background (%)	Signal (%)	Background (%)
Lepton ID, E_T/p_T scale and resolution	1.6	1.8	2.1	3.3
E_T^{miss} modelling	1.1	1.4	0.7	1.8
b -jet identification	0.3	0.3	2.2	2.2
Jet E_T scale and resolution	2.3	2.8	21	15
Fake-lepton background	0	13	0	8
Charge-flip background	0	0.04	0	2.2
Luminosity	1.9	1.6	1.9	1.4
Pile-up estimate	1.1	0.6	0.6	1.6
Trigger efficiency	0.1	0.1	0.1	0.01
Normalization factor	3.8	8	6.0	13
Statistical	1.2	3.2	2.7	5.1

osity, from the experimental and theoretical modelling of the signal acceptance and detection efficiency, and from the background estimation. The effect of the systematic uncertainties on the overall signal and background yields are evaluated separately for the $l\nu l\nu l\nu$ and $l\nu l\nu jj$ channels. The results are summarised in Table 4. The systematic uncertainties are included as nuisance parameters in the profile likelihood described in Sect. 7. Correlations of systematic uncertainties arising from common sources are maintained across signal and background processes and channels.

The experimental uncertainties include the uncertainties on the lepton and jet energy and momentum scales and resolutions, on the efficiencies of the lepton and jet reconstruction and identification, and on the modelling of E_T^{miss} and b -jets. They are evaluated separately for both the signal and background estimations. For the expected signal yield, the major contributions in the $l\nu l\nu l\nu$ channel come from uncertainties in the lepton reconstruction and identification efficiencies as well as lepton energy/momentum resolution and scale modelling ($\pm 1.6\%$), E_T^{miss} modelling ($\pm 1.1\%$), and jet energy scale and resolution ($\pm 2.3\%$). The contributions in the $l\nu l\nu jj$ channel come from uncertainties in the lepton efficiencies and energy/momentum modelling ($\pm 2.1\%$), E_T^{miss} modelling ($\pm 0.7\%$), b -jet identification ($\pm 2.2\%$), and jet energy resolution and scale modelling ($\pm 21\%$). Larger systematic uncertainties due to the jet energy scale and resolution are expected in the $l\nu l\nu jj$ channel due to the dijet requirements, in particular in the dijet invariant mass. For the background yields estimated from MC simulation, the major contributions in the $l\nu l\nu l\nu$ channel come from uncertainties in lepton reconstruction and identification efficiencies ($\pm 1.8\%$), E_T^{miss} modelling ($\pm 1.4\%$), and jet energy modelling ($\pm 2.8\%$). The major contributions in the $l\nu l\nu jj$ channel come from uncertainties in lepton efficiencies and energy

modelling ($\pm 3.3\%$), E_T^{miss} modelling ($\pm 1.8\%$), b -jet identification ($\pm 2.2\%$), and jet energy modelling ($\pm 15\%$).

The estimates of the data-driven fake-lepton background also have uncertainties specific to each channel. In the $l\nu l\nu l\nu$ channel, the systematic uncertainty results from the uncertainties on the probabilities of candidate leptons that satisfy the looser lepton selection criteria to also satisfy the signal lepton selection criteria. For prompt leptons this uncertainty is $\pm(5$ to $10)\%$ while for fake leptons and misidentified/non-prompt leptons this uncertainty is $\pm(80$ to $90)\%$. The latter uncertainty is a conservative estimate which accounts for differences in the heavy-flavour and light-flavour composition between the signal region and the control region where the fake-lepton efficiency is determined for these leptons. In the $l\nu l\nu jj$ channel, the systematic uncertainty results from the uncertainties in the measurement of the fake factors, which is estimated to be $\pm(20$ to $30)\%$. Statistical uncertainties in the samples used for the matrix method and the fake-factor method also contribute to the overall uncertainty of the estimation of the fake-lepton background. The total uncertainty in the overall fake-lepton background yield is $\pm 13\%$ in the $l\nu l\nu l\nu$ channel and $\pm 8\%$ in the $l\nu l\nu jj$ channel.

The charge-flip background is only relevant for the $e^\pm e^\pm / e^\pm \mu^\pm$ final state in the $l\nu l\nu jj$ channel and for the 0-SFOS region in the $l\nu l\nu l\nu$ channel. Its uncertainty is dominated by the statistical precision with which the electron charge misidentification rate is determined from the available data. Since the charge-flip background estimation uses the number of $Z(\rightarrow e^+e^-) + 2$ jets events, the number of events in the data also contributes to the overall systematic uncertainty. In the $l\nu l\nu l\nu$ channel, the uncertainty on the charge-flip background estimate is $\pm 0.5\%$ in the 0-SFOS region but is $\pm 0.04\%$ for the total background estimate in all three signal regions. In the $l\nu l\nu jj$ channel, the total system-

Table 5 Numbers of expected signal and background events, and their statistical and systematic uncertainties, together with the observed yields in the data in the signal regions for the two channels

$lv\ell\nu\ell\nu$	0 SFOS				1 SFOS				2 SFOS						
$W^\pm W^\pm W^\mp$ signal	1.34	\pm	0.02	\pm	0.07	1.39	\pm	0.02	\pm	0.08	0.61	\pm	0.01	\pm	0.03
WZ	0.59	\pm	0.00	\pm	0.07	11.9	\pm	0.1	\pm	1.3	9.1	\pm	0.1	\pm	1.0
Other prompt background	0.21	\pm	0.01	\pm	0.02	0.78	\pm	0.02	\pm	0.11	0.60	\pm	0.02	\pm	0.10
Charge-flip background	0.04	\pm	0.00	\pm	0.01	–					–				
$V\gamma$	–					0.20	\pm	0.13	\pm	0.29	0.11	\pm	0.10	\pm	0.29
Fake-lepton background	1.5	\pm	0.3	\pm	1.4	1.9	\pm	0.3	\pm	1.9	0.49	\pm	0.16	\pm	0.47
Total background	2.4	\pm	0.3	\pm	1.4	14.8	\pm	0.4	\pm	2.3	10.3	\pm	0.2	\pm	1.2
Signal + background	3.7	\pm	0.3	\pm	1.4	16.2	\pm	0.4	\pm	2.3	10.9	\pm	0.2	\pm	1.2
Data	5				13				6						
$lv\ell\nu jj$	$e^\pm e^\pm$				$e^\pm \mu^\pm$				$\mu^\pm \mu^\pm$						
$W^\pm W^\pm W^\mp$ signal	0.46	\pm	0.03	\pm	0.07	1.35	\pm	0.05	\pm	0.19	1.65	\pm	0.06	\pm	0.30
WZ	0.74	\pm	0.13	\pm	0.44	2.77	\pm	0.27	\pm	0.66	3.28	\pm	0.29	\pm	0.71
Other prompt background	0.46	\pm	0.05	\pm	0.16	1.33	\pm	0.10	\pm	0.38	1.33	\pm	0.15	\pm	0.38
Charge-flip background	1.13	\pm	0.13	\pm	0.24	0.74	\pm	0.08	\pm	0.16	–				
$V\gamma$	0.75	\pm	0.35	\pm	0.21	2.5	\pm	0.7	\pm	0.7	–				
Fake-lepton background	0.96	\pm	0.15	\pm	0.39	2.04	\pm	0.22	\pm	0.89	0.43	\pm	0.06	\pm	0.25
Total background	4.0	\pm	0.4	\pm	0.7	9.4	\pm	0.8	\pm	1.4	5.0	\pm	0.3	\pm	0.8
Signal + background	4.5	\pm	0.4	\pm	0.7	10.7	\pm	0.8	\pm	1.4	6.7	\pm	0.3	\pm	0.9
Data	0				15				6						

atic uncertainty in the overall background yield due to the uncertainty in the charge-flip background estimate is found to be $\pm 2.2\%$.

There are also uncertainties in the overall normalization of the signal and MC background cross sections. Uncertainties in the signal cross section are those described in Sect. 4. These are not, however, included as uncertainties in the model and merely serve as a comparison for the final measurement in Sect. 7. The normalizations of the SM background cross sections described in Sect. 5.1 have their own associated uncertainties. The uncertainty in the predicted WZ +jets background cross section is the most important one since it is the largest irreducible background. The size of the uncertainty relative to the predicted WZ +jets background is $\pm 10\%$ in the $lv\ell\nu\ell\nu$ channel and $\pm(16$ to $23)\%$ in the $lv\ell\nu jj$ channel depending on the production mechanism. This uncertainty is based on the measurement performed in the control region, for the $lv\ell\nu\ell\nu$ channel as described in Sect. 5, while it is a combination of the scale, PDF and parton shower uncertainties estimated as in Ref. [12], for the $lv\ell\nu jj$ channel. The remaining uncertainties are mostly negligible in the overall background prediction. The normalization uncertainty in the total background prediction is around $\pm 8\%$ in the $lv\ell\nu\ell\nu$ channel and $\pm 13\%$ in the $lv\ell\nu jj$ channel.

The uncertainty on the integrated luminosity is $\pm 1.9\%$, affecting the overall normalization of both the signal and background processes estimated from MC simulation. It is derived following the methodology detailed in Ref. [18]. The uncertainties associated with the pile-up reweighting of the events are estimated to be no more than $\pm 0.1\%$ for the signal and the backgrounds.

7 Cross-section measurement

The signal and background predictions together with their uncertainties are compared to the data for six signal regions in Table 5. The expected signal yields are calculated using the SM $W^\pm W^\pm W^\mp$ cross sections listed in Sect. 4. The expected numbers of signal plus background events are consistent with the numbers of events observed in data in all regions. Figure 3 shows the $m_T^{3\ell}$ distribution for the $lv\ell\nu\ell\nu$ channel and the distribution of the sum of the scalar p_T for all selected objects, $\Sigma p_T = p_T^{\ell,1} + p_T^{\ell,2} + p_T^{j,1} + p_T^{j,2} + E_T^{\text{miss}}$, for the $lv\ell\nu jj$ channel, after summing over the three signal regions in each channel. Good agreement between data and the signal-plus-background model is observed for both distributions.

The amount of $W^\pm W^\pm W^\mp$ signal in the selected data set is determined using the numbers of expected signal

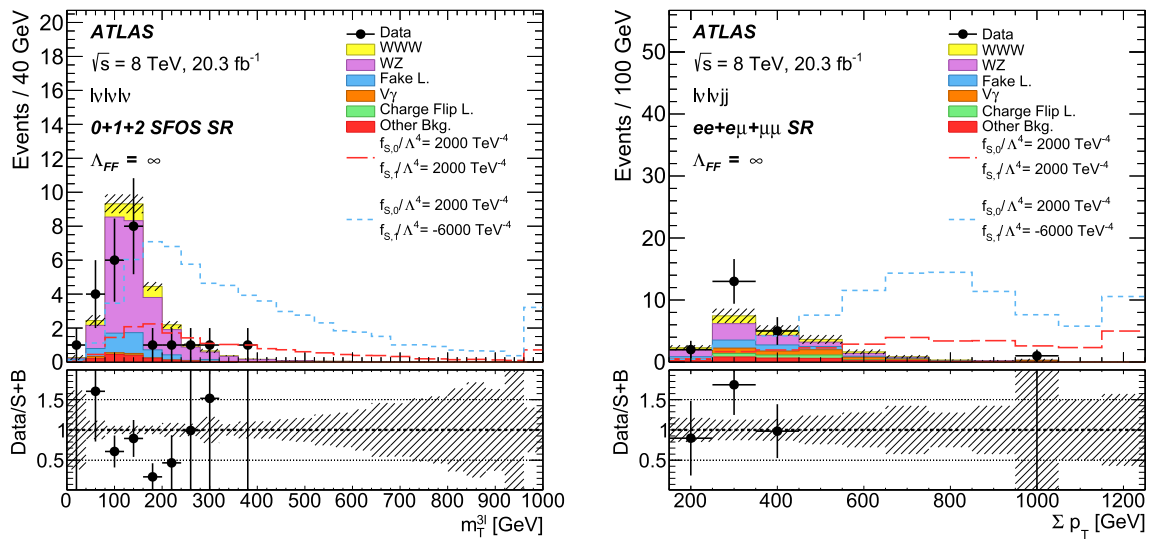


Fig. 3 The distribution of $m_T^{3\ell}$ for the $l\nu l\nu l\nu$ channel (left) and the distribution of Σp_T for the $l\nu l\nu jj$ channel (right) as observed in the data (dots with error bars indicating the statistical uncertainties) and as expected from SM signal and background processes. The ratios between the observed numbers of events in data and the expected SM signal plus background contributions are shown in the lower panels. The hashed bands results from the systematic uncertainties on the

and background events as well the numbers of observed events in the data. The signal strength, μ , is the parameter of interest, defined as a scale factor multiplying the cross section times branching ratio predicted by the SM. A test statistic based on the profile-likelihood ratio [58] is used to extract μ from a maximum-likelihood fit of the signal-plus-background model to the data. The likelihood, \mathcal{L} , is given by

$$\mathcal{L} = \prod_c \prod_i \text{Poisson} \left[n_{i_c}^{\text{obs}} \mid \mu \times n_{i_c}^{\text{sig,SM}}(\theta_k) + n_{i_c}^{\text{bkg}}(\theta_k) \right] \times \prod_k g(\theta_k) \tag{1}$$

where the index c represents one of the two analysis channels, i represents one of the three signal regions in each channel, n^{obs} is number of observed events, $n^{\text{sig,SM}}$ is the expected number of signal events based on the SM calculations, and n^{bkg} is the expected number of background events. The effect of a systematic uncertainty k on the likelihood is modelled with a nuisance parameter, θ_k , constrained with a corresponding Gaussian probability density function $g(\theta_k)$.

The test statistic, t_μ , is defined as

$$t_\mu = -2 \ln \lambda(\mu) = -2 \ln \frac{\mathcal{L}(\mu, \hat{\theta}(\mu))}{\mathcal{L}(\hat{\mu}, \hat{\theta})} \tag{2}$$

where $\hat{\mu}$ is the unconditional maximum-likelihood (ML) estimators of the independent signal strength in the categories

being compared, $\hat{\theta}$ are the unconditional ML estimators of the nuisance parameters, and $\hat{\theta}(\mu)$ are the conditional ML estimators of θ for a given value of μ . The significance of μ is obtained with the above test statistic, and is estimated using 100,000 MC pseudo-experiments to determine how well the fit result agrees with the background-only hypothesis. The observed (expected) significance of a positive signal cross section is 0.96σ (1.05σ) for the combination of the two channels. Most of the sensitivity comes from the 0-SFOS category in the $l\nu l\nu l\nu$ channel and the $\mu^\pm \mu^\pm$ category in the $l\nu l\nu jj$ channel. The most significant deviation from the signal-plus-background hypothesis occurs in the $e^\pm e^\pm$ region, where zero events are observed and 4.0 background and 0.46 signal events are expected. The probability that the background fluctuates down to zero events is 2.3%.

The central value of μ corresponds to the minimum of the negative log-likelihood distribution. The measured fiducial cross section in each channel is obtained by multiplying μ by the expected value of the fiducial cross section in that channel. The measured total cross section is obtained by combining the results for the two channels and then extrapolating to the total phase space using the signal acceptance. The log-likelihood scans for the total cross-section measurement are evaluated with and without systematic uncertainties and are shown in Fig. 4. The expected and observed fiducial and total cross sections are summarized in Table 6.

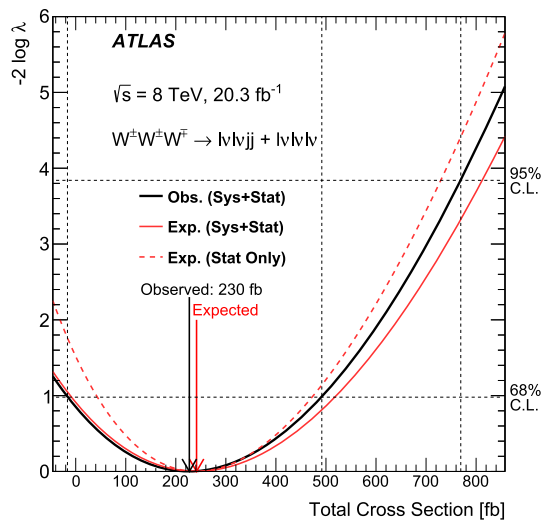


Fig. 4 Profile-likelihood scans as a function of the total cross section for the combination of all six signal regions. The expected (red) scans are shown when considering only statistical uncertainties (dashed line) and when considering both statistical and systematic uncertainties (solid line). The observed (black solid line) scan is also shown. The dotted black grid-lines pinpoint the location of the 68 and 95% CL uncertainties in the measurement of the signal strength

The presence of the $W^\pm W^\pm W^\mp$ signal is also assessed using a one-sided 95% CL upper limit on the production cross section using the CL_s method of Ref. [59]. The limits are evaluated using 2000 MC pseudo-experiments. The observed (expected) upper limit on the fiducial cross section in the absence of $W^\pm W^\pm W^\mp$ production is found to be 1.3 fb (1.1 fb) in the $\ell\nu\ell\nu\ell\nu$ channel and 1.1 fb (0.9 fb) in the $\ell\nu\ell\nu jj$ channel. The observed (expected) upper limit in the absence of $W^\pm W^\pm W^\mp$ production on the total cross section is 730 fb (560 fb) when the two channels are combined. If the SM $W^\pm W^\pm W^\mp$ signal is also considered, the expected upper limit on the total cross section is 850 fb.

8 Limits on anomalous quartic gauge couplings (aQGCs)

Contributions from sources beyond the SM to the $W^\pm W^\pm W^\mp$ production process can be expressed in a model-independent way using higher-dimensional operators leading to $W W W W$

aQGCs. The parameterization of aQGCs is based on Ref. [60] in a linear representation [61] considering only dimension-eight operators involving four gauge bosons. There are 18 dimension-eight operators built from the covariant derivative of the Higgs field $D_\mu \Phi$, the $SU(2)_L$ field strength $W_{\mu\nu}^i$, and $U(1)_Y$ field strength $B_{\mu\nu}$. Only the two terms built exclusively from $D_\mu \Phi$ and with aQGC parameters $f_{S,0}/\Lambda^4$ and $f_{S,1}/\Lambda^4$ are considered in this analysis:

$$\mathcal{L}_{S,0} = \frac{f_{S,0}}{\Lambda^4} [(D_\mu \Phi)^\dagger D_\nu \Phi] \times [(D^\mu \Phi)^\dagger D^\nu \Phi], \tag{3}$$

$$\mathcal{L}_{S,1} = \frac{f_{S,1}}{\Lambda^4} [(D_\mu \Phi)^\dagger D^\mu \Phi] \times [(D_\nu \Phi)^\dagger D^\nu \Phi], \tag{4}$$

where Λ is the energy scale of the new physics. These two operators only affect massive bosons and do not depend on the gauge boson momenta since no $SU(2)_L$ or $U(1)_Y$ field strengths are included. As a result, they are important for the study of longitudinal vector-boson scattering. Similar parameters were studied before by the ATLAS and CMS Collaborations in Refs. [8, 10, 16].

The effective Lagrangian approach leads to tree-level unitarity violation. This can be avoided by introducing a form factor [62] as

$$\alpha \rightarrow \frac{\alpha_0}{(1 + \hat{s}/\Lambda_{FF}^2)} \tag{5}$$

where α corresponds to one of the two couplings, α_0 is the value of the aQGC at low energy, \hat{s} is the square of the partonic centre-of-mass energy, and Λ_{FF} is the form-factor cut-off scale. However, there is no theoretical algorithm to predict for which form-factor cutoff scale the cross section would violate unitarity. Therefore different values of Λ_{FF} are considered with $\Lambda_{FF} = 0.5, 1, 2,$ and 3 TeV as well as $\Lambda_{FF} = \infty$, which corresponds to the non-unitarized case.

Events with aQGCs are generated with VBFNLO at LO and passed through the ATLAS detector simulation. A grid of samples is obtained using different parameters of $f_{S,0}/\Lambda^4$ and $f_{S,1}/\Lambda^4$ values. The interpolation between these points is performed with a 2-dimensional quadratic function in the $(f_{S,0}/\Lambda^4, f_{S,1}/\Lambda^4)$ space. The LO samples are scaled using

Table 6 The predicted and observed fiducial cross sections for the $\ell\nu\ell\nu\ell\nu$ and $\ell\nu\ell\nu jj$ channels and the predicted and observed total cross section for the combination of the two channels

	Cross section (fb)	
	Theory	Observed
Fiducial		
$\ell\nu\ell\nu\ell\nu$	0.309 ± 0.007 (stat.) ± 0.015 (PDF) ± 0.008 (scale)	$0.31^{+0.35}_{-0.33}$ (stat.) $^{+0.32}_{-0.35}$ (syst.)
$\ell\nu\ell\nu jj$	0.286 ± 0.006 (stat.) ± 0.015 (PDF) ± 0.010 (scale)	$0.24^{+0.39}_{-0.33}$ (stat.) $^{+0.19}_{-0.19}$ (syst.)
Total	241.5 ± 0.1 (stat.) ± 10.3 (PDF) ± 6.3 (scale)	230 ± 200 (stat.) $^{+150}_{-160}$ (syst.)

Table 7 Expected and observed 95% CI on $f_{S,0}/\Lambda^4$ ($f_{S,1}/\Lambda^4$) for different Λ_{FF} values, assuming $f_{S,1}/\Lambda^4$ ($f_{S,0}/\Lambda^4$) to be zero

Λ_{FF} (TeV)	Expected CI ($\times 10^4 \text{ TeV}^{-4}$)		Observed CI ($\times 10^4 \text{ TeV}^{-4}$)	
	$f_{S,0}/\Lambda^4$	$f_{S,1}/\Lambda^4$	$f_{S,0}/\Lambda^4$	$f_{S,1}/\Lambda^4$
0.5	[-0.79, 0.89]	[-1.06, 1.27]	[-0.74, 0.86]	[-0.99, 1.20]
1	[-0.36, 0.41]	[-0.52, 0.60]	[-0.34, 0.40]	[-0.48, 0.58]
2	[-0.22, 0.25]	[-0.33, 0.39]	[-0.20, 0.24]	[-0.29, 0.36]
3	[-0.19, 0.22]	[-0.29, 0.36]	[-0.16, 0.21]	[-0.25, 0.33]
∞	[-0.16, 0.19]	[-0.25, 0.30]	[-0.13, 0.18]	[-0.21, 0.27]

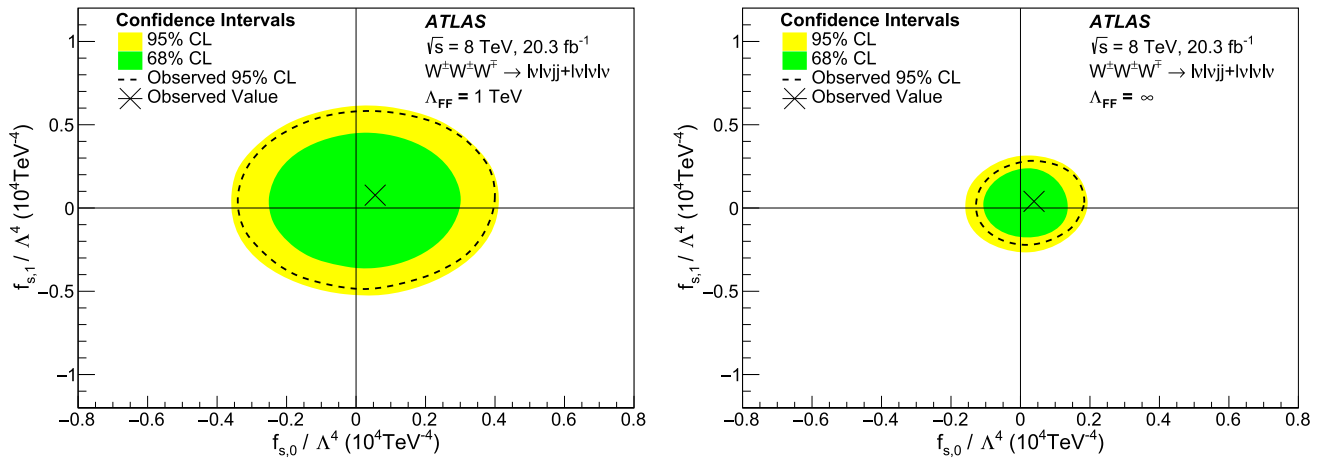


Fig. 5 Expected 68 and 95% CL contours for $f_{S,1}/\Lambda^4$ vs $f_{S,0}/\Lambda^4$ compared to the observed 95% CL contour and the observed best-fit value for cases when $\Lambda_{\text{FF}} = 1 \text{ TeV}$ (left) and $\Lambda_{\text{FF}} = \infty$ (right)

a factor derived from the ratio of the SM LO to NLO predictions. Figure 3 show the expected distribution for the non-unitarized ($\Lambda_{\text{FF}} = \infty$) aQGC signal samples being generated with parameters $f_{S,0}/\Lambda^4 = 2000 \text{ TeV}^{-4}$, $f_{S,1}/\Lambda^4 = 2000 \text{ TeV}^{-4}$ in red and parameters $f_{S,0}/\Lambda^4 = 2000 \text{ TeV}^{-4}$, $f_{S,1}/\Lambda^4 = -6000 \text{ TeV}^{-4}$ in blue as a function of the $m_T^{3\ell}$ distribution in the $\ell\nu\ell\nu\ell\nu$ channel and the Σp_T distribution in the $\ell\nu\ell\nu jj$ channel, summed over the three signal regions in each channel. Even though aQGC events tend to have leptons or jets with larger momenta, the detection efficiency for events in the fiducial region is found to be consistent with the one obtained for the SM sample within 20%. The efficiencies of the aQGC samples are used with their statistical and systematic uncertainties to derive the 95% confidence intervals (CI) on aQGC, while the largest observed deviation of the aQGC efficiencies from the SM one is used as an extra systematic uncertainty. Frequentist CI on the anomalous couplings are computed by forming a profile-likelihood-ratio test that incorporates the observed and expected numbers of signal events for different values of the anomalous couplings. Table 7 shows the expected and observed 95% CI on $f_{S,0}/\Lambda^4$ ($f_{S,1}/\Lambda^4$) with different Λ_{FF} values, assuming $f_{S,1}/\Lambda^4$ ($f_{S,0}/\Lambda^4$) to be zero. Figure 5 shows the two-dimensional 95% CL contour limits of $f_{S,0}/\Lambda^4$ vs $f_{S,1}/\Lambda^4$ in

the cases where $\Lambda_{\text{FF}} = 1 \text{ TeV}$ and $\Lambda_{\text{FF}} = \infty$. For $\Lambda_{\text{FF}} = \infty$, the limits can be compared to the stronger limits obtained by the CMS Collaboration in Ref. [16] in a different production channel. Other parameterization (α_4, α_5) of new physics have been introduced in Refs. [63–65]. The limits presented in this paper can be converted into limits on α_4 and α_5 following the formalism defined in the Appendix of Ref. [60] and using Equations (60) and (61) in Ref. [66]. For example, non-unitarized limits obtained for $\Lambda_{\text{FF}} = \infty$ are: α_4 expected [-0.61, 0.78], α_4 observed [-0.49, 0.75] and α_5 expected [-0.57, 0.69], α_5 observed [-0.48, 0.62]. Limits derived by the ATLAS Collaboration in other final states are reported in Refs. [8, 10]. The latter were obtained using a different unitarization scheme. Since that scheme is not applicable to tri-boson production, a combination of the limits is not possible.

9 Summary

A search for triboson $W^{\pm}W^{\pm}W^{\mp}$ production in two decay channels ($W^{\pm}W^{\pm}W^{\mp} \rightarrow \ell^{\pm}\nu\ell^{\pm}\nu\ell^{\mp}\nu$ and $W^{\pm}W^{\pm}W^{\mp} \rightarrow \ell^{\pm}\nu\ell^{\pm}\nu jj$ with $\ell = e, \mu$) is reported, using proton-proton collision data corresponding to an integrated luminosity of 20.3 fb^{-1} at a centre-of-mass energy of 8 TeV

collected by the ATLAS detector at the LHC. Events with exactly three charged leptons or two same-charge leptons in association with two jets are selected. The data are found to be in good agreement with the SM predictions in all signal regions. The observed 95% CL upper limit on the SM $W^\pm W^\pm W^\mp$ production cross section is found to be 730 fb with an expected limit of 560 fb in the absence of $W^\pm W^\pm W^\mp$ production. Limits are also set on the aQGC parameters $f_{S,0}/\Lambda^4$ and $f_{S,1}/\Lambda^4$.

Acknowledgements We thank CERN for the very successful operation of the LHC, as well as the support staff from our institutions without whom ATLAS could not be operated efficiently. We acknowledge the support of ANPCyT, Argentina; YerPhI, Armenia; ARC, Australia; BMWFW and FWF, Austria; ANAS, Azerbaijan; SSTC, Belarus; CNPq and FAPESP, Brazil; NSERC, NRC and CFI, Canada; CERN; CONICYT, Chile; CAS, MOST and NSFC, China; COLCIENCIAS, Colombia; MSMT CR, MPO CR and VSC CR, Czech Republic; DNRF and DNSRC, Denmark; IN2P3-CNRS, CEA-DSM/IRFU, France; GNSF, Georgia; BMBF, HGF, and MPG, Germany; GSRT, Greece; RGC, Hong Kong SAR, China; ISF, I-CORE and Benozio Center, Israel; INFN, Italy; MEXT and JSPS, Japan; CNRST, Morocco; FOM and NWO, Netherlands; RCN, Norway; MNiSW and NCN, Poland; FCT, Portugal; MNE/IFA, Romania; MES of Russia and NRC KI, Russian Federation; JINR; MESTD, Serbia; MSSR, Slovakia; ARRS and MIZŠ, Slovenia; DST/NRF, South Africa; MINECO, Spain; SRC and Wallenberg Foundation, Sweden; SERI, SNSF and Cantons of Bern and Geneva, Switzerland; MOST, Taiwan; TAEK, Turkey; STFC, United Kingdom; DOE and NSF, United States of America. In addition, individual groups and members have received support from BCKDF, the Canada Council, CANARIE, CRC, Compute Canada, FQRNT, and the Ontario Innovation Trust, Canada; EPLANET, ERC, ERDF, FP7, Horizon 2020 and Marie Skłodowska-Curie Actions, European Union; Investissements d’Avenir Labex and Idex, ANR, Région Auvergne and Fondation Partager le Savoir, France; DFG and AvH Foundation, Germany; Herakleitos, Thales and Aristeia programmes co-financed by EU-ESF and the Greek NSRF; BSF, GIF and Minerva, Israel; BRF, Norway; CERCA Programme Generalitat de Catalunya, Generalitat Valenciana, Spain; the Royal Society and Leverhulme Trust, United Kingdom. The crucial computing support from all WLCG partners is acknowledged gratefully, in particular from CERN, the ATLAS Tier-1 facilities at TRIUMF (Canada), NDGF (Denmark, Norway, Sweden), CC-IN2P3 (France), KIT/GridKA (Germany), INFN-CNAF (Italy), NL-T1 (Netherlands), PIC (Spain), ASGC (Taiwan), RAL (UK) and BNL (USA), the Tier-2 facilities worldwide and large non-WLCG resource providers. Major contributors of computing resources are listed in Ref. [67].

Open Access This article is distributed under the terms of the Creative Commons Attribution 4.0 International License (<http://creativecommons.org/licenses/by/4.0/>), which permits unrestricted use, distribution, and reproduction in any medium, provided you give appropriate credit to the original author(s) and the source, provide a link to the Creative Commons license, and indicate if changes were made. Funded by SCOAP³.

References

1. DELPHI Collaboration, J. Abdallah et al., Measurement of the $e^+e^- \rightarrow W^+W^-\gamma$ cross-section and limits on anomalous quartic gauge couplings with DELPHI. *Eur. Phys. J. C* **31**, 139 (2003). doi:10.1140/epjc/s2003-01350-x. arXiv:hep-ex/0311004 [hep-ex]
2. L3 Collaboration, P. Achard et al., The $e^+e^- \rightarrow Z\gamma\gamma \rightarrow q\bar{q}\gamma\gamma$ reaction at LEP and constraints on anomalous quartic gauge boson couplings. *Phys. Lett. B* **540**, 43 (2002). doi:10.1016/S0370-2693(02)02127-5. arXiv:hep-ex/0206050 [hep-ex]
3. L3 Collaboration, P. Achard et al., Study of the $W^+W^-\gamma$ process and limits on anomalous quartic gauge boson couplings at LEP. *Phys. Lett. B* **527**, 29 (2002). doi:10.1016/S0370-2693(02)01167-X. arXiv:hep-ex/0111029 [hep-ex]
4. OPAL Collaboration, G. Abbiendi et al., Measurement of the $W^+W^-\gamma$ cross-section and first direct limits on anomalous electroweak quartic gauge couplings. *Phys. Lett. B* **471**, 293 (1999). doi:10.1016/S0370-2693(99)01357-X. arXiv:hep-ex/9910069 [hep-ex]
5. OPAL Collaboration, G. Abbiendi et al., A Study of $W^+W^-\gamma$ events at LEP. *Phys. Lett. B* **580**, 17 (2004). doi:10.1016/j.physletb.2003.10.063. arXiv:hep-ex/0309013 [hep-ex]
6. OPAL Collaboration, G. Abbiendi et al., Constraints on anomalous quartic gauge boson couplings from $\nu\bar{\nu}\gamma\gamma$ and $q\bar{q}\gamma\gamma$ events at LEP-2. *Phys. Rev. D* **70**, 032005 (2004). doi:10.1103/PhysRevD.70.032005. arXiv:hep-ex/0402021 [hep-ex]
7. D0 Collaboration, V. Abazov et al., Search for anomalous quartic $W\gamma\gamma$ couplings in dielectron and missing energy final states in $p\bar{p}$ collisions at $\sqrt{s} = 1.96$ TeV. *Phys. Rev. D* **88**, 012005 (2013). doi:10.1103/PhysRevD.88.012005. arXiv:1305.1258 [hep-ex]
8. ATLAS Collaboration, Evidence for electroweak production of $W^\pm W^\pm jj$ in pp collisions at $\sqrt{s} = 8$ TeV with the ATLAS detector. *Phys. Rev. Lett.* **113**, 141803 (2014). doi:10.1103/PhysRevLett.113.141803. arXiv:1405.6241 [hep-ex]
9. ATLAS Collaboration, Evidence of $W\gamma\gamma$ production in pp collisions at $\sqrt{s} = 8$ TeV and limits on anomalous quartic gauge couplings with the ATLAS detector. *Phys. Rev. Lett.* **115**, 031802 (2015). doi:10.1103/PhysRevLett.115.031802. arXiv:1503.03243 [hep-ex]
10. ATLAS Collaboration, Measurements of $W^\pm Z$ production cross sections in pp collisions at $\sqrt{s} = 8$ TeV with the ATLAS detector and limits on anomalous gauge boson self-couplings. *Phys. Rev. D* **93**, 092004 (2016). doi:10.1103/PhysRevD.93.092004. arXiv:1603.02151 [hep-ex]
11. ATLAS Collaboration, Measurements of $Z\gamma$ and $Z\gamma\gamma$ production in pp collisions at $\sqrt{s} = 8$ TeV with the ATLAS detector. *Phys. Rev. D* **93**, 112002 (2016). doi:10.1103/PhysRevD.93.112002. arXiv:1604.05232 [hep-ex]
12. ATLAS Collaboration, Measurement of $W^\pm W^\pm$ vector-boson scattering and limits on anomalous quartic gauge couplings with the ATLAS detector (2016). doi:10.3204/PUBDB-2016-04963. arXiv:1611.02428 [hep-ex]
13. ATLAS Collaboration, Measurement of exclusive $\gamma\gamma \rightarrow W^+W^-$ production and search for exclusive Higgs boson production in pp collisions at $\sqrt{s} = 8$ TeV using the ATLAS detector. *Phys. Rev. D* **94**(3), 032011 (2016). arXiv:1607.03745 [hep-ex]. <https://inspirehep.net/search?p=find+eprint+1607.03745>
14. ATLAS Collaboration, Search for anomalous electroweak production of WW/WZ in association with a high-mass dijet system in pp collisions at $\sqrt{s} = 8$ TeV with the ATLAS detector. *Phys. Rev. D* **95**(3), 032001 (2017). arXiv:1609.05122 [hep-ex]. <https://inspirehep.net/search?p=find+eprint+1609.05122>
15. CMS Collaboration, Search for $WW\gamma$ and $WZ\gamma$ production and constraints on anomalous quartic gauge couplings in pp collisions at $\sqrt{s} = 8$ TeV. *Phys. Rev. D* **90**, 032008 (2014). doi:10.1103/PhysRevD.90.032008. arXiv:1404.4619 [hep-ex]
16. CMS Collaboration, Study of vector boson scattering and search for new physics in events with two same-sign leptons and two jets. *Phys. Rev. Lett.* **114**, 051801 (2015). doi:10.1103/PhysRevLett.114.051801. arXiv:1410.6315 [hep-ex]
17. CMS Collaboration, Evidence for exclusive $\gamma\gamma$ to W^+W^- production and constraints on anomalous quartic gauge couplings at

- $\sqrt{s} = 7$ and 8 TeV. JHEP **08**, 119 (2016). [arXiv:1604.04464](https://arxiv.org/abs/1604.04464) [hep-ex]. <https://inspirehep.net/search?p=find+eprint+1604.04464>
18. ATLAS Collaboration, Luminosity determination in pp collisions at $\sqrt{s} = 8$ TeV using the ATLAS detector at the LHC. Eur. Phys. J. C **76**(12), 653 (2016). [arXiv:1608.03953](https://arxiv.org/abs/1608.03953) [hep-ex]. <https://inspirehep.net/search?p=find+eprint+1608.03953>
 19. ATLAS Collaboration, The ATLAS Experiment at the CERN Large Hadron Collider. JINST **3**, S08003 (2008). doi:[10.1088/1748-0221/3/08/S08003](https://doi.org/10.1088/1748-0221/3/08/S08003)
 20. ATLAS Collaboration, Electron reconstruction and identification efficiency measurements with the ATLAS detector using the 2011 LHC proton-proton collision data. Eur. Phys. J. C **74**, 2941 (2014). doi:[10.1140/epjc/s10052-014-2941-0](https://doi.org/10.1140/epjc/s10052-014-2941-0). [arXiv:1404.2240](https://arxiv.org/abs/1404.2240) [hep-ex]
 21. ATLAS Collaboration, Electron efficiency measurements with the ATLAS detector using the 2012 LHC proton-proton collision data, tech.rep. ATLAS-CONF-2014-032, CERN (2014). <http://cds.cern.ch/record/1706245>
 22. ATLAS Collaboration, Measurement of the muon reconstruction performance of the ATLAS detector using 2011 and 2012 LHC proton-proton collision data. Eur. Phys. J. C **74**, 3130 (2014). doi:[10.1140/epjc/s10052-014-3130-x](https://doi.org/10.1140/epjc/s10052-014-3130-x). [arXiv:1407.3935](https://arxiv.org/abs/1407.3935) [hep-ex]
 23. M. Cacciari, G.P. Salam, G. Soyez, The Anti-k(t) jet clustering algorithm. JHEP **04**, 063 (2008). doi:[10.1088/1126-6708/2008/04/063](https://doi.org/10.1088/1126-6708/2008/04/063). [arXiv:0802.1189](https://arxiv.org/abs/0802.1189) [hep-ph]
 24. ATLAS Collaboration, Jet energy measurement and its systematic uncertainty in proton-proton collisions at $\sqrt{s} = 7$ TeV with the ATLAS detector. Eur. Phys. J. C **75**, 17 (2015). doi:[10.1140/epjc/s10052-014-3190-y](https://doi.org/10.1140/epjc/s10052-014-3190-y). [arXiv:1406.0076](https://arxiv.org/abs/1406.0076) [hep-ex]
 25. ATLAS Collaboration, Performance of b -jet identification in the ATLAS experiment. JINST **11**, P04008 (2016). doi:[10.1088/1748-0221/11/04/P04008](https://doi.org/10.1088/1748-0221/11/04/P04008). [arXiv:1512.01094](https://arxiv.org/abs/1512.01094) [hep-ex]
 26. ATLAS Collaboration, Calibration of the performance of b -tagging for c and light-flavour jets in the 2012 ATLAS data, tech. rep. ATLAS-CONF-2014-046, CERN (2014). <http://cds.cern.ch/record/1741020>
 27. ATLAS Collaboration, Performance of Missing Transverse Momentum Reconstruction in Proton-Proton Collisions at 7 TeV with ATLAS. Eur. Phys. J. C **72**, 1844 (2012). doi:[10.1140/epjc/s10052-011-1844-6](https://doi.org/10.1140/epjc/s10052-011-1844-6). [arXiv:1108.5602](https://arxiv.org/abs/1108.5602) [hep-ex]
 28. K.A. Olive et al. (Particle Data Group), Review of particle physics. Chin. Phys. C **38**, 090001 (2014). doi:[10.1088/1674-1137/38/9/090001](https://doi.org/10.1088/1674-1137/38/9/090001)
 29. F. Campanario et al., QCD corrections to charged triple vector boson production with leptonic decay. Phys. Rev. D **78**, 094012 (2008). doi:[10.1103/PhysRevD.78.094012](https://doi.org/10.1103/PhysRevD.78.094012). [arXiv:0809.0790](https://arxiv.org/abs/0809.0790) [hep-ph]
 30. S. Yong-Bai et al., NLO QCD + EW corrections to WWW production with leptonic decays at the LHC (2016). [arXiv:1605.00554](https://arxiv.org/abs/1605.00554) [hep-ph]
 31. J. Alwall et al., The automated computation of tree-level and next-to-leading order differential cross sections, and their matching to parton shower simulations. JHEP **07**, 079 (2014). doi:[10.1007/JHEP07\(2014\)079](https://doi.org/10.1007/JHEP07(2014)079). [arXiv:1405.0301](https://arxiv.org/abs/1405.0301) [hep-ph]
 32. H.-L. Lai et al., New parton distributions for collider physics. Phys. Rev. D **82**, 074024 (2010). doi:[10.1103/PhysRevD.82.074024](https://doi.org/10.1103/PhysRevD.82.074024). [arXiv:1007.2241](https://arxiv.org/abs/1007.2241) [hep-ph]
 33. T. Sjöstrand, S. Mrenna, P.Z. Skands, A brief introduction to PYTHIA 8.1, Comput. Phys. Commun. **178**, 852 (2008). doi:[10.1016/j.cpc.2008.01.036](https://doi.org/10.1016/j.cpc.2008.01.036). [arXiv:0710.3820](https://arxiv.org/abs/0710.3820) [hep-ph]
 34. ATLAS Collaboration, Proposal for truth particle observable definitions in physics measurements, tech. rep. ATL-PHYS-PUB-2015-013, CERN (2015). <http://cds.cern.ch/record/2022743>
 35. R.D. Ball et al., Parton distributions for the LHC Run II. JHEP **04**, 040 (2015). doi:[10.1007/JHEP04\(2015\)040](https://doi.org/10.1007/JHEP04(2015)040). [arXiv:1410.8849](https://arxiv.org/abs/1410.8849) [hep-ph]
 36. A.D. Martin et al., Parton distributions for the LHC. Eur. Phys. J. C **63**, 189 (2009). doi:[10.1140/epjc/s10052-009-1072-5](https://doi.org/10.1140/epjc/s10052-009-1072-5). [arXiv:0901.0002](https://arxiv.org/abs/0901.0002) [hep-ph]
 37. S. Alekhin et al., The PDF4LHC Working Group Interim Report (2011). [arXiv:1101.0538](https://arxiv.org/abs/1101.0538) [hep-ph]
 38. K. Arnold et al., VBFNLO: a parton level Monte Carlo for processes with electroweak bosons. Comput. Phys. Commun. **180**, 1661 (2009). doi:[10.1016/j.cpc.2009.03.006](https://doi.org/10.1016/j.cpc.2009.03.006). [arXiv:0811.4559](https://arxiv.org/abs/0811.4559) [hep-ph]
 39. K. Arnold et al., VBFNLO: a parton level Monte Carlo for Processes with electroweak bosons—manual for version 2.5.0 (2011). [arXiv:1107.4038](https://arxiv.org/abs/1107.4038) [hep-ph]
 40. J. Baglio et al., Release Note—VBFNLO 2.7.0 (2014). [arXiv:1404.3940](https://arxiv.org/abs/1404.3940) [hep-ph]
 41. ATLAS Collaboration, The ATLAS simulation infrastructure. Eur. Phys. J. C **70**, 823 (2010). doi:[10.1140/epjc/s10052-010-1429-9](https://doi.org/10.1140/epjc/s10052-010-1429-9). [arXiv:1005.4568](https://arxiv.org/abs/1005.4568) [physics.ins-det]
 42. S. Agostinelli et al., GEANT4: a simulation toolkit. Nucl. Instrum. Methods A **506**, 250 (2003). doi:[10.1016/S0168-9002\(03\)01368-8](https://doi.org/10.1016/S0168-9002(03)01368-8)
 43. P. Nason, A New method for combining NLO QCD with shower Monte Carlo algorithms. JHEP **11**, 040 (2004). doi:[10.1088/1126-6708/2004/11/040](https://doi.org/10.1088/1126-6708/2004/11/040). [arXiv:hep-ph/0409146](https://arxiv.org/abs/hep-ph/0409146) [hep-ph]
 44. S. Frixione, P. Nason, C. Oleari, Matching NLO QCD computations with parton shower simulations: the POWHEG method. JHEP **11**, 070 (2007). doi:[10.1088/1126-6708/2007/11/070](https://doi.org/10.1088/1126-6708/2007/11/070). [arXiv:0709.2092](https://arxiv.org/abs/0709.2092) [hep-ph]
 45. S. Alioli et al., A general framework for implementing NLO calculations in shower Monte Carlo programs: the POWHEG BOX. JHEP **1006**, 043 (2010). doi:[10.1007/JHEP06\(2010\)043](https://doi.org/10.1007/JHEP06(2010)043). [arXiv:1002.2581](https://arxiv.org/abs/1002.2581) [hep-ph]
 46. T. Melia et al., W^+W^- , WZ and ZZ production in the POWHEG BOX. JHEP **11**, 078 (2011). doi:[10.1007/JHEP11\(2011\)078](https://doi.org/10.1007/JHEP11(2011)078). [arXiv:1107.5051](https://arxiv.org/abs/1107.5051) [hep-ph]
 47. T. Gleisberg et al., Event generation with SHERPA 1.1. JHEP **02**, 007 (2009). doi:[10.1088/1126-6708/2009/02/007](https://doi.org/10.1088/1126-6708/2009/02/007). [arXiv:0811.4622](https://arxiv.org/abs/0811.4622) [hep-ph]
 48. F. Campanario et al., NLO QCD corrections to WZ +jet production with leptonic decays. JHEP **07**, 076 (2010). doi:[10.1007/JHEP07\(2010\)076](https://doi.org/10.1007/JHEP07(2010)076). [arXiv:1006.0390](https://arxiv.org/abs/1006.0390) [hep-ph]
 49. F. Campanario et al., Next-to-leading order QCD corrections to $W\gamma$ production in association with two jets. Eur. Phys. J. C **74**, 2882 (2014). doi:[10.1140/epjc/s10052-014-2882-7](https://doi.org/10.1140/epjc/s10052-014-2882-7). [arXiv:1402.0505](https://arxiv.org/abs/1402.0505) [hep-ph]
 50. M.L. Mangano et al., ALPGEN, a generator for hard multiparton processes in hadronic collisions. JHEP **07**, 001 (2003). doi:[10.1088/1126-6708/2003/07/001](https://doi.org/10.1088/1126-6708/2003/07/001). [arXiv:hep-ph/0206293](https://arxiv.org/abs/hep-ph/0206293) [hep-ph]
 51. G. Corcella et al., HERWIG 6: an event generator for hadron emission reactions with interfering gluons (including supersymmetric processes). JHEP **01**, 010 (2001). doi:[10.1088/1126-6708/2001/01/010](https://doi.org/10.1088/1126-6708/2001/01/010). [arXiv:hep-ph/0011363](https://arxiv.org/abs/hep-ph/0011363) [hep-ph]
 52. J.M. Butterworth, J.R. Forshaw, M.H. Seymour, Multiparton interactions in photoproduction at HERA. Z. Phys. C **72**, 637 (1996). doi:[10.1007/s002880050286](https://doi.org/10.1007/s002880050286). [arXiv:hep-ph/9601371](https://arxiv.org/abs/hep-ph/9601371) [hep-ph]
 53. F. Campanario, N. Kaiser, D. Zeppenfeld, $W\gamma$ production in vector boson fusion at NLO in QCD. Phys. Rev. D **89**, 014009 (2014). doi:[10.1103/PhysRevD.89.014009](https://doi.org/10.1103/PhysRevD.89.014009). [arXiv:1309.7259](https://arxiv.org/abs/1309.7259) [hep-ph]
 54. S. Frixione et al., Electroweak and QCD corrections to top-pair hadroproduction in association with heavy bosons. JHEP **06**, 184 (2015). doi:[10.1007/JHEP06\(2015\)184](https://doi.org/10.1007/JHEP06(2015)184). [arXiv:1504.03446](https://arxiv.org/abs/1504.03446) [hep-ph]
 55. T. Binoth et al., NLO QCD corrections to tri-boson production. JHEP **06**, 082 (2008). doi:[10.1088/1126-6708/2008/06/082](https://doi.org/10.1088/1126-6708/2008/06/082). [arXiv:0804.0350](https://arxiv.org/abs/0804.0350) [hep-ph]
 56. F. Campanario et al., Next-to-leading order QCD corrections to W^+W^+ and W^-W^- production in association with two jets. Phys.

57. T.P.S. Gillam, C.G. Lester, Improving estimates of the number of ‘fake’ leptons and other mis-reconstructed objects in hadron collider events: BoB’s your UNCLE. *JHEP* **11**, 031 (2014). doi:10.1007/JHEP11(2014)031. arXiv:1407.5624 [hep-ph]
58. G. Cowan et al., Asymptotic formulae for likelihood-based tests of new physics. *Eur. Phys. J. C* **71**, 1554 (2011). doi:10.1140/epjc/s10052-011-1554-0, doi:10.1140/epjc/s10052-013-2501-z. arXiv: 1007.1727 [physics.data-an]. [Erratum: *Eur. Phys. J. C* **73**, 2501 (2013)]
59. A.L. Read, Presentation of search results: the CL_s technique. *J. Phys. G Nucl. Part. Phys.* **28**, 2693 (2002). <http://stacks.iop.org/0954-3889/28/i=10/a=313>
60. O.J.P. Eboli, M.C. Gonzalez-Garcia, J.K. Mizukoshi, $pp \rightarrow jje^\pm\mu^\pm\nu\nu$ and $jje^\pm\mu^\mp\nu\nu$ at $\mathcal{O}(\alpha_s^4)$ and $\mathcal{O}(\alpha_s^2)$ for the study of the quartic electroweak gauge boson vertex at CERN LHC. *Phys. Rev. D* **74**, 073005 (2006). doi:10.1103/PhysRevD.74.073005. arXiv:hep-ph/0606118 [hep-ph]
61. G. Belanger et al., Bosonic quartic couplings at LEP-2. *Eur. Phys. J. C* **13**, 283 (2000). doi:10.1007/s100520000305. arXiv:hep-ph/9908254 [hep-ph]
62. O.J.P. Eboli, M.C. Gonzalez-Garcia, S.M. Lietti, Bosonic quartic couplings at CERN LHC. *Phys. Rev. D* **69**, 095005 (2004). doi:10.1103/PhysRevD.69.095005. arXiv:hep-ph/0310141 [hep-ph]
63. T. Appelquist, C. Bernard, Strongly interacting Higgs bosons. *Phys. Rev. D* **22**, 200–213 (1980). doi:10.1103/PhysRevD.22.200. <http://link.aps.org/>. doi:10.1103/PhysRevD.22.200
64. A.C. Longhitano, Heavy Higgs bosons in the Weinberg-Salam model. *Phys. Rev. D* **22**, 1166–1175 (1980). doi:10.1103/PhysRevD.22.1166. <http://link.aps.org/>. doi:10.1103/PhysRevD.22.1166
65. A.C. Longhitano, Low-energy impact of a heavy Higgs boson sector. *Nucl. Phys. B* **188**, 118–154 (1981). <http://www.sciencedirect.com/science/article/pii/0550321381901097>
66. C. Degrande et al., Monte Carlo tools for studies of non-standard electroweak gauge boson interactions in multi-boson processes: a snowmass White Paper. Community Summer Study 2013: Snowmass on the Mississippi (CSS2013) Minneapolis, July 29–August 6, 2013 (2013). arXiv:1309.7890 [hep-ph]
67. ATLAS Collaboration, ATLAS Computing Acknowledgements 2016–2017, ATL-GEN-PUB-2016-002 (2016). <http://cds.cern.ch/record/2202407>

ATLAS Collaboration

M. Aaboud^{136d}, G. Aad⁸⁷, B. Abbott¹¹⁴, J. Abdallah⁸, O. Abdinov¹², B. Abeloos¹¹⁸, R. Aben¹⁰⁸, O. S. AbouZeid¹³⁸, N. L. Abraham¹⁵², H. Abramowicz¹⁵⁶, H. Abreu¹⁵⁵, R. Abreu¹¹⁷, Y. Abulaiti^{149a,149b}, B. S. Acharya^{168a,168b,a}, S. Adachi¹⁵⁸, L. Adamczyk^{40a}, D. L. Adams²⁷, J. Adelman¹⁰⁹, S. Adomeit¹⁰¹, T. Adye¹³², A. A. Affolder⁷⁶, T. Agatonovic-Jovin¹⁴, J. Agricola⁵⁶, J. A. Aguilar-Saavedra^{127a,127f}, S. P. Ahlen²⁴, F. Ahmadov^{67,b}, G. Aielli^{134a,134b}, H. Akerstedt^{149a,149b}, T. P. A. Åkesson⁸³, A. V. Akimov⁹⁷, G. L. Alberghi^{22a,22b}, J. Albert¹⁷³, S. Albrand⁵⁷, M. J. Alconada Verzini⁷³, M. Aleksa³², I. N. Aleksandrov⁶⁷, C. Alexa^{28b}, G. Alexander¹⁵⁶, T. Alexopoulos¹⁰, M. Alhroob¹¹⁴, B. Ali¹²⁹, M. Aliev^{75a,75b}, G. Alimonti^{93a}, J. Alison³³, S. P. Alkire³⁷, B. M. M. Allbrooke¹⁵², B. W. Allen¹¹⁷, P. P. Allport¹⁹, A. Aloisio^{105a,105b}, A. Alonso³⁸, F. Alonso⁷³, C. Alpigiani¹³⁹, A. A. Alshehri⁵⁵, M. Alstady⁸⁷, B. Alvarez Gonzalez³², D. Álvarez Piqueras¹⁷¹, M. G. Alvigi^{105a,105b}, B. T. Amadio¹⁶, K. Amako⁶⁸, Y. Amaral Coutinho^{26a}, C. Amelung²⁵, D. Amidei⁹¹, S. P. Amor Dos Santos^{127a,127c}, A. Amorim^{127a,127b}, S. Amoroso³², G. Amundsen²⁵, C. Anastopoulos¹⁴², L. S. Ancu⁵¹, N. Andari¹⁹, T. Andeen¹¹, C. F. Anders^{60b}, G. Anders³², J. K. Anders⁷⁶, K. J. Anderson³³, A. Andreazza^{93a,93b}, V. Andrei^{60a}, S. Angelidakis⁹, I. Angelozzi¹⁰⁸, P. Anger⁴⁶, A. Angerami³⁷, F. Anghinolfi³², A. V. Anisenkov^{110,c}, N. Anjos¹³, A. Annovi^{125a,125b}, C. Antel^{60a}, M. Antonelli⁴⁹, A. Antonov^{99,*}, F. Anulli^{133a}, M. Aoki⁶⁸, L. Aperio Bella¹⁹, G. Arabidze⁹², Y. Arai⁶⁸, J. P. Araque^{127a}, A. T. H. Arce⁴⁷, F. A. Arduh⁷³, J.-F. Arguin⁹⁶, S. Argyropoulos⁶⁵, M. Arik^{20a}, A. J. Armbruster¹⁴⁶, L. J. Armitage⁷⁸, O. Arnaez³², H. Arnold⁵⁰, M. Arratia³⁰, O. Arslan²³, A. Artamonov⁹⁸, G. Artoni¹²¹, S. Artz⁸⁵, S. Asai¹⁵⁸, N. Asbah⁴⁴, A. Ashkenazi¹⁵⁶, B. Åsman^{149a,149b}, L. Asquith¹⁵², K. Assamagan²⁷, R. Astalos^{147a}, M. Atkinson¹⁷⁰, N. B. Atlay¹⁴⁴, K. Augsten¹²⁹, G. Avolio³², B. Axen¹⁶, M. K. Ayoub¹¹⁸, G. Azuelos^{96,d}, M. A. Baak³², A. E. Baas^{60a}, M. J. Baca¹⁹, H. Bachacou¹³⁷, K. Bachas^{75a,75b}, M. Backes¹²¹, M. Backhaus³², P. Bagiachi^{133a,133b}, P. Bagnaia^{133a,133b}, Y. Bai^{35a}, J. T. Baines¹³², O. K. Baker¹⁸⁰, E. M. Baldin^{110,c}, P. Balek¹⁷⁶, T. Balestri¹⁵¹, F. Balli¹³⁷, W. K. Balunas¹²³, E. Banas⁴¹, Sw. Banerjee^{177,e}, A. A. E. Bannoura¹⁷⁹, L. Barak³², E. L. Barberio⁹⁰, D. Barberis^{52a,52b}, M. Barbero⁸⁷, T. Barillari¹⁰², M.-S. Barisits³², T. Barklow¹⁴⁶, N. Barlow³⁰, S. L. Barnes⁸⁶, B. M. Barnett¹³², R. M. Barnett¹⁶, Z. Barnovska-Blenessy⁵, A. Baroncelli^{135a}, G. Barone²⁵, A. J. Barr¹²¹, L. Barranco Navarro¹⁷¹, F. Barreiro⁸⁴, J. Barreiro Guimarães da Costa^{35a}, R. Bartoldus¹⁴⁶, A. E. Barton⁷⁴, P. Bartos^{147a}, A. Basalae¹²⁴, A. Bassalat^{118,f}, R. L. Bates⁵⁵, S. J. Batista¹⁶², J. R. Batley³⁰, M. Battaglia¹³⁸, M. Bause^{133a,133b}, F. Bauer¹³⁷, H. S. Bawa^{146,g}, J. B. Beacham¹¹², M. D. Beattie⁷⁴, T. Beau⁸², P. H. Beauchemin¹⁶⁶, P. Bechtel²³, H. P. Beck^{18,h}, K. Becker¹²¹, M. Becker⁸⁵, M. Beckingham¹⁷⁴, C. Becot¹¹¹, A. J. Beddall^{20d}, A. Beddall^{20b}, V. A. Bednyakov⁶⁷, M. Bedognetti¹⁰⁸, C. P. Bee¹⁵¹, L. J. Beemster¹⁰⁸, T. A. Beermann³², M. Begel²⁷, J. K. Behr⁴⁴, C. Belanger-Champagne⁸⁹, A. S. Bell⁸⁰, G. Bella¹⁵⁶, L. Bellagamba^{22a}, A. Bellerive³¹, M. Bellomo⁸⁸, K. Belotskiy⁹⁹, O. Beltramello³², N. L. Belyaev⁹⁹, O. Benary^{156,*}, D. Bencheikroun^{136a}, M. Bender¹⁰¹, K. Bendtz^{149a,149b}, N. Benekos¹⁰, Y. Benhammou¹⁵⁶, E. Benhar Nocchioli¹⁸⁰, J. Benitez⁶⁵, D. P. Benjamin⁴⁷, J. R. Bensinger²⁵, S. Bentvelsen¹⁰⁸, L. Beresford¹²¹, M. Beretta⁴⁹, D. Berge¹⁰⁸, E. Bergeaas Kuutmann¹⁶⁹, N. Berger⁵, J. Beringer¹⁶, S. Berlendis⁵⁷, N. R. Bernard⁸⁸, C. Bernius¹¹¹, F. U. Bernlochner²³, T. Berry⁷⁹, P. Berta¹³⁰, C. Bertella⁸⁵, G. Bertoli^{149a,149b}

F. Bertolucci^{125a,125b}, I. A. Bertram⁷⁴, C. Bertsche⁴⁴, D. Bertsche¹¹⁴, G. J. Besjes³⁸, O. Bessidskaia Bylund^{149a,149b}, M. Bessner⁴⁴, N. Besson¹³⁷, C. Betancourt⁵⁰, A. Bethani⁵⁷, S. Bethke¹⁰², A. J. Bevan⁷⁸, R. M. Bianchi¹²⁶, L. Bianchini²⁵, M. Bianco³², O. Biebel¹⁰¹, D. Biedermann¹⁷, R. Bielski⁸⁶, N. V. Biesuz^{125a,125b}, M. Biglietti^{135a}, J. Bilbao De Mendizabal⁵¹, T. R. V. Billoud⁹⁶, H. Bilokon⁴⁹, M. Bindi⁵⁶, S. Binet¹¹⁸, A. Bingul^{20b}, C. Bini^{133a,133b}, S. Biondi^{22a,22b}, T. Bisanz⁵⁶, D. M. Bjergaard⁴⁷, C. W. Black¹⁵³, J. E. Black¹⁴⁶, K. M. Black²⁴, D. Blackburn¹³⁹, R. E. Blair⁶, J.-B. Blanchard¹³⁷, T. Blazek^{147a}, I. Bloch⁴⁴, C. Blocker²⁵, A. Blue⁵⁵, W. Blum^{85,*}, U. Blumenschein⁵⁶, S. Blunier^{34a}, G. J. Bobbink¹⁰⁸, V. S. Bobrovnikov^{110,c}, S. S. Bocchetta⁸³, A. Bocci⁴⁷, C. Bock¹⁰¹, M. Boehler⁵⁰, D. Boerner¹⁷⁹, J. A. Bogaerts³², D. Bogavac¹⁴, A. G. Bogdanchikov¹¹⁰, C. Bohm^{149a}, V. Boisvert⁷⁹, P. Bokan¹⁴, T. Bold^{40a}, A. S. Boldyrev^{168a,168c}, M. Bomben⁸², M. Bona⁷⁸, M. Boonekamp¹³⁷, A. Borisov¹³¹, G. Borissov⁷⁴, J. Bortfeldt³², D. Bortoletto¹²¹, V. Bortolotto^{62a,62b,62c}, K. Bos¹⁰⁸, D. Boscherini^{22a}, M. Bosman¹³, J. D. Bossio Sola²⁹, J. Boudreau¹²⁶, J. Bouffard², E. V. Bouhova-Thacker⁷⁴, D. Boumediene³⁶, C. Bourdarios¹¹⁸, S. K. Boutle⁵⁵, A. Boveia³², J. Boyd³², I. R. Boyko⁶⁷, J. Bracini¹⁹, A. Brandt⁸, G. Brandt⁵⁶, O. Brandt^{60a}, U. Bratzler¹⁵⁹, B. Brau⁸⁸, J. E. Brau¹¹⁷, W. D. Breaden Madden⁵⁵, K. Brendlinger¹²³, A. J. Brennan⁹⁰, L. Brenner¹⁰⁸, R. Brenner¹⁶⁹, S. Bressler¹⁷⁶, T. M. Bristow⁴⁸, D. Britton⁵⁵, D. Britzger⁴⁴, F. M. Brochu³⁰, I. Brock²³, R. Brock⁹², G. Brooijmans³⁷, T. Brooks⁷⁹, W. K. Brooks^{34b}, J. Brosamer¹⁶, E. Brost¹⁰⁹, J. H. Broughton¹⁹, P. A. Bruckman de Renstrom⁴¹, D. Bruncko^{147b}, R. Bruneliere⁵⁰, A. Bruni^{22a}, G. Bruni^{22a}, L. S. Bruni¹⁰⁸, B. H. Brunt³⁰, M. Bruschi^{22a}, N. Bruscinò²³, P. Bryant³³, L. Bryngemark⁸³, T. Buanes¹⁵, Q. Buat¹⁴⁵, P. Buchholz¹⁴⁴, A. G. Buckley⁵⁵, I. A. Budagov⁶⁷, F. Buehrer⁵⁰, M. K. Bugge¹²⁰, O. Bulekov⁹⁹, D. Bullock⁸, H. Burckhart³², S. Burdin⁷⁶, C. D. Burgard⁵⁰, B. Burghgrave¹⁰⁹, K. Burka⁴¹, S. Burke¹³², I. Burmeister⁴⁵, J. T. P. Burr¹²¹, E. Busato³⁶, D. Büscher⁵⁰, V. Büscher⁸⁵, P. Bussey⁵⁵, J. M. Butler²⁴, C. M. Buttar⁵⁵, J. M. Butterworth⁸⁰, P. Butti¹⁰⁸, W. Buttinger²⁷, A. Buzatu⁵⁵, A. R. Buzykaev^{110,c}, S. Cabrera Urbán¹⁷¹, D. Caforio¹²⁹, V. M. Cairo^{39a,39b}, O. Kakir^{4a}, N. Calace⁵¹, P. Calafiura¹⁶, A. Calandri⁸⁷, G. Calderini⁸², P. Calfayan¹⁰¹, G. Callea^{39a,39b}, L. P. Caloba^{26a}, S. Calvente Lopez⁸⁴, D. Calvet³⁶, S. Calvet³⁶, T. P. Calvet⁸⁷, R. Camacho Toro³³, S. Camarda³², P. Camarri^{134a,134b}, D. Cameron¹²⁰, R. Caminal Armadans¹⁷⁰, C. Camincher⁵⁷, S. Campana³², M. Campanelli⁸⁰, A. Camplani^{93a,93b}, A. Campoverde¹⁴⁴, V. Canale^{105a,105b}, A. Canepa^{164a}, M. Cano Bret¹⁴¹, J. Cantero¹¹⁵, T. Cao⁴², M. D. M. Capeans Garrido³², I. Caprini^{28b}, M. Caprini^{28b}, M. Capua^{39a,39b}, R. M. Carbone³⁷, R. Cardarelli^{134a}, F. Cardillo⁵⁰, I. Carli¹³⁰, T. Carli³², G. Carlino^{105a}, L. Carminati^{93a,93b}, S. Caron¹⁰⁷, E. Carquin^{34b}, G. D. Carrillo-Montoya³², J. R. Carter³⁰, J. Carvalho^{127a,127c}, D. Casadei¹⁹, M. P. Casado^{13,i}, M. Casolino¹³, D. W. Casper¹⁶⁷, E. Castaneda-Miranda^{148a}, R. Castelijns¹⁰⁸, A. Castelli¹⁰⁸, V. Castillo Gimenez¹⁷¹, N. F. Castro^{127a,j}, A. Catinaccio³², J. R. Catmore¹²⁰, A. Cattai³², J. Caudron²³, V. Cavaliere¹⁷⁰, E. Cavallaro¹³, D. Cavalli^{93a}, M. Cavalli-Sforza¹³, V. Cavasinni^{125a,125b}, F. Ceradini^{135a,135b}, L. Cerda Alberich¹⁷¹, B. C. Cerio⁴⁷, A. S. Cerqueira^{26b}, A. Cerri¹⁵², L. Cerrito^{134a,134b}, F. Cerutti¹⁶, M. Cerv³², A. Cervelli¹⁸, S. A. Cetin^{20c}, A. Chafaq^{136a}, D. Chakraborty¹⁰⁹, S. K. Chan⁵⁸, Y. L. Chan^{62a}, P. Chang¹⁷⁰, J. D. Chapman³⁰, D. G. Charlton¹⁹, A. Chatterjee⁵¹, C. C. Chau¹⁶², C. A. Chavez Barajas¹⁵², S. Che¹¹², S. Cheatham^{168a,168c}, A. Chegwidan⁹², S. Chekanov⁶, S. V. Chekulaev^{164a}, G. A. Chelkov^{67,k}, M. A. Chelstowska⁹¹, C. Chen⁶⁶, H. Chen²⁷, K. Chen¹⁵¹, S. Chen^{35b}, S. Chen¹⁵⁸, X. Chen^{35c}, Y. Chen⁶⁹, H. C. Cheng⁹¹, H. J. Cheng^{35a}, Y. Cheng³³, A. Cheplakov⁶⁷, E. Cherenmushkina¹³¹, R. Cherkaoui El Moursli^{136e}, V. Chernyatin^{27,*}, E. Cheu⁷, L. Chevalier¹³⁷, V. Chiarella⁴⁹, G. Chiarelli^{125a,125b}, G. Chiodini^{75a}, A. S. Chisholm³², A. Chitan^{28b}, M. V. Chizhov⁶⁷, K. Choi⁶³, A. R. Chomont³⁶, S. Chouridou⁹, B. K. B. Chow¹⁰¹, V. Christodoulou⁸⁰, D. Chromek-Burckhart³², J. Chudoba¹²⁸, A. J. Chuinard⁸⁹, J. J. Chwastowski⁴¹, L. Chytka¹¹⁶, G. Ciapetti^{133a,133b}, A. K. Ciftci^{4a}, D. Cinca⁴⁵, V. Cindro⁷⁷, I. A. Cioara²³, C. Ciocca^{22a,22b}, A. Ciocio¹⁶, F. Ciotto^{105a,105b}, Z. H. Citron¹⁷⁶, M. Citterio^{93a}, M. Ciubancan^{28b}, A. Clark⁵¹, B. L. Clark⁵⁸, M. R. Clark³⁷, P. J. Clark⁴⁸, R. N. Clarke¹⁶, C. Clement^{149a,149b}, Y. Coadou⁸⁷, M. Cobl^{168a,168c}, A. Coccaro⁵¹, J. Cochran⁶⁶, L. Colasurdo¹⁰⁷, B. Cole³⁷, A. P. Colijn¹⁰⁸, J. Collot⁵⁷, T. Colombo¹⁶⁷, G. Compostella¹⁰², P. Conde Muñio^{127a,127b}, E. Coniavitis⁵⁰, S. H. Connell^{148b}, I. A. Connelly⁷⁹, V. Consorti⁵⁰, S. Constantinescu^{28b}, G. Conti³², F. Conventi^{105a,1}, M. Cooke¹⁶, B. D. Cooper⁸⁰, A. M. Cooper-Sarkar¹²¹, K. J. R. Cormier¹⁶², T. Cornelissen¹⁷⁹, M. Corradi^{133a,133b}, F. Corriveau^{89,m}, A. Cortes-Gonzalez³², G. Cortiana¹⁰², G. Costa^{93a}, M. J. Costa¹⁷¹, D. Costanzo¹⁴², G. Cottin³⁰, G. Cowan⁷⁹, B. E. Cox⁸⁶, K. Cranmer¹¹¹, S. J. Crawley⁵⁵, G. Cree³¹, S. Crépe-Renaudin⁵⁷, F. Crescioli⁸², W. A. Cribbs^{149a,149b}, M. Crispin Ortuzar¹²¹, M. Cristinziani²³, V. Croft¹⁰⁷, G. Crosetti^{39a,39b}, A. Cueto⁸⁴, T. Cuhadar Donszelmann¹⁴², J. Cummings¹⁸⁰, M. Curatolo⁴⁹, J. Cúth⁸⁵, H. Czirr¹⁴⁴, P. Czodrowski³, G. D'amen^{22a,22b}, S. D'Auria⁵⁵, M. D'Onofrio⁷⁶, M. J. Da Cunha Sargedas De Sousa^{127a,127b}, C. Da Via⁸⁶, W. Dabrowski^{40a}, T. Dado^{147a}, T. Dai⁹¹, O. Dale¹⁵, F. Dallaire⁹⁶, C. Dallapiccola⁸⁸, M. Dam³⁸, J. R. Dandoy³³, N. P. Dang⁵⁰, A. C. Daniells¹⁹, N. S. Dann⁸⁶, M. Danninger¹⁷², M. Dano Hoffmann¹³⁷, V. Dao⁵⁰, G. Darbo^{52a}, S. Darmora⁸, J. Dassoulas³, A. Dattagupta¹¹⁷, W. Davey²³, C. David¹⁷³, T. Davidek¹³⁰, M. Davies¹⁵⁶, P. Davison⁸⁰, E. Dawe⁹⁰, I. Dawson¹⁴², K. De⁸, R. de Asmundis^{105a}, A. De Benedetti¹¹⁴, S. De Castro^{22a,22b}, S. De Cecco⁸², N. De Groot¹⁰⁷, P. de Jong¹⁰⁸, H. De la Torre⁹², F. De Lorenzi⁶⁶, A. De Maria⁵⁶, D. De Pedis^{133a}, A. De Salvo^{133a}, U. De Sanctis¹⁵²

A. De Santo¹⁵², J. B. De Vivie De Regie¹¹⁸, W. J. Dearnaley⁷⁴, R. Debbe²⁷, C. Debenedetti¹³⁸, D. V. Dedovich⁶⁷, N. Dehghanian³, I. Deigaard¹⁰⁸, M. Del Gaudio^{39a,39b}, J. Del Peso⁸⁴, T. Del Prete^{125a,125b}, D. Delgove¹¹⁸, F. Deliot¹³⁷, C. M. Delitzsch⁵¹, A. Dell'Acqua³², L. Dell'Asta²⁴, M. Dell'Orso^{125a,125b}, M. Della Pietra^{105a,1}, D. della Volpe⁵¹, M. Delmastro⁵, P. A. Delsart⁵⁷, D. A. DeMarco¹⁶², S. Demers¹⁸⁰, M. Demichev⁶⁷, A. Demilly⁸², S. P. Denisov¹³¹, D. Denysiuk¹³⁷, D. Derendarz⁴¹, J. E. Derkaoui^{136d}, F. Derue⁸², P. Dervan⁷⁶, K. Desch²³, C. Deterre⁴⁴, K. Dette⁴⁵, P. O. Deviveiros³², A. Dewhurst¹³², S. Dhaliwal²⁵, A. Di Ciaccio^{134a,134b}, L. Di Ciaccio⁵, W. K. Di Clemente¹²³, C. Di Donato^{133a,133b}, A. Di Girolamo³², B. Di Girolamo³², B. Di Micco^{135a,135b}, R. Di Nardo³², A. Di Simone⁵⁰, R. Di Sipio¹⁶², D. Di Valentino³¹, C. Diaconu⁸⁷, M. Diamond¹⁶², F. A. Dias⁴⁸, M. A. Diaz^{34a}, E. B. Diehl⁹¹, J. Dietrich¹⁷, S. Díez Cornell⁴⁴, A. Dimitrievska¹⁴, J. Dingfelder²³, P. Dita^{28b}, S. Dita^{28b}, F. Dittus³², F. Djama⁸⁷, T. Djobava^{53b}, J. I. Djuvsland^{60a}, M. A. B. do Vale^{26c}, D. Dobos³², M. Dobre^{28b}, C. Doglioni⁸³, J. Dolejsi¹³⁰, Z. Dolezal¹³⁰, M. Donadelli^{26d}, S. Donati^{125a,125b}, P. Dondero^{122a,122b}, J. Donini³⁶, J. Dopke¹³², A. Doria^{105a}, M. T. Dova⁷³, A. T. Doyle⁵⁵, E. Drechsler⁵⁶, M. Dris¹⁰, Y. Du¹⁴⁰, J. Duarte-Campderros¹⁵⁶, E. Duchovni¹⁷⁶, G. Duckeck¹⁰¹, O. A. Ducu^{96,n}, D. Duda¹⁰⁸, A. Dudarev³², A. Chr. Dudder⁸⁵, E. M. Duffield¹⁶, L. Dufflot¹¹⁸, M. Dührssen³², M. Dumancic¹⁷⁶, M. Dunford^{60a}, H. Duran Yildiz^{4a}, M. Düren⁵⁴, A. Durglishvili^{53b}, D. Duschinger⁴⁶, B. Dutta⁴⁴, M. Dyndal⁴⁴, C. Eckardt⁴⁴, K. M. Ecker¹⁰², R. C. Edgar⁹¹, N. C. Edwards⁴⁸, T. Eifert³², G. Eigen¹⁵, K. Einsweiler¹⁶, T. Ekelof¹⁶⁹, M. El Kacimi^{136c}, V. Ellajosyula⁸⁷, M. Ellert¹⁶⁹, S. Elles⁵, F. Ellinghaus¹⁷⁹, A. A. Elliot¹⁷³, N. Ellis³², J. Elmsheuser²⁷, M. Elsing³², D. Emelianov¹³², Y. Enari¹⁵⁸, O. C. Endner⁸⁵, J. S. Ennis¹⁷⁴, J. Erdmann⁴⁵, A. Ereditato¹⁸, G. Ernis¹⁷⁹, J. Ernst², M. Ernst²⁷, S. Errede¹⁷⁰, E. Ertel⁸⁵, M. Escalier¹¹⁸, H. Esch⁴⁵, C. Escobar¹²⁶, B. Esposito⁴⁹, A. I. Etienvre¹³⁷, E. Etzion¹⁵⁶, H. Evans⁶³, A. Ezhilov¹²⁴, M. Ezzi^{136e}, F. Fabbri^{22a,22b}, L. Fabbri^{22a,22b}, G. Facini³³, R. M. Fakhruddinov¹³¹, S. Falciano^{133a}, R. J. Falla⁸⁰, J. Faltova³², Y. Fang^{35a}, M. Fanti^{93a,93b}, A. Farbin⁸, A. Farilla^{135a}, C. Farina¹²⁶, E. M. Farina^{122a,122b}, T. Farooque¹³, S. Farrell¹⁶, S. M. Farrington¹⁷⁴, P. Farthouat³², F. Fassi^{136e}, P. Fassnacht³², D. Fassoulitis⁹, M. Fauci Giannelli⁷⁹, A. Favareto^{52a,52b}, W. J. Fawcett¹²¹, L. Fayard¹¹⁸, O. L. Fedin^{124,o}, W. Fedorko¹⁷², S. Feigl¹²⁰, L. Felgioni⁸⁷, C. Feng¹⁴⁰, E. J. Feng³², H. Feng⁹¹, A. B. Fenyuk¹³¹, L. Feremenga⁸, P. Fernandez Martinez¹⁷¹, S. Fernandez Perez¹³, J. Ferrando⁴⁴, A. Ferrari¹⁶⁹, P. Ferrari¹⁰⁸, R. Ferrari^{122a}, D. E. Ferreira de Lima^{60b}, A. Ferrer¹⁷¹, D. Ferrere⁵¹, C. Ferretti⁹¹, A. Ferretto Parodi^{52a,52b}, F. Fiedler⁸⁵, A. Filipčić⁷⁷, M. Filipuzzi⁴⁴, F. Filthaut¹⁰⁷, M. Fincke-Keeler¹⁷³, K. D. Finelli¹⁵³, M. C. N. Fiolhais^{127a,127c}, L. Fiorini¹⁷¹, A. Firan⁴², A. Fischer², C. Fischer¹³, J. Fischer¹⁷⁹, W. C. Fisher⁹², N. Flaschel⁴⁴, I. Fleck¹⁴⁴, P. Fleischmann⁹¹, G. T. Fletcher¹⁴², R. R. M. Fletcher¹²³, T. Flick¹⁷⁹, L. R. Flores Castillo^{62a}, M. J. Flowerdew¹⁰², G. T. Forcolin⁸⁶, A. Formica¹³⁷, A. Forti⁸⁶, A. G. Foster¹⁹, D. Fournier¹¹⁸, H. Fox⁷⁴, S. Fracchia¹³, P. Francavilla⁸², M. Franchini^{22a,22b}, D. Francis³², L. Franconi¹²⁰, M. Franklin⁵⁸, M. Frate¹⁶⁷, M. Fraternali^{122a,122b}, D. Freeborn⁸⁰, S. M. Fressard-Batranceanu³², F. Friedrich⁴⁶, D. Froidevaux³², J. A. Frost¹²¹, C. Fukunaga¹⁵⁹, E. Fullana Torregrosa⁸⁵, T. Fusayasu¹⁰³, J. Fuster¹⁷¹, C. Gabaldon⁵⁷, O. Gabizon¹⁷⁹, A. Gabrielli^{22a,22b}, A. Gabrielli¹⁶, G. P. Gach^{40a}, S. Gadatsch³², S. Gadomski⁷⁹, G. Gagliardi^{52a,52b}, L. G. Gagnon⁹⁶, P. Gagnon⁶³, C. Galea¹⁰⁷, B. Galhardo^{127a,127c}, E. J. Gallas¹²¹, B. J. Gallop¹³², P. Gallus¹²⁹, G. Galster³⁸, K. K. Gan¹¹², J. Gao⁵⁹, Y. Gao⁴⁸, Y. S. Gao^{146,g}, F. M. Garay Walls⁴⁸, C. García¹⁷¹, J. E. García Navarro¹⁷¹, M. Garcia-Sciveres¹⁶, R. W. Gardner³³, N. Garelli¹⁴⁶, V. Garonne¹²⁰, A. Gascon Bravo⁴⁴, K. Gasnikova⁴⁴, C. Gatti⁴⁹, A. Gaudiello^{52a,52b}, G. Gaudio^{122a}, L. Gauthier⁹⁶, I. L. Gavrilenko⁹⁷, C. Gay¹⁷², G. Gaycken²³, E. N. Gazis¹⁰, Z. Gece¹⁷², C. N. P. Gee¹³², Ch. Geich-Gimbel²³, M. Geisen⁸⁵, M. P. Geisler^{60a}, K. Gellerstedt^{149a,149b}, C. Gemme^{52a}, M. H. Genest⁵⁷, C. Geng^{59,p}, S. Gentile^{133a,133b}, C. Gentsos¹⁵⁷, S. George⁷⁹, D. Gerbaudo¹³, A. Gershon¹⁵⁶, S. Ghasemi¹⁴⁴, M. Ghneimat²³, B. Giacobbe^{22a}, S. Giagu^{133a,133b}, P. Giannetti^{125a,125b}, B. Gibbard²⁷, S. M. Gibson⁷⁹, M. Gignac¹⁷², M. Gilchriese¹⁶, T. P. S. Gillam³⁰, D. Gillberg³¹, G. Gilles¹⁷⁹, D. M. Gingrich^{3,d}, N. Giokaris⁹, M. P. Giordani^{168a,168c}, F. M. Giorgi^{22a}, F. M. Giorgi¹⁷, P. F. Giraud¹³⁷, P. Giromini⁵⁸, D. Giugni^{93a}, F. Giuli¹²¹, C. Giuliani¹⁰², M. Giulini^{60b}, B. K. Gjelsten¹²⁰, S. Gkaitatzis¹⁵⁷, I. Gkialas¹⁵⁷, E. L. Gkoukousis¹¹⁸, L. K. Gladilin¹⁰⁰, C. Glasman⁸⁴, J. Glatzer⁵⁰, P. C. F. Glaysheer⁴⁸, A. Glazov⁴⁴, M. Goblirsch-Kolb²⁵, J. Godlewski⁴¹, S. Goldfarb⁹⁰, T. Golling⁵¹, D. Golubkov¹³¹, A. Gomes^{127a,127b,127d}, R. Gonçalo^{127a}, J. Goncalves Pinto Firmino Da Costa¹³⁷, G. Gonella⁵⁰, L. Gonella¹⁹, A. Gongadze⁶⁷, S. González de la Hoz¹⁷¹, G. Gonzalez Parra¹³, S. Gonzalez-Sevilla⁵¹, L. Goossens³², P. A. Gorbounov⁹⁸, H. A. Gordon²⁷, I. Gorelov¹⁰⁶, B. Gorini³², E. Gorini^{75a,75b}, A. Gorišek⁷⁷, E. Gornicki⁴¹, A. T. Goshaw⁴⁷, C. Gössling⁴⁵, M. I. Gostkin⁶⁷, C. R. Goudet¹¹⁸, D. Goujdami^{136c}, A. G. Goussiou¹³⁹, N. Govender^{148b,q}, E. Gozani¹⁵⁵, L. Graber⁵⁶, I. Grabowska-Bold^{40a}, P. O. J. Gradin⁵⁷, P. Grafström^{22a,22b}, J. Gramling⁵¹, E. Gramstad¹²⁰, S. Grancagnolo¹⁷, V. Gratchev¹²⁴, P. M. Gravila^{28e}, H. M. Gray³², E. Graziani^{135a}, Z. D. Greenwood^{81,r}, C. Grefe²³, K. Gregersen⁸⁰, I. M. Gregor⁴⁴, P. Grenier¹⁴⁶, K. Grevtsov⁵, J. Griffiths⁸, A. A. Grillo¹³⁸, K. Grimm⁷⁴, S. Grinstein^{13,s}, Ph. Gris³⁶, J.-F. Grivaz¹¹⁸, S. Groh⁸⁵, J. P. Grohs⁴⁶, E. Gross¹⁷⁶, J. Grosse-Knetter⁵⁶, G. C. Grossi⁸¹, Z. J. Grout⁸⁰, L. Guan⁹¹, W. Guan¹⁷⁷, J. Guenther⁶⁴, F. Guescini⁵¹, D. Guest¹⁶⁷, O. Gueta¹⁵⁶, E. Guido^{52a,52b}, T. Guillemin⁵, S. Guindon², U. Gul⁵⁵, C. Gumpert³², J. Guo¹⁴¹, Y. Guo^{59,p}, R. Gupta⁴², S. Gupta¹²¹, G. Gustavino^{133a,133b}, P. Gutierrez¹¹⁴,

N. G. Gutierrez Ortiz⁸⁰, C. Gutsche⁴⁶, C. Guyot¹³⁷, C. Gwenlan¹²¹, C. B. Gwilliam⁷⁶, A. Haas¹¹¹, C. Haber¹⁶, H. K. Hadavand⁸, N. Haddad^{136c}, A. Hader⁸⁷, S. Hageböck²³, M. Hagihara¹⁶⁵, Z. Hajduk⁴¹, H. Hakobyan^{181,*}, M. Haleem⁴⁴, J. Haley¹¹⁵, G. Halladjian⁹², G. D. Hallewell⁸⁷, K. Hamacher¹⁷⁹, P. Hamal¹¹⁶, K. Hamano¹⁷³, A. Hamilton^{148a}, G. N. Hamity¹⁴², P. G. Hamnett⁴⁴, L. Han⁵⁹, K. Hanagaki^{68,t}, K. Hanawa¹⁵⁸, M. Hance¹³⁸, B. Haney¹²³, P. Hanke^{60a}, R. Hanna¹³⁷, J. B. Hansen³⁸, J. D. Hansen³⁸, M. C. Hansen²³, P. H. Hansen³⁸, K. Hara¹⁶⁵, A. S. Hard¹⁷⁷, T. Harenberg¹⁷⁹, F. Hariri¹¹⁸, S. Harkusha⁹⁴, R. D. Harrington⁴⁸, P. F. Harrison¹⁷⁴, F. Hartjes¹⁰⁸, N. M. Hartmann¹⁰¹, M. Hasegawa⁶⁹, Y. Hasegawa¹⁴³, A. Hasib¹¹⁴, S. Hassani¹³⁷, S. Haug¹⁸, R. Hauser⁹², L. Hauswald⁴⁶, M. Havranek¹²⁸, C. M. Hawkes¹⁹, R. J. Hawkings³², D. Hayakawa¹⁶⁰, D. Hayden⁹², C. P. Hays¹²¹, J. M. Hays⁷⁸, H. S. Hayward⁷⁶, S. J. Haywood¹³², S. J. Head¹⁹, T. Heck⁸⁵, V. Hedberg⁸³, L. Heelan⁸, S. Heim¹²³, T. Heim¹⁶, B. Heinemann¹⁶, J. J. Heinrich¹⁰¹, L. Heinrich¹¹¹, C. Heinz⁵⁴, J. Hejbal¹²⁸, L. Helary³², S. Hellman^{149a,149b}, C. Hensens³², J. Henderson¹²¹, R. C. W. Henderson⁷⁴, Y. Heng¹⁷⁷, S. Henkelmann¹⁷², A. M. Henriques Correia³², S. Henrot-Versille¹¹⁸, G. H. Herbert¹⁷, H. Herde²⁵, V. Herget¹⁷⁸, Y. Hernández Jiménez¹⁷¹, G. Herten⁵⁰, R. Hertenberger¹⁰¹, L. Hervas³², G. G. Hesketh⁸⁰, N. P. Hessey¹⁰⁸, J. W. Hetherly⁴², R. Hickling⁷⁸, E. Higón-Rodríguez¹⁷¹, E. Hill¹⁷³, J. C. Hill³⁰, K. H. Hiller⁴⁴, S. J. Hillier¹⁹, I. Hinchliffe¹⁶, E. Hines¹²³, R. R. Hinman¹⁶, M. Hirose⁵⁰, D. Hirschbuehl¹⁷⁹, J. Hobbs¹⁵¹, N. Hod^{164a}, M. C. Hodgkinson¹⁴², P. Hodgson¹⁴², A. Hoecker³², M. R. Hoferkamp¹⁰⁶, F. Hoenic¹⁰¹, D. Hohn²³, T. R. Holmes¹⁶, M. Homann⁴⁵, T. Honda⁶⁸, T. M. Hong¹²⁶, B. H. Hooberman¹⁷⁰, W. H. Hopkins¹¹⁷, Y. Horii¹⁰⁴, A. J. Horton¹⁴⁵, J.-Y. Hostachy⁵⁷, S. Hou¹⁵⁴, A. Houmada^{136a}, J. Howarth⁴⁴, J. Hoya⁷³, M. Hrabovsky¹¹⁶, I. Hristova¹⁷, J. Hrivnac¹¹⁸, T. Hryn'ova⁵, A. Hrynevich⁹⁵, C. Hsu^{148c}, P. J. Hsu^{154,u}, S.-C. Hsu¹³⁹, Q. Hu⁵⁹, S. Hu¹⁴¹, Y. Huang⁴⁴, Z. Hubacek¹²⁹, F. Hubaut⁸⁷, F. Huegging²³, T. B. Huffman¹²¹, E. W. Hughes³⁷, G. Hughes⁷⁴, M. Huhtinen³², P. Huo¹⁵¹, N. Huseynov^{67,b}, J. Huston⁹², J. Huth⁵⁸, G. Iacobucci⁵¹, G. Iakovidis²⁷, I. Ibragimov¹⁴⁴, L. Iconomidou-Fayard¹¹⁸, E. Ideal¹⁸⁰, Z. Idrissi^{136c}, P. Iengo³², O. Igonkina^{108,v}, T. Iizawa¹⁷⁵, Y. Ikegami⁶⁸, M. Ikeno⁶⁸, Y. Ilchenko^{11,w}, D. Iliadis¹⁵⁷, N. Ilic¹⁴⁶, T. Ince¹⁰², G. Introzzi^{122a,122b}, P. Ioannou^{9,*}, M. Iodice^{135a}, K. Iordanidou³⁷, V. Ippolito⁵⁸, N. Ishijima¹¹⁹, M. Ishino¹⁵⁸, M. Ishitsuka¹⁶⁰, R. Ishmukhametov¹¹², C. Issever¹²¹, S. Istin^{20a}, F. Ito¹⁶⁵, J. M. Iturbe Ponce⁸⁶, R. Iuppa^{163a,163b}, W. Iwanski⁶⁴, H. Iwasaki⁶⁸, J. M. Izen⁴³, V. Izzo^{105a}, S. Jabbar³, B. Jackson¹²³, P. Jackson¹, V. Jain², K. B. Jakobi⁸⁵, K. Jakobs⁵⁰, S. Jakobsen³², T. Jakoubek¹²⁸, D. O. Jamin¹¹⁵, D. K. Jana⁸¹, R. Jansky⁶⁴, J. Janssen²³, M. Janus⁵⁶, G. Jarlskog⁸³, N. Javadov^{67,b}, T. Javůrek⁵⁰, F. Jeanneau¹³⁷, L. Jeanty¹⁶, G.-Y. Jeng¹⁵³, D. Jennens⁹⁰, P. Jenni^{50,x}, C. Jeske¹⁷⁴, S. Jézéquel⁵, H. Ji¹⁷⁷, J. Jia¹⁵¹, H. Jiang⁶⁶, Y. Jiang⁵⁹, S. Jiggins⁸⁰, J. Jimenez Pena¹⁷¹, S. Jin^{35a}, A. Jinaru^{28b}, O. Jinnouchi¹⁶⁰, H. Jivan^{148c}, P. Johansson¹⁴², K. A. Johns⁷, W. J. Johnson¹³⁹, K. Jon-And^{149a,149b}, G. Jones¹⁷⁴, R. W. L. Jones⁷⁴, S. Jones⁷, T. J. Jones⁷⁶, J. Jongmanns^{60a}, P. M. Jorge^{127a,127b}, J. Jovicevic^{164a}, X. Ju¹⁷⁷, A. Juste Rozas^{13,s}, M. K. Köhler¹⁷⁶, A. Kaczmarzka⁴¹, M. Kado¹¹⁸, H. Kagan¹¹², M. Kagan¹⁴⁶, S. J. Kahn⁸⁷, T. Kaji¹⁷⁵, E. Kajomovitz⁴⁷, C. W. Kalderon¹²¹, A. Kaluza⁸⁵, S. Kama⁴², A. Kamenshchikov¹³¹, N. Kanaya¹⁵⁸, S. Kaneti³⁰, L. Kanjir⁷⁷, V. A. Kantserov⁹⁹, J. Kanzaki⁶⁸, B. Kaplan¹¹¹, L. S. Kaplan¹⁷⁷, A. Kapliy³³, D. Kar^{148c}, K. Karakostas¹⁰, A. Karamaoun³, N. Karastathis¹⁰, M. J. Kareem⁵⁶, E. Karentzos¹⁰, M. Karnevskiy⁸⁵, S. N. Karpov⁶⁷, Z. M. Karpova⁶⁷, K. Karthik¹¹¹, V. Kartvelishvili⁷⁴, A. N. Karyukhin¹³¹, K. Kasahara¹⁶⁵, L. Kashif¹⁷⁷, R. D. Kass¹¹², A. Kastanas¹⁵, Y. Kataoka¹⁵⁸, C. Kato¹⁵⁸, A. Katre⁵¹, J. Katzy⁴⁴, K. Kawade¹⁰⁴, K. Kawagoe⁷², T. Kawamoto¹⁵⁸, G. Kawamura⁵⁶, V. F. Kazanin^{110,c}, R. Keeler¹⁷³, R. Kehoe⁴², J. S. Keller⁴⁴, J. J. Kempster⁷⁹, H. Keoshkerian¹⁶², O. Kepka¹²⁸, B. P. Kerševan⁷⁷, S. Kersten¹⁷⁹, R. A. Keyes⁸⁹, M. Khader¹⁷⁰, F. Khalil-zada¹², A. Khanov¹¹⁵, A. G. Kharlamov^{110,c}, T. Kharlamova¹¹⁰, T. J. Khoo⁵¹, V. Khovanskij⁹⁸, E. Khramov⁶⁷, J. Khubua^{53b,y}, S. Kido⁶⁹, C. R. Kilby⁷⁹, H. Y. Kim⁸, S. H. Kim¹⁶⁵, Y. K. Kim³³, N. Kimura¹⁵⁷, O. M. Kind¹⁷, B. T. King⁷⁶, M. King¹⁷¹, J. Kirk¹³², A. E. Kiryunin¹⁰², T. Kishimoto¹⁵⁸, D. Kisielewska^{40a}, F. Kiss⁵⁰, K. Kiuchi¹⁶⁵, O. Kivernyk¹³⁷, E. Kladiva^{147b}, M. H. Klein³⁷, M. Klein⁷⁶, U. Klein⁷⁶, K. Kleinknecht⁸⁵, P. Klimek¹⁰⁹, A. Klimentov²⁷, R. Klingenberg⁴⁵, J. A. Klinger¹⁴², T. Klioutchnikova³², E.-E. Kluge^{60a}, P. Kluit¹⁰⁸, S. Kluth¹⁰², J. Knapik⁴¹, E. Kneringer⁶⁴, E. B. F. G. Knoops⁸⁷, A. Knue⁵⁵, A. Kobayashi¹⁵⁸, D. Kobayashi¹⁶⁰, T. Kobayashi¹⁵⁸, M. Kobel⁴⁶, M. Kocian¹⁴⁶, P. Kodys¹³⁰, N. M. Koehler¹⁰², T. Koffas³¹, E. Koffeman¹⁰⁸, T. Koi¹⁴⁶, H. Kolanoski¹⁷, M. Kolb^{60b}, I. Koletsou⁵, A. A. Komar^{97,*}, Y. Komori¹⁵⁸, T. Kondo⁶⁸, N. Kondrashova⁴⁴, K. Köneke⁵⁰, A. C. König¹⁰⁷, T. Kono^{68,z}, R. Konoplich^{111,aa}, N. Konstantinidis⁸⁰, R. Kopeliansky⁶³, S. Koperny^{40a}, L. Köpke⁸⁵, A. K. Kopp⁵⁰, K. Korcyl⁴¹, K. Kordas¹⁵⁷, A. Korn⁸⁰, A. A. Korol^{110,c}, I. Korolkov¹³, E. V. Korolkova¹⁴², O. Kortner¹⁰², S. Kortner¹⁰², T. Kosek¹³⁰, V. V. Kostyukhin²³, A. Kotwal⁴⁷, A. Kourkoumeli-Charalampidi^{122a,122b}, C. Kourkoumelis⁹, V. Kouskoura²⁷, A. B. Kowalewska⁴¹, R. Kowalewski¹⁷³, T. Z. Kowalski^{40a}, C. Kozakai¹⁵⁸, W. Kozanecki¹³⁷, A. S. Kozhin¹³¹, V. A. Kramarenko¹⁰⁰, G. Kramberger⁷⁷, D. Krasnopevtsev⁹⁹, M. W. Krasny⁸², A. Krasznahorkay³², A. Kravchenko²⁷, M. Kretz^{60c}, J. Kretzschmar⁷⁶, K. Kreutzfeldt⁵⁴, P. Krieger¹⁶², K. Krizka³³, K. Kroeninger⁴⁵, H. Kroha¹⁰², J. Kroll¹²³, J. Kroseberg²³, J. Krstic¹⁴, U. Kruchonak⁶⁷, H. Krüger²³, N. Krumnack⁶⁶, M. C. Kruse⁴⁷, M. Kruskal²⁴, T. Kubota⁹⁰, H. Kucuk⁸⁰, S. Kuday^{4b}, J. T. Kuechler¹⁷⁹, S. Kuehn⁵⁰, A. Kugel^{60c}, F. Kuger¹⁷⁸, A. Kuhl¹³⁸, T. Kuhl⁴⁴, V. Kukhtin⁶⁷, R. Kukla¹³⁷, Y. Kulchitsky⁹⁴, S. Kuleshov^{34b}, M. Kuna^{133a,133b}, T. Kunigo⁷⁰, A. Kupco¹²⁸,

H. Kurashige⁶⁹, Y. A. Kurochkin⁹⁴, V. Kus¹²⁸, E. S. Kuwertz¹⁷³, M. Kuze¹⁶⁰, J. Kvita¹¹⁶, T. Kwan¹⁷³, D. Kyriazopoulos¹⁴², A. La Rosa¹⁰², J. L. La Rosa Navarro^{26d}, L. La Rotonda^{39a,39b}, C. Lacasta¹⁷¹, F. Lacava^{133a,133b}, J. Lacey³¹, H. Lacker¹⁷, D. Lacour⁸², V. R. Lacuesta¹⁷¹, E. Ladygin⁶⁷, R. Lafaye⁵, B. Laforge⁸², T. Lagouri¹⁸⁰, S. Lai⁵⁶, S. Lammers⁶³, W. Lampl⁷, E. Lançon¹³⁷, U. Landgraf⁵⁰, M. P. J. Landon⁷⁸, M. C. Lanfermann⁵¹, V. S. Lang^{60a}, J. C. Lange¹³, A. J. Lankford¹⁶⁷, F. Lanni²⁷, K. Lantzsch²³, A. Lanza^{122a}, S. Laplace⁸², C. Lapoire³², J. F. Laporte¹³⁷, T. Lari^{93a}, F. Lasagni Manghi^{22a,22b}, M. Lassnig³², P. Laurelli⁴⁹, W. Lavrijsen¹⁶, A. T. Law¹³⁸, P. Laycock⁷⁶, T. Lazovich⁵⁸, M. Lazzaroni^{93a,93b}, B. Le⁹⁰, O. Le Dortz⁸², E. Le Guirriec⁸⁷, E. P. Le Quilleuc¹³⁷, M. LeBlanc¹⁷³, T. LeCompte⁶, F. Ledroit-Guillon⁵⁷, C. A. Lee²⁷, S. C. Lee¹⁵⁴, L. Lee¹, B. Lefebvre⁸⁹, G. Lefebvre⁸², M. Lefebvre¹⁷³, F. Legger¹⁰¹, C. Leggett¹⁶, A. Lehan⁷⁶, G. Lehmann Miotto³², X. Lei⁷, W. A. Leight³¹, A. Leisos^{157,ab}, A. G. Leister¹⁸⁰, M. A. L. Leite^{26d}, R. Leitner¹³⁰, D. Lellouch¹⁷⁶, B. Lemmer⁵⁶, K. J. C. Leney⁸⁰, T. Lenz²³, B. Lenzi³², R. Leone⁷, S. Leone^{125a,125b}, C. Leonidopoulos⁴⁸, S. Leontsinis¹⁰, G. Lerner¹⁵², C. Leroy⁹⁶, A. A. J. Lesage¹³⁷, C. G. Lester³⁰, M. Levchenko¹²⁴, J. Levêque⁵, D. Levin⁹¹, L. J. Levinson¹⁷⁶, M. Levy¹⁹, D. Lewis⁷⁸, A. M. Leyko²³, M. Leyton⁴³, B. Li^{59,p}, C. Li⁵⁹, H. Li¹⁵¹, H. L. Li³³, L. Li⁴⁷, L. Li¹⁴¹, Q. Li^{35a}, S. Li⁴⁷, X. Li⁸⁶, Y. Li¹⁴⁴, Z. Liang^{35a}, B. Liberti^{134a}, A. Liblong¹⁶², P. Lichard³², K. Lie¹⁷⁰, J. Liebal²³, W. Liebig¹⁵, A. Limosani¹⁵³, S. C. Lin^{154,ac}, T. H. Lin⁸⁵, B. E. Lindquist¹⁵¹, A. E. Lioni⁵¹, E. Lipeles¹²³, A. Lipniacka¹⁵, M. Lisovsky^{60b}, T. M. Liss¹⁷⁰, A. Lister¹⁷², A. M. Litke¹³⁸, B. Liu^{154,ad}, D. Liu¹⁵⁴, H. Liu⁹¹, H. Liu²⁷, J. Liu⁸⁷, J. B. Liu⁵⁹, K. Liu⁸⁷, L. Liu¹⁷⁰, M. Liu⁴⁷, M. Liu⁵⁹, Y. L. Liu⁵⁹, Y. Liu⁵⁹, M. Livan^{122a,122b}, A. Lleres⁵⁷, J. Llorente Merino^{35a}, S. L. Lloyd⁷⁸, F. Lo Sterzo¹⁵⁴, E. M. Lobodzinska⁴⁴, P. Loch⁷, W. S. Lockman¹³⁸, F. K. Loebinger⁸⁶, A. E. Loevschall-Jensen³⁸, K. M. Loew²⁵, A. Loginov^{180,*}, T. Lohse¹⁷, K. Lohwasser⁴⁴, M. Lokajicek¹²⁸, B. A. Long²⁴, J. D. Long¹⁷⁰, R. E. Long⁷⁴, L. Longo^{75a,75b}, K. A. Looper¹¹², J. A. López^{34b}, D. Lopez Mateos⁵⁸, B. Lopez Paredes¹⁴², I. Lopez Paz¹³, A. Lopez Solis⁸², J. Lorenz¹⁰¹, N. Lorenzo Martinez⁶³, M. Losada²¹, P. J. Lösel¹⁰¹, X. Lou^{35a}, A. Lounis¹¹⁸, J. Love⁶, P. A. Love⁷⁴, H. Lu^{62a}, N. Lu⁹¹, H. J. Lubatti¹³⁹, C. Luci^{133a,133b}, A. Lucotte⁵⁷, C. Luedtke⁵⁰, F. Luehring⁶³, W. Lukas⁶⁴, L. Luminari^{133a}, O. Lundberg^{149a,149b}, B. Lund-Jensen¹⁵⁰, P. M. Luzzi⁸², D. Lynn²⁷, R. Lysak¹²⁸, E. Lytken⁸³, V. Lyubushkin⁶⁷, H. Ma²⁷, L. L. Ma¹⁴⁰, Y. Ma¹⁴⁰, G. Maccarrone⁴⁹, A. Macchiolo¹⁰², C. M. Macdonald¹⁴², B. Maček⁷⁷, J. Machado Miguens^{123,127b}, D. Madaffari⁸⁷, R. Madar³⁶, H. J. Maddocks¹⁶⁹, W. F. Mader⁴⁶, A. Madsen⁴⁴, J. Maeda⁶⁹, S. Maeland¹⁵, T. Maeno²⁷, A. Maevskiy¹⁰⁰, E. Magradze⁵⁶, J. Mahlstedt¹⁰⁸, C. Maiani¹¹⁸, C. Maidantchik^{26a}, A. A. Maier¹⁰², T. Maier¹⁰¹, A. Maio^{127a,127b,127d}, S. Majewski¹¹⁷, Y. Makida⁶⁸, N. Makovec¹¹⁸, B. Malaescu⁸², Pa. Malecki⁴¹, V. P. Maleev¹²⁴, F. Malek⁵⁷, U. Mallik⁶⁵, D. Malon⁶, C. Malone¹⁴⁶, C. Malone³⁰, S. Maltezos¹⁰, S. Malyukov³², J. Mamuzic¹⁷¹, G. Mancini⁴⁹, L. Mandelli^{93a}, I. Mandić⁷⁷, J. Maneira^{127a,127b}, L. Manhaes de Andrade Filho^{26b}, J. Manjarres Ramos^{164b}, A. Mann¹⁰¹, A. Manousos³², B. Mansoulie¹³⁷, J. D. Mansour^{35a}, R. Mantifel⁸⁹, M. Mantoani⁵⁶, S. Manzoni^{93a,93b}, L. Mapelli³², G. Marceca²⁹, L. March⁵¹, G. Marchiori⁸², M. Marcisovsky¹²⁸, M. Marjanovic¹⁴, D. E. Marley⁹¹, F. Marroquim^{26a}, S. P. Marsden⁸⁶, Z. Marshall¹⁶, S. Marti-Garcia¹⁷¹, B. Martin⁹², T. A. Martin¹⁷⁴, V. J. Martin⁴⁸, B. Martin dit Latour¹⁵, M. Martinez^{13,s}, V. I. Martinez Outschoorn¹⁷⁰, S. Martin-Haugh¹³², V. S. Martoiu^{28b}, A. C. Martyniuk⁸⁰, A. Marzin³², L. Masetti⁸⁵, T. Mashimo¹⁵⁸, R. Mashinistov⁹⁷, J. Masik⁸⁶, A. L. Maslennikov^{110,c}, I. Massa^{22a,22b}, L. Massa^{22a,22b}, P. Mastrandrea⁵, A. Mastroberardino^{39a,39b}, T. Masubuchi¹⁵⁸, P. Mättig¹⁷⁹, J. Mattmann⁸⁵, J. Maurer^{28b}, S. J. Maxfield⁷⁶, D. A. Maximov^{110,c}, R. Mazini¹⁵⁴, S. M. Mazza^{93a,93b}, N. C. Mc Fadden¹⁰⁶, G. Mc Goldrick¹⁶², S. P. Mc Kee⁹¹, A. McCarn⁹¹, R. L. McCarthy¹⁵¹, T. G. McCarthy¹⁰², L. I. McClymont⁸⁰, E. F. McDonald⁹⁰, J. A. McFayden⁸⁰, G. Mchedlize⁵⁶, S. J. McMahon¹³², R. A. McPherson^{173,m}, M. Medinnis⁴⁴, S. Meehan¹³⁹, S. Mehlhase¹⁰¹, A. Mehta⁷⁶, K. Meier^{60a}, C. Meineck¹⁰¹, B. Meirose⁴³, D. Melini¹⁷¹, B. R. Mellado Garcia^{148c}, M. Melo^{147a}, F. Meloni¹⁸, A. Mengarelli^{22a,22b}, S. Menke¹⁰², E. Meoni¹⁶⁶, S. Mergelmeyer¹⁷, P. Mermoud⁵¹, L. Merola^{105a,105b}, C. Meroni^{93a}, F. S. Merritt³³, A. Messina^{133a,133b}, J. Metcalfe⁶, A. S. Mete¹⁶⁷, C. Meyer⁸⁵, C. Meyer¹²³, J.-P. Meyer¹³⁷, J. Meyer¹⁰⁸, H. Meyer Zu Theenhausen^{60a}, F. Miano¹⁵², R. P. Middleton¹³², S. Miglioranzi^{52a,52b}, L. Mijović⁴⁸, G. Mikenberg¹⁷⁶, M. Mikestikova¹²⁸, M. Mikuž⁷⁷, M. Milesi⁹⁰, A. Milic⁶⁴, D. W. Miller³³, C. Mills⁴⁸, A. Milov¹⁷⁶, D. A. Milstead^{149a,149b}, A. A. Minaenko¹³¹, Y. Minami¹⁵⁸, I. A. Minashvili⁶⁷, A. I. Mincer¹¹¹, B. Mindur^{40a}, M. Mineev⁶⁷, Y. Minegishi¹⁵⁸, Y. Ming¹⁷⁷, L. M. Mir¹³, K. P. Mistry¹²³, T. Mitani¹⁷⁵, J. Mitrevski¹⁰¹, V. A. Mitsou¹⁷¹, A. Miucci¹⁸, P. S. Miyagawa¹⁴², J. U. Mjörnmark⁸³, M. Mlynarikova¹³⁰, T. Moa^{149a,149b}, K. Mochizuki⁹⁶, S. Mohapatra³⁷, S. Molander^{149a,149b}, R. Moles-Valls²³, R. Monden⁷⁰, M. C. Mondragon⁹², K. Mönig⁴⁴, J. Monk³⁸, E. Monnier⁸⁷, A. Montalbano¹⁵¹, J. Montejo Berlingen³², F. Monticelli⁷³, S. Monzani^{93a,93b}, R. W. Moore³, N. Morange¹¹⁸, D. Moreno²¹, M. Moreno Llácer⁵⁶, P. Morettini^{52a}, S. Morgenstern³², D. Mori¹⁴⁵, T. Mori¹⁵⁸, M. Morii⁵⁸, M. Morinaga¹⁵⁸, V. Morisbak¹²⁰, S. Moritz⁸⁵, A. K. Morley¹⁵³, G. Mornacchi³², J. D. Morris⁷⁸, S. S. Mortensen³⁸, L. Morvaj¹⁵¹, M. Mosidze^{53b}, J. Moss^{146,ae}, K. Motohashi¹⁶⁰, R. Mount¹⁴⁶, E. Mountricha²⁷, E. J. W. Moyses⁸⁸, S. Muanza⁸⁷, R. D. Mudd¹⁹, F. Mueller¹⁰², J. Mueller¹²⁶, R. S. P. Mueller¹⁰¹, T. Mueller³⁰, D. Muenstermann⁷⁴, P. Mullen⁵⁵, G. A. Mullier¹⁸, F. J. Munoz Sanchez⁸⁶, J. A. Murillo Quijada¹⁹, W. J. Murray^{174,132}, H. Musheghyan⁵⁶, M. Muškinja⁷⁷, A. G. Myagkov^{131,af}, M. Myska¹²⁹, B. P. Nachman¹⁴⁶,

O. Nackenhorst⁵¹, K. Nagai¹²¹, R. Nagai^{68,z}, K. Nagano⁶⁸, Y. Nagasaka⁶¹, K. Nagata¹⁶⁵, M. Nagel⁵⁰, E. Nagy⁸⁷, A. M. Nairz³², Y. Nakahama¹⁰⁴, K. Nakamura⁶⁸, T. Nakamura¹⁵⁸, I. Nakano¹¹³, H. Namasivayam⁴³, R. F. Naranjo Garcia⁴⁴, R. Narayan¹¹, D. I. Narrias Villar^{60a}, I. Naryshkin¹²⁴, T. Naumann⁴⁴, G. Navarro²¹, R. Nayyar⁷, H. A. Neal⁹¹, P. Yu. Nechaeva⁹⁷, T. J. Neep⁸⁶, A. Negri^{122a,122b}, M. Negrini^{22a}, S. Nektarijevic¹⁰⁷, C. Nellist¹¹⁸, A. Nelson¹⁶⁷, S. Nemecek¹²⁸, P. Nemethy¹¹¹, A. A. Nepomuceno^{26a}, M. Nessi^{32,ag}, M. S. Neubauer¹⁷⁰, M. Neumann¹⁷⁹, R. M. Neves¹¹¹, P. Nevski²⁷, P. R. Newman¹⁹, D. H. Nguyen⁶, T. Nguyen Manh⁹⁶, R. B. Nickerson¹²¹, R. Nicolaidou¹³⁷, J. Nielsen¹³⁸, A. Nikiforov¹⁷, V. Nikolaenko^{131,af}, I. Nikolic-Audit⁸², K. Nikolopoulos¹⁹, J. K. Nilsen¹²⁰, P. Nilsson²⁷, Y. Ninomiya¹⁵⁸, A. Nisati^{133a}, R. Nisius¹⁰², T. Nobe¹⁵⁸, M. Nomachi¹¹⁹, I. Nomidis³¹, T. Nooney⁷⁸, S. Norberg¹¹⁴, M. Nordberg³², N. Norjoharuddeen¹²¹, O. Novgorodova⁴⁶, S. Nowak¹⁰², M. Nozaki⁶⁸, L. Nozka¹¹⁶, K. Ntekas¹⁶⁷, E. Nurse⁸⁰, F. Nuti⁹⁰, F. O'grady⁷, D. C. O'Neil¹⁴⁵, A. A. O'Rourke⁴⁴, V. O'Shea⁵⁵, F. G. Oakham^{31,d}, H. Oberlack¹⁰², T. Obermann²³, J. Ocariz⁸², A. Ochi⁶⁹, I. Ochoa³⁷, J. P. Ochoa-Ricoux^{34a}, S. Oda⁷², S. Odaka⁶⁸, H. Ogren⁶³, A. Oh⁸⁶, S. H. Oh⁴⁷, C. C. Ohm¹⁶, H. Ohman¹⁶⁹, H. Oide³², H. Okawa¹⁶⁵, Y. Okumura¹⁵⁸, T. Okuyama⁶⁸, A. Olariu^{28b}, L. F. Oleiro Seabra^{127a}, S. A. Olivares Pino⁴⁸, D. Oliveira Damazio²⁷, A. Olszewski⁴¹, J. Olszowska⁴¹, A. Onofre^{127a,127e}, K. Onogi¹⁰⁴, P. U. E. Onyisi^{11,w}, M. J. Oreglia³³, Y. Oren¹⁵⁶, D. Orestano^{135a,135b}, N. Orlando^{62b}, R. S. Orr¹⁶², B. Osculati^{52a,52b,*}, R. Ospanov⁸⁶, G. Otero y Garzon²⁹, H. Otono⁷², M. Ouchrif^{136d}, F. Ould-Saada¹²⁰, A. Ouraou¹³⁷, K. P. Oussoren¹⁰⁸, Q. Ouyang^{35a}, M. Owen⁵⁵, R. E. Owen¹⁹, V. E. Ozcan^{20a}, N. Ozturk⁸, K. Pachal¹⁴⁵, A. Pacheco Pages¹³, L. Pacheco Rodriguez¹³⁷, C. Padilla Aranda¹³, M. Pagáčová⁵⁰, S. Pagan Griso¹⁶, M. Paganini¹⁸⁰, F. Paige²⁷, P. Pais⁸⁸, K. Pajchel¹²⁰, G. Palacino^{164b}, S. Palazzo^{39a,39b}, S. Palestini³², M. Palka^{40b}, D. Pallin³⁶, E. St. Panagiotopoulou¹⁰, C. E. Pandini⁸², J. G. Panduro Vazquez⁷⁹, P. Pani^{149a,149b}, S. Panitkin²⁷, D. Pantea^{28b}, L. Paolozzi⁵¹, Th. D. Papadopoulou¹⁰, K. Papageorgiou¹⁵⁷, A. Paramonov⁶, D. Paredes Hernandez¹⁸⁰, A. J. Parker⁷⁴, M. A. Parker³⁰, K. A. Parker¹⁴², F. Parodi^{52a,52b}, J. A. Parsons³⁷, U. Parzefall⁵⁰, V. R. Pascuzzi¹⁶², E. Pasqualucci^{133a}, S. Passaggio^{52a}, Fr. Pastore⁷⁹, G. Pásztor^{31,ah}, S. Patarraia¹⁷⁹, J. R. Pater⁸⁶, T. Pauly³², J. Pearce¹⁷³, B. Pearson¹¹⁴, L. E. Pedersen³⁸, M. Pedersen¹²⁰, S. Pedraza Lopez¹⁷¹, R. Pedro^{127a,127b}, S. V. Peleganchuk^{110,c}, O. Penc¹²⁸, C. Peng^{35a}, H. Peng⁵⁹, J. Penwell⁶³, B. S. Peralva^{26b}, M. M. Perego¹³⁷, D. V. Perepelitsa²⁷, E. Perez Codina^{164a}, L. Perini^{93a,93b}, H. Pernegger³², S. Perrella^{105a,105b}, R. Peschke⁴⁴, V. D. Peshekhonov⁶⁷, K. Peters⁴⁴, R. F. Y. Peters⁸⁶, B. A. Petersen³², T. C. Petersen³⁸, E. Petit⁵⁷, A. Petridis¹, C. Petridou¹⁵⁷, P. Petroff¹¹⁸, E. Petrolo^{133a}, M. Petrov¹²¹, F. Petrucci^{135a,135b}, N. E. Pettersson⁸⁸, A. Peyaud¹³⁷, R. Pezoa^{34b}, P. W. Phillips¹³², G. Piacquadio^{146,ai}, E. Pianori¹⁷⁴, A. Picazio⁸⁸, E. Piccaro⁷⁸, M. Piccinini^{22a,22b}, M. A. Pickering¹²¹, R. Piegai²⁹, J. E. Pilcher³³, A. D. Pilkington⁸⁶, A. W. J. Pin⁸⁶, M. Pinamonti^{168a,168c,aj}, J. L. Pinfold³, A. Pingel³⁸, S. Pires⁸², H. Pirumov⁴⁴, M. Pitt¹⁷⁶, L. Plazak^{147a}, M.-A. Pleier²⁷, V. Pleskot⁸⁵, E. Plotnikova⁶⁷, P. Plucinski⁹², D. Pluth⁶⁶, R. Poettgen^{149a,149b}, L. Poggioli¹¹⁸, D. Pohl²³, G. Polesello^{122a}, A. Poley⁴⁴, A. Policicchio^{39a,39b}, R. Polifka¹⁶², A. Polini^{22a}, C. S. Pollard⁵⁵, V. Polychronakos²⁷, K. Pommès³², L. Pontecorvo^{133a}, B. G. Pope⁹², G. A. Popeneciu^{28c}, A. Poppleton³², S. Pospisil¹²⁹, K. Potamianos¹⁶, I. N. Potrap⁶⁷, C. J. Potter³⁰, C. T. Potter¹¹⁷, G. Poulard³², J. Poveda³², V. Pozdnyakov⁶⁷, M. E. Pozo Astigarraga³², P. Pralavorio⁸⁷, A. Pranko¹⁶, S. Prell⁶⁶, D. Price⁸⁶, L. E. Price⁶, M. Primavera^{75a}, S. Prince⁸⁹, K. Prokofiev^{62c}, F. Prokoshin^{34b}, S. Protopopescu²⁷, J. Proudfoot⁶, M. Przybycien^{40a}, D. Puddu^{135a,135b}, M. Purohit^{27,ak}, P. Puzo¹¹⁸, J. Qian⁹¹, G. Qin⁵⁵, Y. Qin⁸⁶, A. Quadt⁵⁶, W. B. Quayle^{168a,168b}, M. Queitsch-Maitland⁸⁶, D. Quilty⁵⁵, S. Raddum¹²⁰, V. Radeka²⁷, V. Radescu¹²¹, S. K. Radhakrishnan¹⁵¹, P. Radloff¹¹⁷, P. Rados⁹⁰, F. Ragusa^{93a,93b}, G. Rahal¹⁸², J. A. Raine⁸⁶, S. Rajagopalan²⁷, M. Rammensee³², C. Rangel-Smith¹⁶⁹, M. G. Ratti^{93a,93b}, F. Rauscher¹⁰¹, S. Rave⁸⁵, T. Ravenscroft⁵⁵, I. Ravinovich¹⁷⁶, M. Raymond³², A. L. Read¹²⁰, N. P. Readioff⁷⁶, M. Reale^{75a,75b}, D. M. Rebuffi^{122a,122b}, A. Redelbach¹⁷⁸, G. Redlinger²⁷, R. Reece¹³⁸, R. G. Reed^{148c}, K. Reeves⁴³, L. Rehnisch¹⁷, J. Reichert¹²³, A. Reiss⁸⁵, C. Rember³², H. Ren^{35a}, M. Rescigno^{133a}, S. Resconi^{93a}, O. L. Rezanova^{110,c}, P. Reznicek¹³⁰, R. Rezvani⁹⁶, R. Richter¹⁰², S. Richter⁸⁰, E. Richter-Was^{40b}, O. Ricken²³, M. Ridel⁸², P. Rieck¹⁷, C. J. Riegel¹⁷⁹, J. Rieger⁵⁶, O. Rifki¹¹⁴, M. Rijssenbeek¹⁵¹, A. Rimoldi^{122a,122b}, M. Rimoldi¹⁸, L. Rinaldi^{22a}, B. Ristić⁵¹, E. Ritsch³², I. Riu¹³, F. Rizatdinova¹¹⁵, E. Rizvi⁷⁸, C. Rizzi¹³, S. H. Robertson^{89,m}, A. Robichaud-Veronneau⁸⁹, D. Robinson³⁰, J. E. M. Robinson⁴⁴, A. Robson⁵⁵, C. Roda^{125a,125b}, Y. Rodina⁸⁷, A. Rodriguez Perez¹³, D. Rodriguez Rodriguez¹⁷¹, S. Roe³², C. S. Rogan⁵⁸, O. Røhne¹²⁰, A. Romaniouk⁹⁹, M. Romano^{22a,22b}, S. M. Romano Saez³⁶, E. Romero Adam¹⁷¹, N. Rompotis¹³⁹, M. Ronzani⁵⁰, L. Roos⁸², E. Ros¹⁷¹, S. Rosati^{133a}, K. Rosbach⁵⁰, P. Rose¹³⁸, N.-A. Rosien⁵⁶, V. Rossetti^{149a,149b}, E. Rossi^{105a,105b}, L. P. Rossi^{52a}, J. H. N. Rosten³⁰, R. Rosten¹³⁹, M. Rotaru^{28b}, I. Roth¹⁷⁶, J. Rothberg¹³⁹, D. Rousseau¹¹⁸, A. Rozanov⁸⁷, Y. Rozen¹⁵⁵, X. Ruan^{148c}, F. Rubbo¹⁴⁶, M. S. Rudolph¹⁶², F. Rühr⁵⁰, A. Ruiz-Martinez³¹, Z. Rurikova⁵⁰, N. A. Rusakovich⁶⁷, A. Ruschke¹⁰¹, H. L. Russell¹³⁹, J. P. Rutherford⁷, N. Ruthmann³², Y. F. Ryabov¹²⁴, M. Rybar¹⁷⁰, G. Rybkin¹¹⁸, S. Ryu⁶, A. Ryzhov¹³¹, G. F. Rzehorz⁵⁶, A. F. Saavedra¹⁵³, G. Sabato¹⁰⁸, S. Sacerdoti²⁹, H. F.-W. Sadrozinski¹³⁸, R. Sadykov⁶⁷, F. Safai Tehrani^{133a}, P. Saha¹⁰⁹, M. Sahinsoy^{60a}, M. Saimpert¹³⁷, T. Saito¹⁵⁸, H. Sakamoto¹⁵⁸, Y. Sakurai¹⁷⁵, G. Salamanna^{135a,135b}, A. Salamon^{134a,134b}, J. E. Salazar Loyola^{34b}, D. Salek¹⁰⁸, P. H. Sales De Bruin¹³⁹, D. Salihagic¹⁰²,

A. Salnikov¹⁴⁶, J. Salt¹⁷¹, D. Salvatore^{39a,39b}, F. Salvatore¹⁵², A. Salvucci^{62a,62b,62c}, A. Salzburger³², D. Sammel⁵⁰, D. Sampsonidis¹⁵⁷, A. Sanchez^{105a,105b}, J. Sánchez¹⁷¹, V. Sanchez Martinez¹⁷¹, H. Sandaker¹²⁰, R. L. Sandbach⁷⁸, H. G. Sander⁸⁵, M. Sandhoff¹⁷⁹, C. Sandoval²¹, D. P. C. Sankey¹³², M. Sannino^{52a,52b}, A. Sansoni⁴⁹, C. Santoni³⁶, R. Santonico^{134a,134b}, H. Santos^{127a}, I. Santoyo Castillo¹⁵², K. Sapp¹²⁶, A. Saponov⁶⁷, J. G. Saraiva^{127a,127d}, B. Sarrazin²³, O. Sasaki⁶⁸, K. Sato¹⁶⁵, E. Sauvan⁵, G. Savage⁷⁹, P. Savard^{162,d}, N. Savic¹⁰², C. Sawyer¹³², L. Sawyer^{81,r}, J. Saxon³³, C. Sbarra^{22a}, A. Sbrizzi^{22a,22b}, T. Scanlon⁸⁰, D. A. Scannicchio¹⁶⁷, M. Scarcella¹⁵³, V. Scarfone^{39a,39b}, J. Schaarschmidt¹⁷⁶, P. Schacht¹⁰², B. M. Schachtner¹⁰¹, D. Schaefer³², L. Schaefer¹²³, R. Schaefer⁴⁴, J. Schaeffer⁸⁵, S. Schaepe²³, S. Schaezel^{60b}, U. Schäfer⁸⁵, A. C. Schaffer¹¹⁸, D. Schaile¹⁰¹, R. D. Schamberger¹⁵¹, V. Scharf^{60a}, V. A. Schegelsky¹²⁴, D. Scheirich¹³⁰, M. Schernau¹⁶⁷, C. Schiavi^{52a,52b}, S. Schier¹³⁸, C. Schillo⁵⁰, M. Schioppa^{39a,39b}, S. Schlenker³², K. R. Schmidt-Sommerfeld¹⁰², K. Schmieden³², C. Schmitt⁸⁵, S. Schmitt⁴⁴, S. Schmitz⁸⁵, B. Schneider^{164a}, U. Schnoor⁵⁰, L. Schoeffel¹³⁷, A. Schoening^{60b}, B. D. Schoenrock⁹², E. Schopf²³, M. Schott⁸⁵, J. F. P. Schouwenberg¹⁰⁷, J. Schovancova⁸, S. Schramm⁵¹, M. Schreyer¹⁷⁸, N. Schuh⁸⁵, A. Schulte⁸⁵, M. J. Schultens²³, H.-C. Schultz-Coulon^{60a}, H. Schulz¹⁷, M. Schumacher⁵⁰, B. A. Schumm¹³⁸, Ph. Schune¹³⁷, A. Schwartzman¹⁴⁶, T. A. Schwarz⁹¹, H. Schweiger⁸⁶, Ph. Schwemling¹³⁷, R. Schwienhorst⁹², J. Schwindling¹³⁷, T. Schwindt²³, G. Sciolla²⁵, F. Scuri^{125a,125b}, F. Scutti⁹⁰, J. Searcy⁹¹, P. Seema²³, S. C. Seidel¹⁰⁶, A. Seiden¹³⁸, F. Seifert¹²⁹, J. M. Seixas^{26a}, G. Sekhniaidze^{105a}, K. Sekhon⁹¹, S. J. Sekula⁴², D. M. Seliverstov^{124,*}, N. Semprini-Cesari^{22a,22b}, C. Serfon¹²⁰, L. Serin¹¹⁸, L. Serkin^{168a,168b}, M. Sessa^{135a,135b}, R. Seuster¹⁷³, H. Severini¹¹⁴, T. Sfiligoj⁷⁷, F. Sforza³², A. Sfyrla⁵¹, E. Shabalina⁵⁶, N. W. Shaikh^{149a,149b}, L. Y. Shan^{35a}, R. Shang¹⁷⁰, J. T. Shank²⁴, M. Shapiro¹⁶, P. B. Shatalov⁹⁸, K. Shaw^{168a,168b}, S. M. Shaw⁸⁶, A. Shcherbakova^{149a,149b}, C. Y. Shehu¹⁵², P. Sherwood⁸⁰, L. Shi^{154,al}, S. Shimizu⁶⁹, C. O. Shimmin¹⁶⁷, M. Shimojima¹⁰³, S. Shirabe⁷², M. Shiyakova^{67,am}, A. Shmeleva⁹⁷, D. Shoaleh Saadi⁹⁶, M. J. Shochet³³, S. Shojaii^{93a,93b}, D. R. Shope¹¹⁴, S. Shrestha¹¹², E. Shulga⁹⁹, M. A. Shupe⁷, P. Sicho¹²⁸, A. M. Sickles¹⁷⁰, P. E. Sidebo¹⁵⁰, O. Sidiropoulou¹⁷⁸, D. Sidorov¹¹⁵, A. Sidoti^{22a,22b}, F. Siegert⁴⁶, Dj. Sijacki¹⁴, J. Silva^{127a,127d}, S. B. Silverstein^{149a}, V. Simak¹²⁹, Lj. Simic¹⁴, S. Simion¹¹⁸, E. Simioni⁸⁵, B. Simmons⁸⁰, D. Simon³⁶, M. Simon⁸⁵, P. Sinervo¹⁶², N. B. Sinev¹¹⁷, M. Sioli^{22a,22b}, G. Siragusa¹⁷⁸, I. Siral⁹¹, S. Yu. Sivoklov¹⁰⁰, J. Sjölin^{149a,149b}, M. B. Skinner⁷⁴, H. P. Skottowe⁵⁸, P. Skubic¹¹⁴, M. Slater¹⁹, T. Slavicek¹²⁹, M. Slawinska¹⁰⁸, K. Sliwa¹⁶⁶, R. Slovak¹³⁰, V. Smakhtin¹⁷⁶, B. H. Smart⁵, L. Smestad¹⁵, J. Smiesko^{147a}, S. Yu. Smirnov⁹⁹, Y. Smirnov⁹⁹, L. N. Smirnova^{100,an}, O. Smirnova⁸³, M. N. K. Smith³⁷, R. W. Smith³⁷, M. Smizanska⁷⁴, K. Smolek¹²⁹, A. A. Snesarev⁹⁷, I. M. Snyder¹¹⁷, S. Snyder²⁷, R. Sobie^{173,m}, F. Socher⁴⁶, A. Soffer¹⁵⁶, D. A. Soh¹⁵⁴, G. Sokhrannyi⁷⁷, C. A. Solans Sanchez³², M. Solar¹²⁹, E. Yu. Soldatov⁹⁹, U. Soldevila¹⁷¹, A. A. Solodkov¹³¹, A. Soloshenko⁶⁷, O. V. Solovyanov¹³¹, V. Solovye¹²⁴, P. Sommer⁵⁰, H. Son¹⁶⁶, H. Y. Song^{59,ao}, A. Sood¹⁶, A. Sopczak¹²⁹, V. Sopko¹²⁹, V. Sorin¹³, D. Sosa^{60b}, C. L. Sotiropoulou^{125a,125b}, R. Soualah^{168a,168c}, A. M. Soukharev^{110,c}, D. South⁴⁴, B. C. Sowden⁷⁹, S. Spagnolo^{75a,75b}, M. Spalla^{125a,125b}, M. Spangenberg¹⁷⁴, F. Spanò⁷⁹, D. Sperlich¹⁷, F. Spettel¹⁰², R. Spighi^{22a}, G. Spigo³², L. A. Spiller⁹⁰, M. Spousta¹³⁰, R. D. St. Denis^{55,*}, A. Stabile^{93a}, R. Stamen^{60a}, S. Stamm¹⁷, E. Stanecka⁴¹, R. W. Stanek⁶, C. Stanescu^{135a}, M. Stanescu-Bellu⁴⁴, M. M. Stanitzki⁴⁴, S. Stapnes¹²⁰, E. A. Starchenko¹³¹, G. H. Stark³³, J. Stark⁵⁷, P. Staroba¹²⁸, P. Starovoitov^{60a}, S. Stärz³², R. Staszewski⁴¹, P. Steinberg²⁷, B. Stelzer¹⁴⁵, H. J. Stelzer³², O. Stelzer-Chilton^{164a}, H. Stenzel⁵⁴, G. A. Stewart⁵⁵, J. A. Stillings²³, M. C. Stockton⁸⁹, M. Stoebe⁸⁹, G. Stoicea^{28b}, P. Stolte⁵⁶, S. Stonjek¹⁰², A. R. Stradling⁸, A. Straessner⁴⁶, M. E. Stramaglia¹⁸, J. Strandberg¹⁵⁰, S. Strandberg^{149a,149b}, A. Strandlie¹²⁰, M. Strauss¹¹⁴, P. Strizenec^{147b}, R. Ströhmer¹⁷⁸, D. M. Strom¹¹⁷, R. Stroynowski⁴², A. Strubig¹⁰⁷, S. A. Stucci²⁷, B. Stugu¹⁵, N. A. Styles⁴⁴, D. Su¹⁴⁶, J. Su¹²⁶, S. Suchek^{60a}, Y. Sugaya¹¹⁹, M. Suk¹²⁹, V. V. Sulin⁹⁷, S. Sultansoy^{4c}, T. Sumida⁷⁰, S. Sun⁵⁸, X. Sun^{35a}, J. E. Sundermann⁵⁰, K. Suruliz¹⁵², G. Susinno^{39a,39b}, M. R. Sutton¹⁵², S. Suzuki⁶⁸, M. Svatos¹²⁸, M. Swiatlowski³³, I. Sykora^{147a}, T. Sykora¹³⁰, D. Ta⁵⁰, C. Taccini^{135a,135b}, K. Tackmann⁴⁴, J. Taenzer¹⁶², A. Taffard¹⁶⁷, R. Tafirout^{164a}, N. Taiblum¹⁵⁶, H. Takai²⁷, R. Takashima⁷¹, T. Takeshita¹⁴³, Y. Takubo⁶⁸, M. Talby⁸⁷, A. A. Talyshev^{110,c}, K. G. Tan⁹⁰, J. Tanaka¹⁵⁸, M. Tanaka¹⁶⁰, R. Tanaka¹¹⁸, S. Tanaka⁶⁸, R. Tanioka⁶⁹, B. B. Tannenwald¹¹², S. Tapia Araya^{34b}, S. Tapprogge⁸⁵, S. Tarem¹⁵⁵, G. F. Tartarelli^{93a}, P. Tas¹³⁰, M. Tasevsky¹²⁸, T. Tashiro⁷⁰, E. Tassi^{39a,39b}, A. Tavares Delgado^{127a,127b}, Y. Tayalati^{136e}, A. C. Taylor¹⁰⁶, G. N. Taylor⁹⁰, P. T. E. Taylor⁹⁰, W. Taylor^{164b}, F. A. Teischinger³², P. Teixeira-Dias⁷⁹, K. K. Temming⁵⁰, D. Temple¹⁴⁵, H. Ten Kate³², P. K. Teng¹⁵⁴, J. J. Teoh¹¹⁹, F. Tepel¹⁷⁹, S. Terada⁶⁸, K. Terashi¹⁵⁸, J. Terron⁸⁴, S. Terzo¹³, M. Testa⁴⁹, R. J. Teuscher^{162,m}, T. Theveneaux-Pelzer⁸⁷, J. P. Thomas¹⁹, J. Thomas-Wilsker⁷⁹, E. N. Thompson³⁷, P. D. Thompson¹⁹, A. S. Thompson⁵⁵, L. A. Thomsen¹⁸⁰, E. Thomson¹²³, M. Thomson³⁰, M. J. Tibbetts¹⁶, R. E. Ticse Torres⁸⁷, V. O. Tikhomirov^{97,ap}, Yu. A. Tikhonov^{110,c}, S. Timoshenko⁹⁹, P. Tipton¹⁸⁰, S. Tisserant⁸⁷, K. Todome¹⁶⁰, T. Todorov^{5,*}, S. Todorova-Nova¹³⁰, J. Tojo⁷², S. Tokár^{147a}, K. Tokushuku⁶⁸, E. Tolley⁵⁸, L. Tomlinson⁸⁶, M. Tomoto¹⁰⁴, L. Tompkins^{146,aq}, K. Toms¹⁰⁶, B. Tong⁵⁸, P. Tornambe⁵⁰, E. Torrence¹¹⁷, H. Torres¹⁴⁵, E. Torró Pastor¹³⁹, J. Toth^{87,ar}, F. Touchard⁸⁷, D. R. Tovey¹⁴², T. Trefzger¹⁷⁸, A. Tricoli²⁷, I. M. Trigger^{164a}, S. Trincaz-Duvold⁸², M. F. Tripiana¹³, W. Trischuk¹⁶², B. Trocme⁵⁷, A. Trofymov⁴⁴, C. Troncon^{93a}, M. Trottier-McDonald¹⁶, M. Trovatelli¹⁷³, L. Truong^{168a,168c}, M. Trzebinski⁴¹

A. Trzupek⁴¹, J. C.-L. Tseng¹²¹, P. V. Tsiarehka⁹⁴, G. Tsipolitis¹⁰, N. Tsirintanis⁹, S. Tsiskaridze¹³, V. Tsiskaridze⁵⁰, E. G. Tskhadadze^{53a}, K. M. Tsui^{62a}, I. I. Tsukerman⁹⁸, V. Tsulaia¹⁶, S. Tsuno⁶⁸, D. Tsybychev¹⁵¹, Y. Tu^{62b}, A. Tudorache^{28b}, V. Tudorache^{28b}, A. N. Tuna⁵⁸, S. A. Tuppuri^{22a,22b}, S. Turchikhin⁶⁷, D. Turecek¹²⁹, D. Turgeman¹⁷⁶, R. Turra^{93a,93b}, P. M. Tuts³⁷, M. Tyndel¹³², G. Ucchielli^{22a,22b}, I. Ueda¹⁵⁸, M. Ughetto^{149a,149b}, F. Ukegawa¹⁶⁵, G. Unal³², A. Undrus²⁷, G. Unel¹⁶⁷, F. C. Ungaro⁹⁰, Y. Unno⁶⁸, C. Unverdorben¹⁰¹, J. Urban^{147b}, P. Urquijo⁹⁰, P. Urrejola⁸⁵, G. Usai⁸, L. Vacavant⁸⁷, V. Vacek¹²⁹, B. Vachon⁸⁹, C. Valderanis¹⁰¹, E. Valdes Santurio^{149a,149b}, N. Valencic¹⁰⁸, S. Valentineti^{22a,22b}, A. Valero¹⁷¹, L. Valery¹³, S. Valkar¹³⁰, J. A. Valls Ferrer¹⁷¹, W. Van Den Wollenberg¹⁰⁸, P. C. Van Der Deijl¹⁰⁸, H. van der Graaf¹⁰⁸, N. van Eldik¹⁵⁵, P. van Gemmeren⁶, J. Van Nieuwkoop¹⁴⁵, I. van Vulpen¹⁰⁸, M. C. van Woerden³², M. Vanadia^{133a,133b}, W. Vandelli³², R. Vanguri¹²³, A. Vaniachine¹⁶¹, P. Vankov¹⁰⁸, G. Vardanyan¹⁸¹, R. Vari^{133a}, E. W. Varnes⁷, T. Varol⁴², D. Varouchas⁸², A. Vartapetian⁸, K. E. Varvell¹⁵³, J. G. Vasquez¹⁸⁰, G. A. Vasquez^{34b}, F. Vazeille³⁶, T. Vazquez Schroeder⁸⁹, J. Veatch⁵⁶, V. Veeraraghavan⁷, L. M. Veloce¹⁶², F. Veloso^{127a,127c}, S. Veneziano^{133a}, A. Ventura^{75a,75b}, M. Venturi¹⁷³, N. Venturi¹⁶², A. Venturini²⁵, V. Vercesi^{122a}, M. Verducci^{133a,133b}, W. Verkerke¹⁰⁸, J. C. Vermeulen¹⁰⁸, A. Vest^{46,as}, M. C. Vetterli^{145,d}, O. Viazlo⁸³, I. Vichou^{170,*}, T. Vickey¹⁴², O. E. Vickey Boeriu¹⁴², G. H. A. Viehhauser¹²¹, S. Viel¹⁶, L. Vigani¹²¹, M. Villa^{22a,22b}, M. Villaplana Perez^{93a,93b}, E. Vilucchi⁴⁹, M. G. Vincker³¹, V. B. Vinogradov⁶⁷, C. Vittori^{22a,22b}, I. Vivarelli¹⁵², S. Vlachos¹⁰, M. Vlasak¹²⁹, M. Vogel¹⁷⁹, P. Vokac¹²⁹, G. Volpi^{125a,125b}, M. Volpi⁹⁰, H. von der Schmitt¹⁰², E. von Toerne²³, V. Vorobel¹³⁰, K. Vorobev⁹⁹, M. Vos¹⁷¹, R. Voss³², J. H. Vossebeld⁷⁶, N. Vranjes¹⁴, M. Vranjes Milosavljevic¹⁴, V. Vrba¹²⁸, M. Vreeswijk¹⁰⁸, R. Vuillemet³², I. Vukotic³³, Z. Vykydal¹²⁹, P. Wagner²³, W. Wagner¹⁷⁹, H. Wahlberg⁷³, S. Wahrenmund⁴⁶, J. Wakabayashi¹⁰⁴, J. Walder⁷⁴, R. Walker¹⁰¹, W. Walkowiak¹⁴⁴, V. Wallangen^{149a,149b}, C. Wang^{35b}, C. Wang^{140,87}, F. Wang¹⁷⁷, H. Wang¹⁶, H. Wang⁴², J. Wang⁴⁴, J. Wang¹⁵³, K. Wang⁸⁹, R. Wang⁶, S. M. Wang¹⁵⁴, T. Wang²³, T. Wang³⁷, W. Wang⁵⁹, X. Wang¹⁸⁰, C. Wanotayaroj¹¹⁷, A. Warburton⁸⁹, C. P. Ward³⁰, D. R. Wardrop⁸⁰, A. Washbrook⁴⁸, P. M. Watkins¹⁹, A. T. Watson¹⁹, M. F. Watson¹⁹, G. Watts¹³⁹, S. Watts⁸⁶, B. M. Waugh⁸⁰, S. Webb⁸⁵, M. S. Weber¹⁸, S. W. Weber¹⁷⁸, S. A. Weber³¹, J. S. Webster⁶, A. R. Weidberg¹²¹, B. Weinert⁶³, J. Weingarten⁵⁶, C. Weiser⁵⁰, H. Weits¹⁰⁸, P. S. Wells³², T. Wenaus²⁷, T. Wengler³², S. Wenig³², N. Wermes²³, M. Werner⁵⁰, M. D. Werner⁶⁶, P. Werner³², M. Wessels^{60a}, J. Wetter¹⁶⁶, K. Whalen¹¹⁷, N. L. Whallon¹³⁹, A. M. Wharton⁷⁴, A. White⁸, M. J. White¹, R. White^{34b}, D. Whiteson¹⁶⁷, F. J. Wickens¹³², W. Wiedenmann¹⁷⁷, M. Wielers¹³², C. Wiglesworth³⁸, L. A. M. Wiik-Fuchs²³, A. Wildauer¹⁰², F. Wilk⁸⁶, H. G. Wilkens³², H. H. Williams¹²³, S. Williams¹⁰⁸, C. Willis⁹², S. Willocq⁸⁸, J. A. Wilson¹⁹, I. Wingerter-Seez⁵, F. Winklmeier¹¹⁷, O. J. Winston¹⁵², B. T. Winter²³, M. Wittgen¹⁴⁶, J. Wittkowski¹⁰¹, T. M. H. Wolf¹⁰⁸, M. W. Wolter⁴¹, H. Wolters^{127a,127c}, S. D. Worm¹³², B. K. Wosiek⁴¹, J. Wotschack³², M. J. Woudstra⁸⁶, K. W. Wozniak⁴¹, M. Wu⁵⁷, M. Wu³³, S. L. Wu¹⁷⁷, X. Wu⁵¹, Y. Wu⁹¹, T. R. Wyatt⁸⁶, B. M. Wynne⁴⁸, S. Xella³⁸, D. Xu^{35a}, L. Xu²⁷, T. Xu¹³⁷, B. Yabsley¹⁵³, S. Yacoob^{148a}, D. Yamaguchi¹⁶⁰, Y. Yamaguchi¹¹⁹, A. Yamamoto⁶⁸, S. Yamamoto¹⁵⁸, T. Yamanaka¹⁵⁸, K. Yamauchi¹⁰⁴, Y. Yamazaki⁶⁹, Z. Yan²⁴, H. Yang¹⁴¹, H. Yang¹⁷⁷, Y. Yang¹⁵⁴, Z. Yang¹⁵, W.-M. Yao¹⁶, Y. C. Yap⁸², Y. Yasu⁶⁸, E. Yatsenko⁵, K. H. Yau Wong²³, J. Ye⁴², S. Ye²⁷, I. Yeletsikh⁶⁷, A. L. Yen⁵⁸, E. Yildirim⁸⁵, K. Yorita¹⁷⁵, R. Yoshida⁶, K. Yoshihara¹²³, C. Young¹⁴⁶, C. J. S. Young³², S. Youssef²⁴, D. R. Yu¹⁶, J. Yu⁸, J. M. Yu⁹¹, J. Yu⁶⁶, L. Yuan⁶⁹, S. P. Y. Yuen²³, I. Yusuff^{30,at}, B. Zabinski⁴¹, R. Zaidan⁶⁵, A. M. Zaitsev^{131,af}, N. Zakharchuk⁴⁴, J. Zalieckas¹⁵, A. Zaman¹⁵¹, S. Zambito⁵⁸, L. Zanello^{133a,133b}, D. Zanzi⁹⁰, C. Zeitnitz¹⁷⁹, M. Zeman¹²⁹, A. Zemla^{40a}, J. C. Zeng¹⁷⁰, Q. Zeng¹⁴⁶, K. Zengel²⁵, O. Zenin¹³¹, T. Ženiš^{147a}, D. Zerwas¹¹⁸, D. Zhang⁹¹, F. Zhang¹⁷⁷, G. Zhang^{59,ao}, H. Zhang^{35b}, J. Zhang⁶, L. Zhang⁵⁰, R. Zhang²³, R. Zhang^{59,au}, X. Zhang¹⁴⁰, Z. Zhang¹¹⁸, X. Zhao⁴², Y. Zhao¹⁴⁰, Z. Zhao⁵⁹, A. Zhemchugov⁶⁷, J. Zhong¹²¹, B. Zhou⁹¹, C. Zhou¹⁷⁷, L. Zhou³⁷, L. Zhou⁴², M. Zhou¹⁵¹, N. Zhou^{35c}, C. G. Zhu¹⁴⁰, H. Zhu^{35a}, J. Zhu⁹¹, Y. Zhu⁵⁹, X. Zhuang^{35a}, K. Zhukov⁹⁷, A. Zibell¹⁷⁸, D. Zieminska⁶³, N. I. Zimine⁶⁷, C. Zimmermann⁸⁵, S. Zimmermann⁵⁰, Z. Zinonos⁵⁶, M. Zinser⁸⁵, M. Ziolkowski¹⁴⁴, L. Živković¹⁴, G. Zobernig¹⁷⁷, A. Zoccoli^{22a,22b}, M. zur Nedden¹⁷, L. Zwalinski³²

¹ Department of Physics, University of Adelaide, Adelaide, Australia

² Physics Department, SUNY Albany, Albany, NY, USA

³ Department of Physics, University of Alberta, Edmonton, AB, Canada

⁴ (a) Department of Physics, Ankara University, Ankara, Turkey; (b) Istanbul Aydin University, Istanbul, Turkey; (c) Division of Physics, TOBB University of Economics and Technology, Ankara, Turkey

⁵ LAPP, CNRS/IN2P3 and Université Savoie Mont Blanc, Annecy-le-Vieux, France

⁶ High Energy Physics Division, Argonne National Laboratory, Argonne, IL, USA

⁷ Department of Physics, University of Arizona, Tucson, AZ, USA

⁸ Department of Physics, The University of Texas at Arlington, Arlington, TX, USA

⁹ Physics Department, University of Athens, Athens, Greece

- ¹⁰ Physics Department, National Technical University of Athens, Zografou, Greece
- ¹¹ Department of Physics, The University of Texas at Austin, Austin, TX, USA
- ¹² Institute of Physics, Azerbaijan Academy of Sciences, Baku, Azerbaijan
- ¹³ Institut de Física d'Altes Energies (IFAE), The Barcelona Institute of Science and Technology, Barcelona, Spain
- ¹⁴ Institute of Physics, University of Belgrade, Belgrade, Serbia
- ¹⁵ Department for Physics and Technology, University of Bergen, Bergen, Norway
- ¹⁶ Physics Division, Lawrence Berkeley National Laboratory and University of California, Berkeley, CA, USA
- ¹⁷ Department of Physics, Humboldt University, Berlin, Germany
- ¹⁸ Albert Einstein Center for Fundamental Physics and Laboratory for High Energy Physics, University of Bern, Bern, Switzerland
- ¹⁹ School of Physics and Astronomy, University of Birmingham, Birmingham, UK
- ²⁰ (a) Department of Physics, Bogazici University, Istanbul, Turkey; (b) Department of Physics Engineering, Gaziantep University, Gaziantep, Turkey; (c) Istanbul Bilgi University, Faculty of Engineering and Natural Sciences, Istanbul, Turkey; (d) Bahcesehir University, Faculty of Engineering and Natural Sciences, Istanbul, Turkey
- ²¹ Centro de Investigaciones, Universidad Antonio Narino, Bogota, Colombia
- ²² (a) INFN Sezione di Bologna, Bologna, Italy; (b) Dipartimento di Fisica e Astronomia, Università di Bologna, Bologna, Italy
- ²³ Physikalisches Institut, University of Bonn, Bonn, Germany
- ²⁴ Department of Physics, Boston University, Boston, MA, USA
- ²⁵ Department of Physics, Brandeis University, Waltham, MA, USA
- ²⁶ (a) Universidade Federal do Rio De Janeiro COPPE/EE/IF, Rio de Janeiro, Brazil; (b) Electrical Circuits Department, Federal University of Juiz de Fora (UFJF), Juiz de Fora, Brazil; (c) Federal University of Sao Joao del Rei (UFSJ), Sao Joao del Rei, Brazil; (d) Instituto de Fisica, Universidade de Sao Paulo, São Paulo, Brazil
- ²⁷ Physics Department, Brookhaven National Laboratory, Upton, NY, USA
- ²⁸ (a) Transilvania University of Brasov, Brasov, Romania; (b) National Institute of Physics and Nuclear Engineering, Bucharest, Romania; (c) Physics Department, National Institute for Research and Development of Isotopic and Molecular Technologies, Cluj Napoca, Romania; (d) University Politehnica Bucharest, Bucharest, Romania; (e) West University in Timisoara, Timisoara, Romania
- ²⁹ Departamento de Física, Universidad de Buenos Aires, Buenos Aires, Argentina
- ³⁰ Cavendish Laboratory, University of Cambridge, Cambridge, UK
- ³¹ Department of Physics, Carleton University, Ottawa, ON, Canada
- ³² CERN, Geneva, Switzerland
- ³³ Enrico Fermi Institute, University of Chicago, Chicago, IL, USA
- ³⁴ (a) Departamento de Física, Pontificia Universidad Católica de Chile, Santiago, Chile; (b) Departamento de Física, Universidad Técnica Federico Santa María, Valparaíso, Chile
- ³⁵ (a) Institute of High Energy Physics, Chinese Academy of Sciences, Beijing, China; (b) Department of Physics, Nanjing University, Jiangsu, China; (c) Physics Department, Tsinghua University, Beijing 100084, China
- ³⁶ Laboratoire de Physique Corpusculaire, Clermont Université and Université Blaise Pascal and CNRS/IN2P3, Clermont-Ferrand, France
- ³⁷ Nevis Laboratory, Columbia University, Irvington, NY, USA
- ³⁸ Niels Bohr Institute, University of Copenhagen, Copenhagen, Denmark
- ³⁹ (a) INFN Gruppo Collegato di Cosenza, Laboratori Nazionali di Frascati, Frascati, Italy; (b) Dipartimento di Fisica, Università della Calabria, Rende, Italy
- ⁴⁰ (a) Faculty of Physics and Applied Computer Science, AGH University of Science and Technology, Kraków, Poland; (b) Marian Smoluchowski Institute of Physics, Jagiellonian University, Kraków, Poland
- ⁴¹ Institute of Nuclear Physics, Polish Academy of Sciences, Kraków, Poland
- ⁴² Physics Department, Southern Methodist University, Dallas, TX, USA
- ⁴³ Physics Department, University of Texas at Dallas, Richardson, TX, USA
- ⁴⁴ DESY, Hamburg and Zeuthen, Germany
- ⁴⁵ Lehrstuhl für Experimentelle Physik IV, Technische Universität Dortmund, Dortmund, Germany
- ⁴⁶ Institut für Kern- und Teilchenphysik, Technische Universität Dresden, Dresden, Germany
- ⁴⁷ Department of Physics, Duke University, Durham, NC, USA
- ⁴⁸ SUPA - School of Physics and Astronomy, University of Edinburgh, Edinburgh, UK

- 49 INFN Laboratori Nazionali di Frascati, Frascati, Italy
- 50 Fakultät für Mathematik und Physik, Albert-Ludwigs-Universität, Freiburg, Germany
- 51 Section de Physique, Université de Genève, Geneva, Switzerland
- 52 (a)INFN Sezione di Genova, Genoa, Italy; (b)Dipartimento di Fisica, Università di Genova, Genoa, Italy
- 53 (a)E. Andronikashvili Institute of Physics, Iv. Javakhishvili Tbilisi State University, Tbilisi, Georgia; (b)High Energy Physics Institute, Tbilisi State University, Tbilisi, Georgia
- 54 II Physikalisches Institut, Justus-Liebig-Universität Giessen, Giessen, Germany
- 55 SUPA - School of Physics and Astronomy, University of Glasgow, Glasgow, UK
- 56 II Physikalisches Institut, Georg-August-Universität, Göttingen, Germany
- 57 Laboratoire de Physique Subatomique et de Cosmologie, Université Grenoble-Alpes, CNRS/IN2P3, Grenoble, France
- 58 Laboratory for Particle Physics and Cosmology, Harvard University, Cambridge, MA, USA
- 59 Department of Modern Physics, University of Science and Technology of China, Anhui, China
- 60 (a)Kirchhoff-Institut für Physik, Ruprecht-Karls-Universität Heidelberg, Heidelberg, Germany; (b)Physikalisches Institut, Ruprecht-Karls-Universität Heidelberg, Heidelberg, Germany; (c)ZITI Institut für technische Informatik, Ruprecht-Karls-Universität Heidelberg, Mannheim, Germany
- 61 Faculty of Applied Information Science, Hiroshima Institute of Technology, Hiroshima, Japan
- 62 (a)Department of Physics, The Chinese University of Hong Kong, Shatin, N.T., Hong Kong; (b)Department of Physics, The University of Hong Kong, Hong Kong, China; (c)Department of Physics, The Hong Kong University of Science and Technology, Clear Water Bay, Kowloon, Hong Kong, China
- 63 Department of Physics, Indiana University, Bloomington, IN, United States of America
- 64 Institut für Astro- und Teilchenphysik, Leopold-Franzens-Universität, Innsbruck, Austria
- 65 University of Iowa, Iowa City, IA, USA
- 66 Department of Physics and Astronomy, Iowa State University, Ames, IA, USA
- 67 Joint Institute for Nuclear Research, JINR Dubna, Dubna, Russia
- 68 KEK, High Energy Accelerator Research Organization, Tsukuba, Japan
- 69 Graduate School of Science, Kobe University, Kobe, Japan
- 70 Faculty of Science, Kyoto University, Kyoto, Japan
- 71 Kyoto University of Education, Kyoto, Japan
- 72 Department of Physics, Kyushu University, Fukuoka, Japan
- 73 Instituto de Física La Plata, Universidad Nacional de La Plata and CONICET, La Plata, Argentina
- 74 Physics Department, Lancaster University, Lancaster, UK
- 75 (a)INFN Sezione di Lecce, Lecce, Italy; (b)Dipartimento di Matematica e Fisica, Università del Salento, Lecce, Italy
- 76 Oliver Lodge Laboratory, University of Liverpool, Liverpool, UK
- 77 Department of Physics, Jožef Stefan Institute, University of Ljubljana, Ljubljana, Slovenia
- 78 School of Physics and Astronomy, Queen Mary University of London, London, UK
- 79 Department of Physics, Royal Holloway University of London, Surrey, UK
- 80 Department of Physics and Astronomy, University College London, London, UK
- 81 Louisiana Tech University, Ruston, LA, USA
- 82 Laboratoire de Physique Nucléaire et de Hautes Energies, UPMC and Université Paris-Diderot and CNRS/IN2P3, Paris, France
- 83 Fysiska institutionen, Lunds universitet, Lund, Sweden
- 84 Departamento de Física Teórica C-15, Universidad Autónoma de Madrid, Madrid, Spain
- 85 Institut für Physik, Universität Mainz, Mainz, Germany
- 86 School of Physics and Astronomy, University of Manchester, Manchester, UK
- 87 CPPM, Aix-Marseille Université and CNRS/IN2P3, Marseille, France
- 88 Department of Physics, University of Massachusetts, Amherst, MA, USA
- 89 Department of Physics, McGill University, Montreal, QC, Canada
- 90 School of Physics, University of Melbourne, Victoria, Australia
- 91 Department of Physics, The University of Michigan, Ann Arbor, MI, USA
- 92 Department of Physics and Astronomy, Michigan State University, East Lansing, MI, USA
- 93 (a)INFN Sezione di Milano, Milan, Italy; (b)Dipartimento di Fisica, Università di Milano, Milan, Italy
- 94 B.I. Stepanov Institute of Physics, National Academy of Sciences of Belarus, Minsk, Republic of Belarus
- 95 National Scientific and Educational Centre for Particle and High Energy Physics, Minsk, Republic of Belarus

- ⁹⁶ Group of Particle Physics, University of Montreal, Montreal, QC, Canada
- ⁹⁷ P.N. Lebedev Physical Institute of the Russian Academy of Sciences, Moscow, Russia
- ⁹⁸ Institute for Theoretical and Experimental Physics (ITEP), Moscow, Russia
- ⁹⁹ National Research Nuclear University MEPhI, Moscow, Russia
- ¹⁰⁰ D.V. Skobeltsyn Institute of Nuclear Physics, M.V. Lomonosov Moscow State University, Moscow, Russia
- ¹⁰¹ Fakultät für Physik, Ludwig-Maximilians-Universität München, Munich, Germany
- ¹⁰² Max-Planck-Institut für Physik (Werner-Heisenberg-Institut), Munich, Germany
- ¹⁰³ Nagasaki Institute of Applied Science, Nagasaki, Japan
- ¹⁰⁴ Graduate School of Science and Kobayashi-Maskawa Institute, Nagoya University, Nagoya, Japan
- ¹⁰⁵ ^(a)INFN Sezione di Napoli, Naples, Italy; ^(b)Dipartimento di Fisica, Università di Napoli, Naples, Italy
- ¹⁰⁶ Department of Physics and Astronomy, University of New Mexico, Albuquerque, NM, USA
- ¹⁰⁷ Institute for Mathematics, Astrophysics and Particle Physics, Radboud University Nijmegen/Nikhef, Nijmegen, The Netherlands
- ¹⁰⁸ Nikhef National Institute for Subatomic Physics and University of Amsterdam, Amsterdam, The Netherlands
- ¹⁰⁹ Department of Physics, Northern Illinois University, DeKalb, IL, USA
- ¹¹⁰ Budker Institute of Nuclear Physics, SB RAS, Novosibirsk, Russia
- ¹¹¹ Department of Physics, New York University, New York, NY, USA
- ¹¹² Ohio State University, Columbus, OH, USA
- ¹¹³ Faculty of Science, Okayama University, Okayama, Japan
- ¹¹⁴ Homer L. Dodge Department of Physics and Astronomy, University of Oklahoma, Norman, OK, USA
- ¹¹⁵ Department of Physics, Oklahoma State University, Stillwater, OK, USA
- ¹¹⁶ Palacký University, RCPTM, Olomouc, Czech Republic
- ¹¹⁷ Center for High Energy Physics, University of Oregon, Eugene, OR, USA
- ¹¹⁸ LAL, Univ. Paris-Sud, CNRS/IN2P3, Université Paris-Saclay, Orsay, France
- ¹¹⁹ Graduate School of Science, Osaka University, Osaka, Japan
- ¹²⁰ Department of Physics, University of Oslo, Oslo, Norway
- ¹²¹ Department of Physics, Oxford University, Oxford, UK
- ¹²² ^(a)INFN Sezione di Pavia, Pavia, Italy; ^(b)Dipartimento di Fisica, Università di Pavia, Pavia, Italy
- ¹²³ Department of Physics, University of Pennsylvania, Philadelphia, PA, USA
- ¹²⁴ National Research Centre “Kurchatov Institute” B.P.Konstantinov Petersburg Nuclear Physics Institute, St. Petersburg, Russia
- ¹²⁵ ^(a)INFN Sezione di Pisa, Pisa, Italy; ^(b)Dipartimento di Fisica E. Fermi, Università di Pisa, Pisa, Italy
- ¹²⁶ Department of Physics and Astronomy, University of Pittsburgh, Pittsburgh, PA, USA
- ¹²⁷ ^(a)Laboratório de Instrumentação e Física Experimental de Partículas-LIP, Lisbon, Portugal; ^(b)Faculdade de Ciências, Universidade de Lisboa, Lisbon, Portugal; ^(c)Department of Physics, University of Coimbra, Coimbra, Portugal; ^(d)Centro de Física Nuclear da Universidade de Lisboa, Lisbon, Portugal; ^(e)Departamento de Física, Universidade do Minho, Braga, Portugal; ^(f)Departamento de Física Teórica y del Cosmos and CAFPE, Universidad de Granada, Granada, Spain; ^(g)Dep Física and CEFITEC of Faculdade de Ciências e Tecnologia, Universidade Nova de Lisboa, Caparica, Portugal
- ¹²⁸ Institute of Physics, Academy of Sciences of the Czech Republic, Prague, Czech Republic
- ¹²⁹ Czech Technical University in Prague, Prague, Czech Republic
- ¹³⁰ Faculty of Mathematics and Physics, Charles University in Prague, Prague, Czech Republic
- ¹³¹ State Research Center Institute for High Energy Physics (Protvino), NRC KI, Protvino, Russia
- ¹³² Particle Physics Department, Rutherford Appleton Laboratory, Didcot, UK
- ¹³³ ^(a)INFN Sezione di Roma, Rome, Italy; ^(b)Dipartimento di Fisica, Sapienza Università di Roma, Rome, Italy
- ¹³⁴ ^(a)INFN Sezione di Roma Tor Vergata, Rome, Italy; ^(b)Dipartimento di Fisica, Università di Roma Tor Vergata, Rome, Italy
- ¹³⁵ ^(a)INFN Sezione di Roma Tre, Rome, Italy; ^(b)Dipartimento di Matematica e Fisica, Università Roma Tre, Rome, Italy
- ¹³⁶ ^(a)Faculté des Sciences Ain Chock, Réseau Universitaire de Physique des Hautes Energies-Université Hassan II,

- Casablanca, Morocco; ^(b)Centre National de l'Energie des Sciences Techniques Nucleaires, Rabat, Morocco; ^(c)Faculté des Sciences Semlalia, Université Cadi Ayyad, LPHEA-Marrakech, Marrakech, Morocco; ^(d)Faculté des Sciences, Université Mohamed Premier and LTPM, Oujda, Morocco; ^(e)Faculté des Sciences, Université Mohammed V, Rabat, Morocco
- 137 DSM/IRFU (Institut de Recherches sur les Lois Fondamentales de l'Univers), CEA Saclay (Commissariat à l'Energie Atomique et aux Energies Alternatives), Gif-sur-Yvette, France
- 138 Santa Cruz Institute for Particle Physics, University of California Santa Cruz, Santa Cruz, CA, USA
- 139 Department of Physics, University of Washington, Seattle, WA, USA
- 140 School of Physics, Shandong University, Shandong, China
- 141 Department of Physics and Astronomy, Shanghai Key Laboratory for Particle Physics and Cosmology, Shanghai Jiao Tong University (also affiliated with PKU-CHEP), Shanghai, China
- 142 Department of Physics and Astronomy, University of Sheffield, Sheffield, UK
- 143 Department of Physics, Shinshu University, Nagano, Japan
- 144 Fachbereich Physik, Universität Siegen, Siegen, Germany
- 145 Department of Physics, Simon Fraser University, Burnaby, BC, Canada
- 146 SLAC National Accelerator Laboratory, Stanford, CA, USA
- 147 ^(a)Faculty of Mathematics, Physics and Informatics, Comenius University, Bratislava, Slovak Republic; ^(b)Department of Subnuclear Physics, Institute of Experimental Physics of the Slovak Academy of Sciences, Kosice, Slovak Republic
- 148 ^(a)Department of Physics, University of Cape Town, Cape Town, South Africa; ^(b)Department of Physics, University of Johannesburg, Johannesburg, South Africa; ^(c)School of Physics, University of the Witwatersrand, Johannesburg, South Africa
- 149 ^(a)Department of Physics, Stockholm University, Stockholm, Sweden; ^(b)The Oskar Klein Centre, Stockholm, Sweden
- 150 Physics Department, Royal Institute of Technology, Stockholm, Sweden
- 151 Departments of Physics and Astronomy and Chemistry, Stony Brook University, Stony Brook, NY, USA
- 152 Department of Physics and Astronomy, University of Sussex, Brighton, UK
- 153 School of Physics, University of Sydney, Sydney, Australia
- 154 Institute of Physics, Academia Sinica, Taipei, Taiwan
- 155 Department of Physics, Technion: Israel Institute of Technology, Haifa, Israel
- 156 Raymond and Beverly Sackler School of Physics and Astronomy, Tel Aviv University, Tel Aviv, Israel
- 157 Department of Physics, Aristotle University of Thessaloniki, Thessaloníki, Greece
- 158 International Center for Elementary Particle Physics and Department of Physics, The University of Tokyo, Tokyo, Japan
- 159 Graduate School of Science and Technology, Tokyo Metropolitan University, Tokyo, Japan
- 160 Department of Physics, Tokyo Institute of Technology, Tokyo, Japan
- 161 Tomsk State University, Tomsk, Russia, Russia
- 162 Department of Physics, University of Toronto, Toronto, ON, Canada
- 163 ^(a)INFN-TIFPA, Trento, Italy; ^(b)University of Trento, Trento, Italy
- 164 ^(a)TRIUMF, Vancouver, BC, Canada; ^(b)Department of Physics and Astronomy, York University, Toronto, ON, Canada
- 165 Faculty of Pure and Applied Sciences, and Center for Integrated Research in Fundamental Science and Engineering, University of Tsukuba, Tsukuba, Japan
- 166 Department of Physics and Astronomy, Tufts University, Medford, MA, USA
- 167 Department of Physics and Astronomy, University of California Irvine, Irvine, CA, USA
- 168 ^(a)INFN Gruppo Collegato di Udine, Sezione di Trieste, Udine, Italy; ^(b)ICTP, Trieste, Italy; ^(c)Dipartimento di Chimica Fisica e Ambiente, Università di Udine, Udine, Italy
- 169 Department of Physics and Astronomy, University of Uppsala, Uppsala, Sweden
- 170 Department of Physics, University of Illinois, Urbana, IL, USA
- 171 Instituto de Física Corpuscular (IFIC) and Departamento de Física Atomica, Molecular y Nuclear and Departamento de Ingeniería Electrónica and Instituto de Microelectrónica de Barcelona (IMB-CNM), University of Valencia and CSIC, Valencia, Spain
- 172 Department of Physics, University of British Columbia, Vancouver, BC, Canada
- 173 Department of Physics and Astronomy, University of Victoria, Victoria, BC, Canada
- 174 Department of Physics, University of Warwick, Coventry, UK
- 175 Waseda University, Tokyo, Japan
- 176 Department of Particle Physics, The Weizmann Institute of Science, Rehovot, Israel

- ¹⁷⁷ Department of Physics, University of Wisconsin, Madison, WI, USA
- ¹⁷⁸ Fakultät für Physik und Astronomie, Julius-Maximilians-Universität, Würzburg, Germany
- ¹⁷⁹ Fakultät für Mathematik und Naturwissenschaften, Fachgruppe Physik, Bergische Universität Wuppertal, Wuppertal, Germany
- ¹⁸⁰ Department of Physics, Yale University, New Haven, CT, USA
- ¹⁸¹ Yerevan Physics Institute, Yerevan, Armenia
- ¹⁸² Centre de Calcul de l'Institut National de Physique Nucléaire et de Physique des Particules (IN2P3), Villeurbanne, France
- ^a Also at Department of Physics, King's College London, London, United Kingdom
- ^b Also at Institute of Physics, Azerbaijan Academy of Sciences, Baku, Azerbaijan
- ^c Also at Novosibirsk State University, Novosibirsk, Russia
- ^d Also at TRIUMF, Vancouver BC, Canada
- ^e Also at Department of Physics & Astronomy, University of Louisville, Louisville, KY, United States of America
- ^f Also at Physics Department, An-Najah National University, Nablus, Palestine
- ^g Also at Department of Physics, California State University, Fresno CA, United States of America
- ^h Also at Department of Physics, University of Fribourg, Fribourg, Switzerland
- ⁱ Also at Departament de Física de la Universitat Autònoma de Barcelona, Barcelona, Spain
- ^j Also at Departamento de Física e Astronomia, Faculdade de Ciências, Universidade do Porto, Portugal
- ^k Also at Tomsk State University, Tomsk, Russia, Russia
- ^l Also at Università di Napoli Parthenope, Napoli, Italy
- ^m Also at Institute of Particle Physics (IPP), Canada
- ⁿ Also at National Institute of Physics and Nuclear Engineering, Bucharest, Romania
- ^o Also at Department of Physics, St. Petersburg State Polytechnical University, St. Petersburg, Russia
- ^p Also at Department of Physics, The University of Michigan, Ann Arbor MI, United States of America
- ^q Also at Centre for High Performance Computing, CSIR Campus, Rosebank, Cape Town, South Africa
- ^r Also at Louisiana Tech University, Ruston LA, United States of America
- ^s Also at Institutio Catalana de Recerca i Estudis Avancats, ICREA, Barcelona, Spain
- ^t Also at Graduate School of Science, Osaka University, Osaka, Japan
- ^u Also at Department of Physics, National Tsing Hua University, Taiwan
- ^v Also at Institute for Mathematics, Astrophysics and Particle Physics, Radboud University Nijmegen/Nikhef, Nijmegen, Netherlands
- ^w Also at Department of Physics, The University of Texas at Austin, Austin TX, United States of America
- ^x Also at CERN, Geneva, Switzerland
- ^y Also at Georgian Technical University (GTU), Tbilisi, Georgia
- ^z Also at O Chadai Academic Production, Ochanomizu University, Tokyo, Japan
- ^{aa} Also at Manhattan College, New York NY, United States of America
- ^{ab} Also at Hellenic Open University, Patras, Greece
- ^{ac} Also at Academia Sinica Grid Computing, Institute of Physics, Academia Sinica, Taipei, Taiwan
- ^{ad} Also at School of Physics, Shandong University, Shandong, China
- ^{ae} Also at Department of Physics, California State University, Sacramento CA, United States of America
- ^{af} Also at Moscow Institute of Physics and Technology State University, Dolgoprudny, Russia
- ^{ag} Also at Section de Physique, Université de Genève, Geneva, Switzerland
- ^{ah} Also at Eotvos Lorand University, Budapest, Hungary
- ^{ai} Also at Departments of Physics & Astronomy and Chemistry, Stony Brook University, Stony Brook NY, United States of America
- ^{aj} Also at International School for Advanced Studies (SISSA), Trieste, Italy
- ^{ak} Also at Department of Physics and Astronomy, University of South Carolina, Columbia SC, United States of America
- ^{al} Also at School of Physics and Engineering, Sun Yat-sen University, Guangzhou, China
- ^{am} Also at Institute for Nuclear Research and Nuclear Energy (INRNE) of the Bulgarian Academy of Sciences, Sofia, Bulgaria
- ^{an} Also at Faculty of Physics, M.V.Lomonosov Moscow State University, Moscow, Russia
- ^{ao} Also at Institute of Physics, Academia Sinica, Taipei, Taiwan
- ^{ap} Also at National Research Nuclear University MEPhI, Moscow, Russia

^{aq} Also at Department of Physics, Stanford University, Stanford CA, United States of America

^{ar} Also at Institute for Particle and Nuclear Physics, Wigner Research Centre for Physics, Budapest, Hungary

^{as} Also at Flensburg University of Applied Sciences, Flensburg, Germany

^{at} Also at University of Malaya, Department of Physics, Kuala Lumpur, Malaysia

^{au} Also at CPPM, Aix-Marseille Université and CNRS/IN2P3, Marseille, France

* Deceased